Place Exchange Reactions of Gold Nanoparticles

by

Adil Kassam

A Thesis submitted to McGill University in partial fulfillment of the requirement for the degree of

Doctor of Philosophy

Department of Chemistry
McGill University
Montréal, Québec, Canada

August 2007

Your file Votre référence
ISBN: 978-0-494-67080-4
Our file Notre référence
ISBN: 978-0-494-67080-4

To my parents for all their hardwork, love and support.
Nothing would be possible without you.

ACKNOWLEDGEMENTS

The experience I've had in Montreal has been fantastic and was due in no small part to the many amazing and wonderful people that have surrounded me since moving here. They have enabled me to not only complete my studies, but also to enjoy the time spent completing them. It would be impossible to enumerate them all, but everyone deserves my thanks for making this a great experience.

My supervisor Prof. Bruce Lennox has enabled me to pursue my studies to the best of my ability. His guidance and support are unparallelled and I feel lucky to have found such a great mentor. Even though you were busy, each meeting we had you gave your full attention and thoughts, which meant a lot to me. As a supervisor and person your knowledge and understanding of the universe still astounds me and I will always strive to follow the example and advice you've given me.

I am grateful to Dr. Wilczek who taught me how to teach. It was a delight to learn and teach in your laboratory. Thanks go to Dr. Farrell, Dr. Wiseman Dr. van de Ven and Dr. Cosa for taking time out of their schedules to discuss science and encouraging me to pursue my academic pursuits.

Sandra Aerssen made me feel like I was the most important graduate student and was surprisingly adept at 'sneaking' in an appointment to see my supervisor, thanks for caring. The graduate student secretaries Chantal Marotte and Renée Charron, took care of me like a son. They made sure I didn't go broke and always kept their doors open to listen to my thoughts and frustrations.

Certainly one aspect I never enjoyed was dealing with complex and frustrating administrative tasks. Thankfully, the chemistry department secretaries really made these dealings enjoyable and simple. Colleen MacNamee, Karen Turner, Alison McCaffrey, and Fay Nurse-'Thank you.'

I would like to thank all the fantastic engineers in the bottom of Otto Maass for helping getting machines working, making new instruments and tools. Rick Rossi (electronics), Dr. Nadim Saade (MS), Frank Rothwell (GC), Bill Bastian (machine

shop), Fred Kluck (machine shop) and George Kopp (glass blowing) all made things 'happen.' A really special thanks goes to Dr. Paul Xia (NMR), who helped me countless times to solve problems no one else could. NMR is certainly a powerful technique and your knowledge and skill certainly saved some projects.

Working long hours and many years in a lab certainly would not be possible without the kind help and encouragement of colleagues around you. While most of the original group has left and replaced by new (and equally amazing) people, this Thesis would not be possible without all of their help. The help of Dr. M. Goren and Dr. N. Cameron when I first started in the lab was v.much appreciated, how you dealt with such a clueless chemist is a testament to your patience and caring. Dr. Vicki Meli your encouragement and great example really made me work harder and strive to become a better chemist. Dr. Lawrence Lee, Dr. Ian Burgess, Dr. Jeff Shepherd and Dr. Brian Seivewright our daily coffee breaks, debates and discussions made everyday exciting and happy even when the chemistry wasn't going well. I was also lucky to supervise 3 great summer students who did too many experiments in the lab. Glen, Elisa and Brad your hardwork (for next to no money) enabled me to finish this thesis without going insane. And I can't forget my three adopted summer students Tara, Christina,Pat and Tom who made life in the lab during the summer enjoyable. Dr. Gerardo Ulibarri really taught me how to work and think as an organic chemist. The year working alongside you were my most productive in terms of development and productivity, and I doubt I will ever be so focused again. While our results unfortunately did not go 'our way' it wasn't due to our lack of hard work. Thank you for being such a great mentor. Finally, no lab is home without an older sister and Dr. Simona Rucareanu was certainly that for me, both in the chemistry sense and in life. I hope you enjoyed your time in Montreal as much as I enjoyed your company. Outside my own lab many fellow graduate students made my time in Otto Maass and Pulp & Paper more enjoyable and deserve acknowledgement. They never said no to me stopping in during the day to talk and were always willing to listen to my thoughts and problems. Of special note are Mike McAlduff, Emily Cranston, David Kolin, Sam Sewall, Pat Farber, Paul Oleynik, and Oleh Tanchak to whom I am especially grateful.

Getting to be able to write this Thesis on a computer was not as easy as I first thought. Many people helped me with their time and knowledge to get my own computer and LaTeX working to write this. I thank Andrew Gosline, Dr. Carl Bartels, Chris

Godbout, Pat Farber, Lawrence Lee, Brian Seivewright and Dave Kolin for their help in all things computer related.

I could not finish the acknowledgements without thanking my friends who had no relation to the Chemistry Department and provided encouragement and support to me over the years. My utmost thanks goes to Chris Boivin, Mike Dwyer, Andrew and Sara Gosline, Olivia Bibollet, Adrielle Houweling and Mike Clay, your friendship and advice has made this thesis possible.

To all members of my various Ultimate teams over the years, thank you for providing me with a venue to escape from the McGill universe to see the rest of the city and country. Special thanks goes to Mike Clay, Andrew Gosline, Andrew Lee, Steph Krajicek and the boys of the Omen and MUT teams.

Last but most importantly I want to thank my family. Mom your unending love, encouragement and food kept me going throughout my degree. My earliest experiments were with you in the kitchen, and although nanoparticles may seem complicated, they are in no way as hard to make (and don't taste as good) as your Bhiriyani. My dad got me hooked into science and technology, whether it was explaining how a lawn mower worked or getting me to fix computers from an early age, thank you for your willingness to teach and your support through these years. My brother Karim, has provided invaluable advice, and allowed me to realize what I can achieve. My sister Rishma, always encouraged me and taught me never to take myself too seriously.

ABSTRACT

The kinetics and mechanism of the place exchange reaction(PER) of alkylthiols with alkylthiol-protected gold nanoparticles(AuNP) are investigated. Using chemically similar alkylthiols it was possible to study the reaction in the absence of perturbing factors, enabling detailed mechanistic and kinetic studies to be explored. It is found that the reactions are zero order in incoming ligand and overall follow a second order diffusion limited Langmuir rate law. In the case where there is little chemical distinction between the incoming and capping ligands, the reactions proceed to an endpoint consistent with a K_{eq}=1. The rate of the reaction is dependent on the chain length of the capping ligand and the AuNP core size. The related dialkyldisulphide-for-alkylthiol AuNP exchange reaction is consistent with the same rate law and also proceeds to a well-defined endpoint. However, the rate constant is 20-fold less than the alkylthiol case. These results lead to a convergent model of PERs where the rate limiting process involves both incoming and outgoing ligands, with diffusion of the incoming ligand to the AuNP surface as the major controlling factor of the reaction rate.

ABRÉGÉ

Le mécanisme et la cinétique de la réaction d'échange de ligand (PER) alkylthiols avec des ligands alkylthiols protégeant la surface d'une nanoparticule d'or (AuNP) ont été étudiés. En utilisant des alkylthiols similaires, il a été possible d'observer ces réactions en l'absence d'interférences, et ainsi d'en explorer en détail les aspects mécanistiques et cinétiques. Il a été démontré que ces réactions sont d'ordre zéro en terme de ligand libre entrant la AuNP, et se conforment à une cinétique de Langmuir d'ordre deux, avec une vitesse maximale dictée par la vitesse de diffusion. Dans le cas où le ligand entrant et le ligand protecteurs sont très similaires, la réaction atteint un qui concorde avec une constante K_{eq}=1. La vitesse de réaction dépend de la longueur de la chaîne du ligand protecteur ainsi que des dimensions des AuNP. La réaction d'échange d'un dialkyldisulfide pour un alkylthiol protecteur procède avec les même ordres de réaction et atteint également un point d'équilibre défini. Cependant, la constante de vitesse dans ce cas est 20 fois moindre que dans le cas d'un alkylthiol comme ligand entrant. Ces résultats suggère un modèle convergent des PER, où l'étape limitante met en jeu à la fois le ligand entrant et le ligand sortant de la AuNP ; la vitesse de diffusion du ligand entrant jusqu'à la surface de l'AuNP étant un élément clé dans la détermination la vitesse de réaction.

Table of Contents

Acknowledgements ii
Abstract v
Abrégé vi
Contributions of Authors viii
List of Abbreviations xv
List of Tables xvii
List of Figures xvii

1 General Introduction **1**
1.1 2D SAM 2
1.2 Creation of 2D Au-RS SAM 3
1.2.1 Kinetics of 2D SAM Formation 3
1.3 Mixed Composition 2D Au-RS SAMs 5
1.3.1 Methods to Create Mixed Composition 2D SAMs 5
1.3.2 Phase properties of 2D SAMs 6
1.3.3 Mechanism and Properties of Exchange Reactions in 2D SAMs 6
1.4 Gold Nanoparticles 9
1.4.1 AuNP Synthesis 9
1.5 AuNP Properties 11
1.5.1 AuNP core properties 12
1.6 Methods to Create Mixed Composition AuNPs 13
1.7 Place Exchange Reactions of AuNPs 14
1.8 History of Thiol-Thiol Exchange Reactions on AuNPs 14
1.8.1 Reaction-Quench Kinetics 16
1.8.2 In-Situ Techniques 19
1.9 AuNP with Mixed Composition Capping Ligands 21
1.10 Kinetics of Place Exchange Reactions on AuNP 22
1.10.1 "Edge and Vertex" Model 23
1.10.2 Chechik Model 24
1.11 Concluding Remarks and Outline of Thesis 26
References 28

2 Methods **32**
2.1 Synthesis of Gold Nanoparticles 32
2.1.1 Synthesis 2nm $C_{10}SH$ stabilized gold nanoparticles 32
2.1.2 Variation on Synthesis 33
2.2 Particle Characterization 33
2.3 Evaluation of Place Exchange Reactions 35
2.3.1 GC analysis of PER products 36
2.3.2 HPLC analysis of PER products 37
2.3.3 Fitting to Kinetic Models 39
References 40

Appendix A NP Size Function **41**
A.1 Program Code 41

3 Place Exchange Reactions of Alkyl Thiols on Gold Nanoparticles **46**
3.1 Abstract 47
3.2 Introduction 47
3.3 Experimental Methods 48
3.4 Results 48
3.5 Conclusion 51
3.6 Acknowledgements 52
References and Notes 52

Appendix B Derivation of Langmuir Kinetics **54**
References 55

Appendix C Fitting of PER Kinetics Data to Models **57**
C.0.1 Traditional Kinetic Models 58
C.0.2 Langmuir Kinetic Models 60
References 63

Appendix D Fitting to Existing Literature Data **64**
References 67

4 The Kinetics and Mechanism of the Place Exchange Reaction on Gold Nanoparticles:Dialkyldisulphide for Alkylthiol **68**
4.1 Abstract 69
4.2 Introduction 69
4.3 Results and Discussion 70
4.4 Conclusion 73
4.5 Methods 73
References and Notes 74

Appendix E Alternative models applied to the dialkyldisulphide PER 76
E.0.1 Alternative Fittings 76
References 84

5 Characteristics of the Alkylthiol-for-Alkylthiol Exchange Reaction Kinetics of Gold Nanoparticles 85
5.1 Abstract 86
5.2 Introduction 86
5.2.1 Previous Work 87
5.3 Methods 87
5.4 Results 88
5.4.1 Effect of NP core size on PER rate 91
5.4.2 Other methods of PER rate control. 94
5.4.3 Mechanism 95
5.5 Conclusion 97
5.6 Acknowledgements 97
References 97

Appendix F Additional Data Reported in Chapter 5 99

6 Conclusions, Contributions, Future Work, and Outlook 101
6.1 Conclusions 101
6.2 Contributions to Original Knowledge 102
6.3 Future Work 103
6.4 Outlook 103
References 104

Contributions of Authors

The main body of this Thesis consists of four chapters (Chapter 2 to Chapter 5). Chapter 2 details the methodology used for the entire Thesis. Two chapters (Chapters 3 and 4) have been published or submitted to peer-reviewed journals and Chapter 5 will shortly be submitted to a peer-refereed journal. The Supplementary Material in the papers making up Chapters 3 and 4 have been elaborated with text and more derivations than appeared in the original manuscripts. An introduction to the field is provided in Chapter 1, and conclusions to the work are provided in Chapter 6.

Chapter 3 Place Exchange Reactions of Alkyl Thiols on Gold Nanoparticles
Co-authoured by Glen Bremner, Brad Clark, Gerardo Ulibarri, and R. Bruce Lennox.
J. Am. Chem. Soc. **2006**. 128 (11), 3476 -3477

Chapter 4 The Kinetics and Mechanism of the Place Exchange Reaction on Gold Nanoparticles: Dialkyldisulphide for Alkylthiol
Co-authoured by Elisa Fuller, and R. Bruce Lennox.
Submitted to *J. Am. Chem. Soc.* on July 16, 2007

Chapter 5 Characteristics of the Alkylthiol-for-Alkylthiol Exchange Reaction Kinetics on Gold Nanoparticles
Co-authoured by Glen Bremner Jeff L. Shepard, and R. Bruce Lennox.
To be submitted to *Langmuir*

The work presented in Chapter 3 was initiated and performed by the author. Glen Bremner and Brad Clark worked as summer students under the supervision of the author. B. Clark performed preliminary methodology experiments which were applied to the methods used in the manuscript. Glen Bremner performed supporting

experiments and performed the "spiking" experiment used in Figure 3.3. Dr. G. Ulibarri provided advice and help during the early stages of the project.

The work presented in Chapter 4 was initiated and performed by the author. Elisa Fuller worked as a summer student under the supervision of the author. E. Fuller performed the experiment used in Figure 4.1.

The work presented in Chapter 5 was initiated and performed by the author. Dr. J. Shepherd worked as a postdoctoral student in the lab and wrote the Matlab program used for particle size analysis. Glen Bremner performed preliminary experiments.

The manuscripts Chapters 2 to 5 are all co-authored by the research director Dr. R. Bruce Lennox, who provided guidance and helped to write the manuscripts.

I hereby give copyright clearance for the inclusion of the following papers, of which I am co-author, in the Thesis of Adil Kassam.

Chapter 4 The Kinetics and Mechanism of the Place Exchange Reaction on Gold Nanoparticles: Dialkyldisulphide for Alkylthiol
Co-authored by Elisa Fuller
Submitted to *J. Am. Chem. Soc.* on July 16, 2007

Chapter 5 Characteristics of the Alkylthiol-for-Alkylthiol Exchange Reaction Kinetics on Gold Nanoparticles
Co-authored by Glen Bremner and Jeff L. Shepherd.
To be submitted to *Langmuir*

R B Lennox Date: Dec. 17/07

Professor R. Bruce Lennox
Department of Chemistry
McGill University

I hereby give copyright clearance for the inclusion of the following papers, of which I am co-author, in the Thesis of Adil Kassam.

Chapter 5 Characteristics of the Alkylthiol-for-Alkylthiol Exchange Reaction Kinetics on Gold Nanoparticles
Co-authored by Jeff L. Shepherd and R. Bruce Lennox.
To be submitted to *Langmuir*

Glen Bremner Date: Dec. 3, 2007

Glen Bremner
Department of Chemistry
University of British Columbia

I hereby give copyright clearance for the inclusion of the following papers, of which I am co-author, in the Thesis of Adil Kassam.

Chapter 4 The Kinetics and Mechanism of the Place Exchange Reaction on Gold Nanoparticles: Dialkyldisulphide for Alkylthiol
Co-authored by R. Bruce Lennox.
Submitted to *J. Am. Chem. Soc.* on July 16, 2007

Elisa Fuller Date: Dec 12th 07.

Elisa Fuller
Department of Chemistry
McGill University

I hereby give copyright clearance for the inclusion of the following papers, of which I am co-author, in the Thesis of Adil Kassam.

Chapter 5 Characteristics of the Alkylthiol-for-Alkylthiol Exchange Reaction Kinetics on Gold Nanoparticles
Co-authored by Glen Bremner and R. Bruce Lennox.
To be submitted to *Langmuir*

Date: Dec 04, 2007

Dr. Jeff L. Shepherd
Department of Chemistry & Biochemistry
Laurentian University

Copyright Information

American Chemical Society's Policy on Theses and Dissertations

If your university requires a signed copy of this letter see contact information below.

Thank you for your request for permission to include **your** paper(s) or portions of text from **your** paper(s) in your thesis. Permission is now automatically granted; please pay special attention to the implications paragraph below. The Copyright Subcommittee of the Joint Board/Council Committees on Publications approved the following:

Copyright permission for published and submitted material from theses and dissertations
ACS extends blanket permission to students to include in their theses and dissertations their own articles, or portions thereof, that have been published in ACS journals or submitted to ACS journals for publication, provided that the ACS copyright credit line is noted on the appropriate page(s).

Publishing implications of electronic publication of theses and dissertation material
Students and their mentors should be aware that posting of theses and dissertation material on the Web prior to submission of material from that thesis or dissertation to an ACS journal may affect publication in that journal. Whether Web posting is considered prior publication may be evaluated on a case-by-case basis by the journal's editor. If an ACS journal editor considers Web posting to be "prior publication", the paper will not be accepted for publication in that journal. If you intend to submit your unpublished paper to ACS for publication, check with the appropriate editor prior to posting your manuscript electronically.

If your paper has **not** yet been published by ACS, we have no objection to your including the text or portions of the text in your thesis/dissertation in **print and microfilm formats**; please note, however, that electronic distribution or Web posting of the unpublished paper as part of your thesis in electronic formats might jeopardize publication of your paper by ACS. Please print the following credit line on the first page of your article: "Reproduced (or 'Reproduced in part') with permission from [JOURNAL NAME], in press (or 'submitted for publication'). Unpublished work copyright [CURRENT YEAR] American Chemical Society." Include appropriate information.

If your paper has already been published by ACS and you want to include the text or portions of the text in your thesis/dissertation in **print or microfilm formats**, please print the ACS copyright credit line on the first page of your article: "Reproduced (or 'Reproduced in part') with permission from [FULL REFERENCE CITATION.] Copyright [YEAR] American Chemical Society." Include appropriate information.

Submission to a Dissertation Distributor: If you plan to submit your thesis to UMI or to another dissertation distributor, you should not include the unpublished ACS paper in your thesis if the thesis will be disseminated electronically, until ACS has published your paper. After publication of the paper by ACS, you may release the entire thesis (**not the individual ACS article by itself**) for electronic dissemination through the distributor; ACS's copyright credit line should be printed on the first page of the ACS paper.

Use on an Intranet: The inclusion of your ACS unpublished or published manuscript is permitted in your thesis in print and microfilm formats. If ACS has published your paper you may include the manuscript in your thesis on an intranet that is not publicly available. Your ACS article cannot be posted electronically on a publicly available medium (i.e. one that is not password protected), such as but not limited to, electronic archives, Internet, library server, etc. The only material from your paper that can be posted on a public electronic medium is the article abstract, figures, and tables, and you may link to the article's DOI or post the article's author-directed URL link provided by ACS. This paragraph does not pertain to the dissertation distributor paragraph above.

Questions? Call +1 202/872-4368/4367. Send e-mail to copyright@acs.org or fax to +1 202-776-8112. 10/10/03, 01/15/04, 06/07/06

List of Abbreviations and Symbols

AgNP	silver nanoparticle
AuNP	gold nanoparticle
PER	place exchange reactions
SAM	self-assembled monolayer
A	reaction endpoint parameter
k	reaction rate constant
Θ	fractional surface coverage
d	diameter
RSH	alkylthiol
RS-Au	alkylthiol gold SAM
RS-AuNP	alkylthiol gold nanoparticle
TO	truncated octahedron
TEM	transmission electron microscopy
FTIR	Fourier transform infrared spectroscopy
DSC	differential scanning calorimetry
TGA	thermogravimetric analysis
NMR	nuclear magnetic resonance
D	diffusion coefficient
EPR	electron paramagnetic resonance
TEMPO	2,2,6,6-tetramethylpiperidine-1-oxyl
THF	tetrahydrofuran
TOAB	tetraoctylammonium bromide
TMS	tetramethylsilane
OCP	open circuit potential

List of Tables

1.1 Methods of creating mixed composition AuNPs 13
1.2 Acid/Base effects on extent of PER 18
1.3 Solvent effects on PER 18
1.4 Factors affecting the kinetics and thermodynamics of PER 25

2.1 Parameters used for TGA analysis of RS-AuNP 33
2.2 Parameters used for GC analysis of alkylthiol solutions 37
2.3 HPLC parameters for the analysis of alkylthiol and dialkyldisulphide solutions 39

3.1 Summary of Alkylthiol Place Exchange Reactions:$C_{12}SH$ with $C_{10}Au$-NP 50

E.1 Rate constants of disulphide exchange from second order Langmuir fittings 84

5.1 Characterization of AuNP samples used in this study 88
5.2 Kinetic data derived from application of second-order diffusion Langmuir rate law. 91
5.3 Rate constants of different sized AuNPs samples. 91
5.4 Mechanistic models applied to alkylthiol-for-alkylthiol and dialkyldisulphide-for-alkylthiol PER. 96

F.1 Rate constants of reaction of different incoming ligands with C_{10}-AuNP. 99

List of Figures

1.1 A typical ω-functionalized alkylthiolate self-assembled monolayer(SAM) 4
1.2 Methods to create 2D mixed composition SAMs 7
1.3 Phase diagram of binary mixed SAM. 8
1.4 A schematic of a truncated octahedron. 12
1.5 Observed trends in reaction endpoints in PER. 16
1.6 "Edges and Vertices" model of PER 17
1.7 Proposed mechanism of Au(I) mediated PER. 18
1.8 TEMPO-based disulphide. 19
1.9 Disulphide model of the PER. 20

2.1 NMR spectra of C_{10}AuNP. 34
2.2 TGA of C_{10}AuNPs 34
2.3 TEM image of a sample of of C_{10}AuNPs and image analysis by Matlab 35
2.4 Calibration plot of C_{10}SH and C_{14}SH using the GC. 38
2.5 Reaction of C_{12}SH with C_{10}S-AuNP using the GC. 38

3.1 Time progress of reactions of C_{12}SH with C_{10}-AuNPs. 49
3.2 Normalized reaction progress for data in Figure 3.1. 50
3.3 Place exchange reaction of C_{10}AuNP with C_{14}SH. 51

C.1 Reaction of C_{12}SH with C_{10}AuNP. 57
C.2 Reaction of C_{12}SH with C_{10}AuNP. 58
C.3 Reaction of C_{12}SH with C_{10}AuNP. 59
C.4 Reaction of C_{12}SH with C_{10}AuNP. 59
C.5 Reaction of C_{12}SH with C_{10}AuNP. 60
C.6 Reaction of C_{12}SH with C_{10}AuNP. 61
C.7 Reaction of C_{12}SH with C_{10}AuNP. 61

C.8 Reaction of $C_{12}SH$ with $C_{10}AuNP$. 62
C.9 Reaction of $C_{12}SH$ with $C_{10}AuNP$ at 6 different concentrations. . . . 62

D.1 Second order diffusion limited Langmuir kinetics fitted to data from Murray and co-workers 65
D.2 Second order diffusion limited Langmuir kinetics fitted to data from Zerbetto and co-workers 66

4.1 Reaction of C_{12} disulphide with $C_{10}S$-AuNP. 71
4.2 Reaction of one equivalent C_{12} disulphide onto $C_{10}S$-AuNP. 72
4.3 Proposed reaction scheme of thiol(A) and disulphide(B) PER. 73

E.1 1^{st} Order Fitting of 1 equivalent C_{12} Disulphide onto $C_{10}S$-AuNP. . . 77
E.2 Observed rate constant (k_{obs}) for concentrations observed. 77
E.3 2^{nd} Order Fitting of 1 equivalent C_{12} Disulphide onto $C_{10}S$-AuNP. . . 78
E.4 1^{st} order Langmuir fitting of 1 equivalent C_{12} disulphide onto $C_{10}S$-AuNP 79
E.5 2^{nd} order Langmuir fitting of 1 equivalent C_{12} disulphide onto $C_{10}S$-AuNP 80
E.6 1^{st} order diffusion Langmuir fitting of 1 equivalent C_{12} disulphide onto $C_{10}S$-AuNP 80
E.7 2^{nd} order diffusion Langmuir fitting of 1 equivalent C_{12} disulphide onto $C_{10}S$-AuNP 81
E.8 Reaction of C_{12} disulphide onto $C_{10}S$-AuNP (0.33 equivalents). 81
E.9 Reaction of C_{12} disulphide onto $C_{10}S$-AuNP (1 equivalent). 82
E.10 Reaction of C_{12} disulphide with $C_{10}S$-AuNP (3 equivalents). 82
E.11 Reaction of C_{12} disulphide onto $C_{10}S$-AuNP 1 equivalent 83

5.1 Reaction of C_6, C_8, C_{12} and C_{14} alkylthiols with C_{10}-AuNPs. 89
5.2 Reaction of C_{10} and C_{14} alkylthiols with C_6-AuNPs. 90
5.3 Reaction of C_6 and C_{10} alkylthiols with C_{14}-AuNPs. 90
5.4 Reaction of C_{12} alkylthiol with three different core sizes of C_{10}-AuNPs. 92
5.5 Proposed scheme of alkylthiol and dialkyldisulphide reaction with alkylthiol-capped AuNPs 95

F.1 Addition of alkylthiols to 3.5nm and 2.0nm AuNP samples. 100

6.1 Proposed reaction scheme of thiol exchange on AuNPs 102

CHAPTER 1

General Introduction

The rapidly expanding field of nanoscience has been driven by key advances in characterization (STM/AFM, HR-TEM), fabrication(μ-contact printing, lithography) and synthetic methods (thin films, nanoparticles). The unique manner these nanometer length structures interact with light, behave in solution, and enhance structural properties allow scientists new ways to address fascinating problems in electronics devices, sensing, medical imaging, etc.[1] From better sensors to new catalysis substrates, the applications envisioned of these materials are vast.

In order to create reproducible and robust materials for these applications the knowledge of how to manipulate and characterize these systems has become crucial.

Nanoparticles (NP; semiconductor, metallic) have been applied to a wide variety of applications because of their facile synthesis, remarkable optical properties, unique size, and surface chemistry. Synthetic methods have been reported to create nanoparticles which are monodisperse($\pm$5%) and range from 0.6 to 100 nm in diameter. They are composed of a range of elements (Au, Ag, Pt), alloys (FePt, PbBi, CoCu) and semiconductors (CdSe, CdTe, HgTe).[2] Depending on the core composition, many of these nanoparticles (NP) have unique optical properties. Many NP strongly luminesce (in both conventional 'down-converting' and unconventional 'up-converting' senses), exhibit intense localized surface plasmon resonance adsorbtions,[3] and even are magnetic when the original material is non-magnetic.[4] Critical to all these properties is the ability to manipulate the surface ligands of these NPs. Surface ligands are invaribly necessary to modulate the NP's solution solubility and stability, but also allow one to use the NP core as a scaffold to introduce ligands with added functionality for applications in sensing, redox activity, drug delivery, etc. A critical factor

in the development of NP systems is the ability to characterize and manipulate their surface ligands.

While many ligand systems have been used and studied, the NP system for which the most is known is the Au-alkylthiol(Au-RS) system. The first reported Au thiol NP synthesis(1994)[5] was eleven years after the surface chemistry of 2D(flat) Au-RS systems was introduced.[6] The 2D system, usually described by the label 'self-assembled monolayers' or "SAMs" has been one of the most intensively studied nanosystems, with ca. 500 papers published from 1983 to 1994, and further ~2000 papers published since 1994. Not only are these systems well-studied, several advances have utilized Au-RS based NP systems for improved sensors for DNA[7] and trace element detection[8] with sensitivity orders of magnitude better then current methods. Several research groups have additionally investigated thiol-AuNPs to deliver and release drugs into cells.[3]

Despite these systems potential for novel applications, little is known about the surface chemistry of AuNP. Of particular importance is the lack of knowledge about the mechanism and kinetics of ligand replacement. This crucial step in the creation of these systems is needed to fully exploit and understand the limitations of these NP systems.

Before tackling this crucial and timely problem, a summary of the field will be presented. An overview of the 2D Au-RS SAM system will be presented, followed by a description of current understanding of that system. The AuNP synthesis methods and the understanding of their creation and manipulation will then be described.

1.1 2D SAM

Alkylthiol SAMs on Au surfaces were first reported by Nuzzo et al. in 1983.[6] Papers in the late 1980s on the analysis and a more thorough characterization by Whitesides and coworkers revealed that alkylthiol SAMs had great potential as a nanotechnology platform.[9, 10] Although a detailed review of 2D alkylthiol SAMs is beyond the scope of this Thesis, it is intimately related to the field of alkylthiol-protected AuNP. Hence a brief summary of the important characteristics and properties of 2D Au-RS SAM is provided in the following. Readers are directed to some excellent reviews for further information on the 2D SAM system.[10, 11]

1.2 Creation of 2D Au-RS SAM

Au-RS SAMs can be created from either the solution or gas phases. Solution-phase preparation is preferred for its simplicity, though the use of solvent complicates the SAM formation. Although still under debate, the most widely accepted chemical reaction for SAM assembly is:

$$RSH + Au_n \longrightarrow RS^- Au^+ Au_{n-1} + \frac{1}{2} H_2 \tag{1.1}$$

No reports have directly detected the formation of H_2 during monolayer formation. However, SAMs formed from dialkyldisulphides are identical to those from alkylthiols as determined by several techniques.[12] Because deuterated thiol groups show no measurable change in the kinetics of formation and final monolayer properties, breaking of the H-S bond is not rate-limiting in the monolayer formation process.
A great deal of research has lead to the following understanding of Au-RS SAMs:

i) Au-S bond strength is 40-50 kcal•mol^{-1}[13, 14]

ii) Ordering of absorbed thiolates is driven by interchain van der Waals forces(1.5-2 kcal•mol^{-1} per CH_2 unit)[15]

iii) Surface density is ca. 4.5 $\times 10^{14}$ molecule•cm^{-2}[16, 17]

iv) Spacing between adjacent surface layers(4.99 Å) is greater than the closest approach between alkyl chains (4.24 Å). This results in a tilt of RS chains (30° to the surface normal for Au(111))[18]

v) XPS spectroscopy measurements have shown that charge of $\sim = 0.2e^-$ resides on the sulphur atom[19, 20]

Figure 1.1 shows the currently accepted schematic of the Au-RS SAM system and provides a reference for both nomenclature and properties of these systems.

1.2.1 Kinetics of 2D SAM Formation

The formation kinetics of RS-Au SAMs have been studied using second-harmonic generation[21], ellipsometry[9], quartz crystal microbalance[22], surface plasmon resonance spectroscopy[23, 24], scanning probe microscopy[25], and interfacial capacitance.[26] The kinetics of SAM formation reported in many publications is approximated by

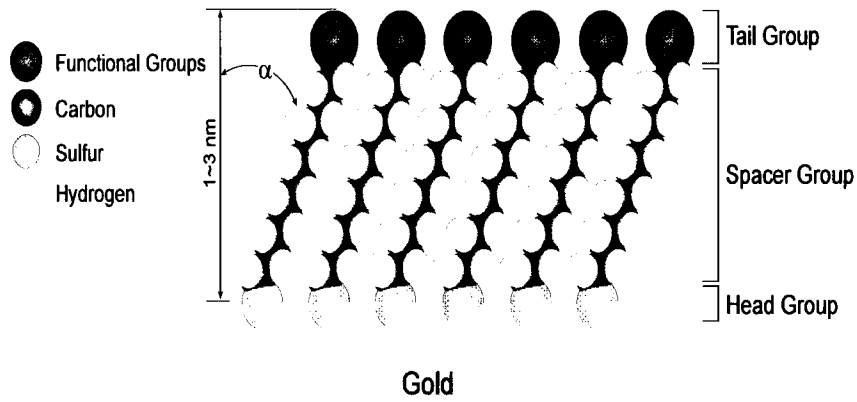

Figure 1.1: A typical ω-functionalized alkylthiolate self-assembled monolayer(SAM)

Langmuir adsorption kinetics.[21–26] However, not all reports agree as to the specific type of adsorption kinetics applicable to SAM formation. Grunze studied SAM formation from a variety of alkane solvents and ethanol and found that they could be approximated by a first-order Langmuir adsorption process.[21] Georgiadis studying the formation and exchange(with HO-C_6SH) of HS-C_6-ssDNA reported that a diffusion-limited Langmuir model with a desorption term was appropriate.[24] Finally, Jennings found that the adsorption kinetics of aqueous micellar C_{10}SH solutions obeyed second order diffusion-limited Langmuir kinetics.[26] It is apparent that Langmuir kinetics are often appropriate when discussing the adsorption of alkylthiols on Au. The particular type of Langmuir kinetics depends on the nature of ligands used and whether secondary effects such as chain-chain interaction, chain packing and solvent solubility (desorption) have a significant effect on the overall process.

1.3 Mixed Composition 2D Au-RS SAMs

1.3.1 Methods to Create Mixed Composition 2D SAMs

The methods used to created mixed alkylthiol SAMs are very relevant to this Thesis. These methods are analogous to the methods used in AuNP derivatization

(see Section 1.6). Because the 2D gold SAMs have been studied in much more detail they give an important reference point in this related system.

There are 5 main methods to create mixed composition SAMs. Each method has its own advantages and disadvantages

i) Co-adsorption of thiols(parallel derivatization):
This is by far the simplest method to create monolayers composed of two or more thiols. Thiols are pre-mixed in solution, before exposure of the substrate to the solution. The major drawback is that the solution composition is not necessarily(and indeed is often not) reflected in the monolayer composition.[27, 28] While the initial stage of monolayer formation is kinetically limited, the time needed to form a monolayer exhibiting close-packed characteristics is often hours, in which case surface-bound alkylthiols most certainly exchange with the alkylthiols in solution in this time regime(see point iv) below).[29]

ii) Sequential adsorption of thiols(serial adsorption):
SAMs formed with short incubation times and/or dilute solutions tend to fill the surface incompletely. These 'vacant sites' can then be filled with a second thiol. Unfortunately exchange kinetics normally begin when the second thiol is introduced in solution(see point iv) below), replacing some of the pre-existing thiol monolayer. This leads to difficulties in making reproducible binary SAMs.

iii) Adsorption of asymmetric disulphides:
A method used to overcome the difficulty of exchange kinetics involves linking the two thiols as an unsymmetric disulphide before introducing them to the substrate (provided of course that the two R groups are chemically similar). This method allows creation of monolayers with a 1:1 ratio of two different thiols on the substrate. The difficulty then is the synthesis of the unsymmetric disulphide and the inability to access a ratio other than the 1:1 stoichiometry provided by the disulphide.

iv) Exchange of a pre-existing monolayer(place exchange reactions):
Thiols in solution will exchange with surface bound alkylthiols in SAMs. In 2D systems the kinetics follow an initial fast reaction (minutes-hours) followed by a slow-plateau type stage(hours-days). The plateau is indicative of a equilibrium type process.[16] Studies by STM and electrochemistry have shown that the

reaction is mediated by defects in the SAMs such as domain boundaries in the underlying gold structure.[30, 31]

v) Reactions on a pre-existing monolayer(post-synthesis derivatization):
Alkylthiols which have already formed a SAM can be modified via conventional reactions at the terminal or other positions in the chain. These reactions have a range of yields which can lead to a SAM derivatized with both the initial thiol, and portions of which that have been converted to other terminal groups.

Figure 1.2 summarizes the 5 methods outlined above in schematic form.

1.3.2 Phase properties of 2D SAMs

In the 2D SAM case, Whitesides and coworkers showed that there is a strong driving force for SAM formed from a binary mixture to remain as a single domain structure, i.e. there is a strong preference for one of the two alkylthiols to form the SAM. In the case of hydroxy vs. methyl terminated thiols, the SAM phase diagram shows an abrupt switch from 100 % alcohol to 100 % methyl as the solution ratio of the alcohol:methyl alkylthiols approaches 100:1.[27, 28] as shown in Figure 1.3. This phase diagram presents an obvious problem that can only be overcome by knowing the kinetics of the reaction, and ideally stopping it before it reaches its thermodynamic endpoint. The binary phase diagram has been established for only a small number of RS pairs, and is further complicated by the fact that the kinetics needed to achieve a thermodynamic equilibrium are also highly dependent upon both the solvent and the particular alkylthiols used.

1.3.3 Mechanism and Properties of Exchange Reactions in 2D SAMs

Longer chain alkylthiols adsorb preferentially cf. shorter chain thiols.[27] This is clearly a thermodynamic effect. However, the timescale necessary to achieve the equilibrium can be long. Most alkylthiol mixtures are kinetically trapped due to the long time necessary for exchange reactions to reach the equilibrium state.[31] Although the initial stage of monolayer formation is a kinetically defined, the stoichiometric endpoints can be reached with prolonged reaction times and/or elevated temperatures.[28] The phenomenon of long chain length preference is usually rationalized by the relative solubilities of the two alkylthiols in solution. For example,

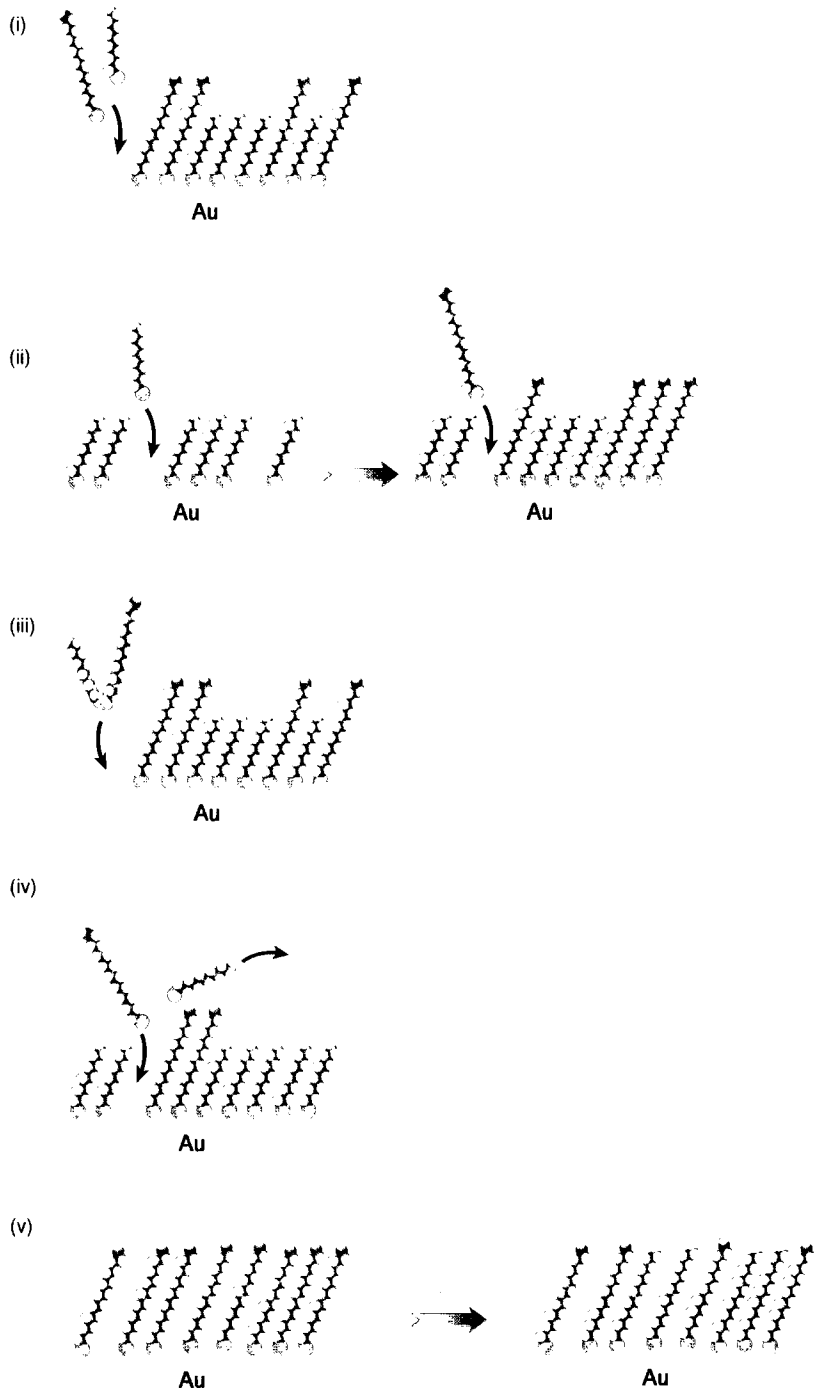

Figure 1.2: Methods to create 2D mixed composition SAMs: i)absorption of unsymmetric disulphides ii)co-absorption of thiols iii)sequential absorption of alkylthiols iv)place exchange reactions v)post-synthetic derivatization

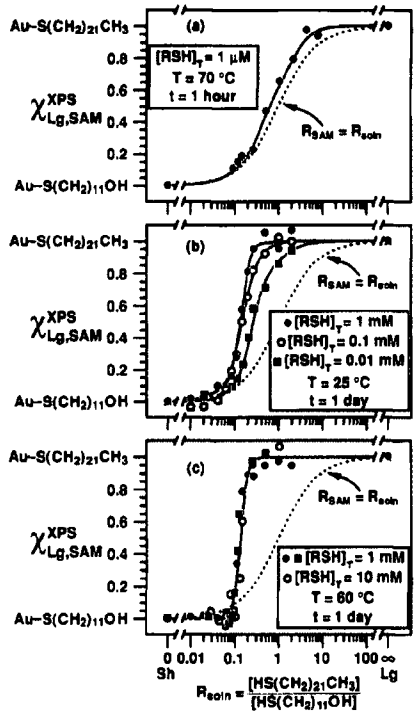

Figure 1.3: Phase diagram of binary mixed SAMs of $HS(CH_2)_{21}CH_3$ and $HS(CH_2)_{11}OH$ formed from ethanolic solution. Dotted curves indicate ideal phase behaviour. Reprinted from [28]. Copyright 1994 American Chemical Society.

longer chains are less soluble in ethanol, and hence their free energies in solution are less negative, leading to a higher affinity for adsorption.[32]

Monolayers of alkylthiols and disulphides form the same quality of SAM.[27] Alkylthiols however react much faster than disulphides in exchange reactions.[9]

Design of mixed composition alkylthiol SAMs thus requires knowledge of kinetics of the reaction because attainment of the thermodynamic state is complex. The problem with this approach is that the mechanism and even kinetics of the reaction are poorly understood. A complexity in understanding the mechanism is that there are likely a number of low-lying (free energy) states of similar value. It is thus relatively easy for a given binary SAM system to reside in a shallow free energy minimum state. Furthermore, these questions require the use of different techniques to examine the reaction. Each technique either modifies the experiment and/or the measurement. Schlenoff and co-workers have used ^{35}S labelling techniques to track the exchange reaction of 2D SAMs and thus chemically identical thiols.[16] The experiments showed that alkylthiols will spontaneously desorb into solution from a 2D SAM, and that

the amount desorption depends on the solvent used (THF, ethanol, water among others). The desorption occurs over the same time scale as the exchange process. The quantity of desorption correlates with the solubility of the alkylthiols. The most probable desorption species is a disulphide, since desorption occurs in aprotic solvents as well. Replacement of the monolayer with another alkylthiol is possible, but this reaction does not go to completion, unless the incoming thiol is added in huge excess (i.e. neat state) to the SAM.[16]

The emerging picture of Au-RS 2D SAMs is that the alkylthiol can remain attached to the Au surface if it is poorly soluble in the solvent used. Desorption occurs in a good solvent and in the presence of another alkylthiol this is accompanied by absorption of solution-based alkylthiols. Whether alkylthiols actively displace preformed monolayers (an associative-like mechanism) or if they simply fill in vacant (dissociative-like) or low coordination sites, is still being studied and debated. The answer to this question is of central importance to using, harnessing, and controlling the exchange reaction in both 2D and NP SAMs.

1.4 Gold Nanoparticles

Alkylthiol AuNP(RS-AuNP) are the 3D analogue of the 2D(flat) gold systems in many respects.[33] These NP have been sought after for their optical properties at the nanometer scale, and in application to drug delivery and sensing problems. Before going into the physical properties of these systems a short history of the synthesis of these materials will be presented.

1.4.1 AuNP Synthesis

The first reported synthesis of AuNP was by Faraday in 1857, who used a gold salt and reduced it with carbon disulphide.[34] Synthesis of relatively large (14 to 24 nm) AuNPs with a relatively narrow size distribution($\pm$10%) was reported by Turkevich in 1951[35] and improved upon by Frens in 1973.[36] The Turkevich/Frens syntheses used citrate as both reductant and capping agent and produce nanoparticles whose diameter is 5-100 nm. The next significant advance in synthesis of AuNP was that of the Au_{55} cluster pioneered by Schmid et al.[37] These researchers used diborane to reduce a gold salt, in the presence of triphenylphosphine. The phosphine served as a stabilizing ligand for the developing NP. These methods serve as routes to creating NPs of various sizes. However the subsequent NPs are not sufficently stable to survive

further manipulation or even drying and re-dispersion.

Brust-Schiffrin Synthesis

Brust and Schiffrin reported the first synthesis of alkylthiol-protected AuNP in 1994.[5] The method involves a two-phase reaction with toluene and water. Briefly, the reaction begins with phase transfer of a gold salt (typically $HAuCl_4$) from the aqueous phase into the organic phase using TOAB. Subsequent addition of an alkylthiol leads to reduction of the Au(III) salt into a Au(I) polymer[1] The Au(I) polymer is then reduced using an aqueous solution of sodium borohydride to yield alkylthiol protected AuNPs.

$$Au\,(III)_{aq} + TOAB \rightarrow Au\,(III)_{toluene} + TOA^{+}_{toluene} + Br^{-}_{aq} \quad (1.2)$$

$$Au\,(III)_{toluene} + C_nSH \rightarrow Au\,(I)\,(SC_n)_m \quad (1.3)$$

$$Au\,(I)\,(SC_n)_m + H^{-} \rightarrow C_nS - AuNP \quad (1.4)$$

The ratio of Au to alkylthiol used in the synthesis largely determines the particle size. Other factors such as temperature, reaction duration, and rate of reagent addition also effect the size and dispersity;[39] of these factors only temperature has a significant effect. Decreasing the reaction temperature allows smaller particles to be synthesized under the same conditions. This reaction methodology provides a route to AuNPs from 1.1nm to ~5nm but is limited in the type of ω-alkylthiols used for stabilization.[39] Heath and Gelbart[40] showed that the observed maxima and minima in size are related to the interplay between the alkylthiol's preference to exist as a monomer in solution and the free energy obtained by lowering the NP surface energy (which is dependant on the particle size.) At room temperature the minimum size is $\sim$ 1.6nm, and the maximum is around 5nm.
Several functionalized alkylthiols have been used in the Brust-Schiffrin synthesis. Many experiments[41] have established that the alkylthiols must:

- withstand the synthesis conditions, both strong oxidizing(from the Au(III) salt) and relatively strong reducing conditions($NaBH_4$)
- the alkylthiol and resulting NP must be soluble in toluene and not water

[1]This Au(I) polymer was later shown to be isolatable and characterizable. The polymer can then be re-dispersed and the synthesis can continue.[38]

In addition the Brust-Schiffrin synthesis requires a large excess of alkylthiol, that is subsequently removed by the repetitive washing of the solid NP mass.

Brust and Schiffrin also extended the range of thiols usable in the synthesis by performing the reaction in one phase using methanol, thus avoiding the use of the phase transfer agent TOAB.[42] Another important addition to the Brust-Schiffrin reaction was reported by Ulman and co-workers, who utilized Superhydride ($Li(C_2H_5)_3BH$) which allows the synthesis to take place in one phase using THF as a solvent.[43] This increases the range of ligands which can be used for AuNP protection but also excludes many ligands. The synthesis still requires an excess of alkylthiol, and is thus not suitable when costly or rare ligands are required.

Although good synthesis methods for the preparation of RS-AuNPs are available, techniques that expand the range of ligands and conserve their use are needed in order for these AuNPs to be able to be introduced to applications requiring specific NPs, often in 0.1-10g quantaties.

1.5 AuNP Properties

The molecule-to-bulk transition of AuNPs has been reported to occur in the range of 13 to 55 Au atoms, where Au_{13} is 0.5 nm in diameter and Au_{55} is 1.4 nm in diameter. AuNP larger than 1.4 nm exhibit metallic properties.[44] NP larger than $\sim$2.4nm possess a strong optical absorbance(due to their surface confined electrons) known as the surface plasmon resonance absorption.[3] This absorption maximum red-shifts with increasing particle diameter. Several powerful sensor platforms based on the reversible aggregation of AuNPs(see for example [7]) have been developed.

Compared to the 2-D RS-Au SAMs described in Section 1.1, alkylthiol-coated AuNPs offer ca. 10^6-fold more surface area($\sim 100 m^2/g$.) This enables many techniques such as FTIR, DSC, TGA, NMR to be used to study the SAM formed on these particles.[33]

C_{10}-AuNPs have a diffusion constant, D, of $\sim 2 \times 10^{-6}$ cm^2/s[45] which is ca. 4-fold slower than the estimated D, for $C_{10}SH$ (7.6×10^{-6} cm^2/s). [46]

Labelling alkylthiols with deuterium at various positions allows one to monitor the mobility of specific methylenes along the chain. The chain ends(C_n-CH_3 n>4) of alkylthiols tethered to AuNP have similar mobilities, using ^2H and ^1H NMR techniques, to that of free alkylthiols in solution, while those at the β position to the thiol group have very little mobility and are effectively locked. The methylenes from

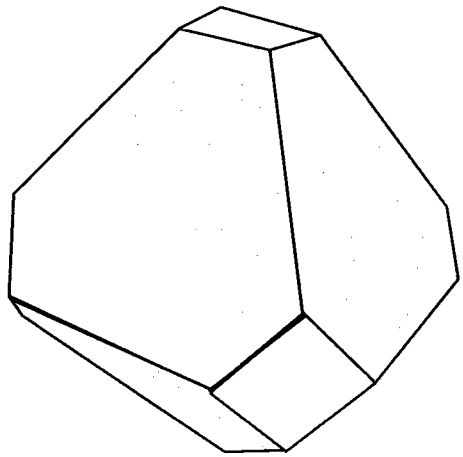

Figure 1.4: A schematic of a truncated octahedron.

the C_3 position along to the chain terminus exhibit an increasing (linear) mobility as they are further and further from the AuNP core. This mobility is strongly dependent upon the temperature and undergoes discontinuities similar to those observed at phospholipid membrane phase transitions.[33]

1.5.1 AuNP core properties

The exact nature of the gold core is a subject of great interest and importance. Whetten and co-workers have reported extensive studies using a combination of TEM and XRD data on the nature of the core and have shown that AuNP exist as faceted structures.[47, 48] The morphology for AuNP $\geq$ 1.4nm diameter is a regular truncated octahedron (TO). A computational study by Landman[49] concurred that AuNP should form truncated octahedron structures at Au_{140}. Landman's calculations also suggest that the RS chain packing on larger particles(Au_{1289}) should 'bundle' and RS chains on smaller particles(Au_{140}) should exhibit disorder at a specific temperatures[50]. DSC and NMR evidence is indeed consistent with concepts of chain bundling.[51] Analysis of 2D projection high resolution TEM images of 3D TO are also consistent with the Whetten TO description.[52]

1.6 Methods to Create Mixed Composition AuNPs

Analogous to the 2D Au-RS systems, several methods have been developed to create multifunctional AuNP.[53] Many reports use combinations of alkylthiols in the

synthesis procedure. However the solution ratio and the particle composition outcome are not necessarily the same.[54] Post-synthetic analysis of the NP's composition is thus required in almost all cases. An improvement was observed using unsymmetrical disulphides to create NP with a defined stoichiometric ratio.[54] This procedure however necessitates the purification and separation of the unsymmetrical disulphide starting materials, leading to another experimental problem. Moreover, it only leads to NP whose 2 ligands types exist in a 1:1 ratio. Table 1.1 provides a summary of the methods to create mixed composition AuNP.

Unlike the 2D system, where clean bare gold is experimentally achievable, 'naked' AuNP in solution are unstable. Methods that seek or rely on there being vacant Au surface sites are thus not practical. A range of ligands (citrate, phosphines, amines, alkylthiols) have varying binding strengths amenable to exploitation via exchange reactions. If there is insufficient solution concentration to maintain complete or near-complete coverage of the AuNP surface, then coalescence and/or precipitation of the NP will readily occur. Table 1.1 provides an overview to the methods used in stabilizing AuNP. Certainly the most commonly used and versatile method is the place exchange reaction (PER).

Table 1.1: Methods of creating mixed composition AuNPs

Method	Advantages	Disadvantages
Mixed thiols/ disulphides in synthesis	Potentially fast/easy	May require new cleaning method Requires excess thiols Reaction conditions may destroy ligands Final composition must be empirically studied
Post synthetic modifications	Low thiol usuage	Complicated Incomplete conversion (yields)
Place exchange reactions	Facile Mild reaction	May require new cleaning method No understanding of final composition Length of reaction

1.7 Place Exchange Reactions of AuNPs

The most used and flexible method to modify pre-existing AuNPs is the PER. Relatively few papers exploit the other *de novo* synthesis methods. There currently are two main strategies used in PER:

i) Pre-synthesised AuNP having weak-binding ligands(citrate, amine, phosphine) are reacted with less than stoichiometric quantities of the desired thiol ligand. Special care must be taken to maintain constant particle size. Purification often requires use of size exclusion chromatography[55–57]. The resulting AuNPs are often less stable than the starting material since not all ligands are thiols. If complete coverage of the surface by alkylthiols is obtained by addition of additional thiols(serial derivatization), the kinetics of the alkylthiol-for-alkylthiol reaction becomes relevant in this regieme. A detailed understanding of the mechanism is needed to rationally design AuNPs using this format of the PER.

ii) Synthesis of alkylthiol-protected AuNPs, followed by subsequent exchange with a second alkylthiol in solution. This reaction, thiol-for-thiol exchange reaction is the subject of this Thesis.

1.8 History of Thiol-Thiol Exchange Reactions on AuNPs

The subject of exchange reactions will be outlined. The first several publications that used this reaction are presented as a basis for discussing the overall field. Specific publications will then be discussed, grouped on the basis of the technique used to monitor the reaction.

The first report of a PER on AuNP was reported by the group of Royce Murray at UNC Chapel Hill.[58] Using $C_8$and C_{12}thiol-protected AuNP, Murray and colleagues reacted several different ω-functionalized thiols. Incoming thiols and the starting RS-AuNP were mixed in toluene for 24 hrs, after which the solvent was evaporated at room-temperature under vaccum. The resulting NP were purified by washing with ethanol to remove any free thiols (the free thiols are ethanol-soluble while the AuNP are not). ^{1}H NMR integration of the methyl signal of the initial alkylthiol and the ω-CH_2 protons of the incoming ligands leads to a quantitative tracking of reaction progress. IR spectroscopy and an electrochemical analysis of the exchange reaction of ferrocene-C_8thiols was used to confirm that the exchange reaction had indeed taken place.

A follow-up publication showed that it was possible to simultaneously exchange several alkylthiols onto RS-AuNP.[59] Although the different alkylthiols reacted at different rates, the relative ratios of the new RS ligands bound to the AuNP did not

vary with time, consistent with there being thermodynamic control of the reaction under these conditions.

A subsequent publication presented a detailed kinetic model and a proposed mechanism. A number of PER on AuNP were assessed by using ligands that have unique NMR signals. A variety of different alkylthiols and reaction conditions were tested. *In situ* observation of the reaction of a benzylthiol with a C_4S-AuNP showed that the reaction proceeds with a 1:1 stoichiometry. No evidence for other species in solution (such as oxidized sulphur species like sulphites or sulphates) were detected by NMR. The extent of reaction (after 96 hours) for the case where methyl-ester C_{12}thiol as the incoming ligand was monitored, with RS-AuNP ranging from C_4 to C_{16}. While complete displacement of short chain thiols(C_4SH) was observed, longer chain thiols (C_{12},C_{16}) showed increasingly less exchange over the same time period. This is consistent with previous work in the 2D RS-Au SAM literature,[27] and the fact that longer chain RS-AuNP are generally more stable over prolonged times cf. shorter chain analogues.[60] A model was proposed which used the 2D SAM exchange reaction, as a model, where the reaction occurs primarily at defect sites.[30] In the NP case such defects naturally reside at the edges or vertexes of the spherically symmetrical crystal. A reverse exchange reaction (where RS-AuNP were reacted with methyl-ester C_{12}SH for a short time and then re-reacted with RSH) was used to test this model. However it was not possible to 'exchange-off' all the methyl-ester C_{12}thiol ligands. This was attributed to the limitations of a surface diffusion process, where the ligands move from edges and verticies to more central(terrace) sites. The resulting model, refered to as the "edge and vertex" model (Figure 1.6) has dominated the literature and experimental interpretation since its first description in 1999.

The kinetics of the reaction are described in detail in Section(1.10). Interestingly Murray and co-workers do not correlate the thermodynamic and kinetic aspects of the experiments leaving open the question whether the observed trends in reaction rates are due to kinetic or thermodynamic factors.

A summary of experiments which seek to modulate the rate of PER, and thus provide insight into the reaction mechanism are now presented.

1.8.1 Reaction-Quench Kinetics

Quench techniques rely on the sudden termination of the reaction and subsequent analysis of the alkylthiol composition of the solution and AuNP. Quenching is performed at arbitrary intervals during the reaction course. Reaction-quench tech-

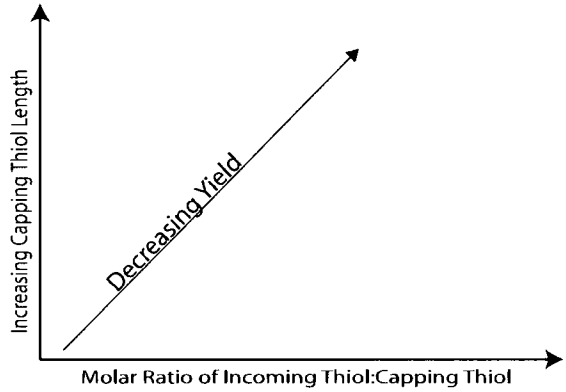

Figure 1.5: Observed trends in reaction endpoints in PER. Adapted from [61].

niques require access to an accurate and quantitative separation of the alkylthiols initially residing on the AuNP. This in turn requires an appropriate solvent such that the AuNP precipitate and the free alkylthiols(i.e. non-Au-bound) remain in solution. The precipitation step is necessary because the NP of interest are too small to be removed by centrifugation or filtration.

NMR spectroscopy

Murray et al. have extensively used the quench technique coupled to NMR analysis. Of note is their study of AuNP's ability to act as redox active species[62, 63] as a means to modulate the PER kinetics. A NMR decomposition technique was used to assess the kinetics when using electrochemically-derivatized C_6AuNP.[64] To improve their reaction assessment, the authors liberated the thiols attached to the purified AuNP by exposing them to iodine.[65] This enables better quantitation in the NMR as the thiols unattached to AuNP give sharper signals. AuNP that had been electrochemically oxidized exhibit faster kinetics and a greater extent of exchange. The 'apparent' equilibrium position of the reaction(the number of ligands exchanged after 20 hours) was assessed to test the effect of several solvents and so-called acid-base effects (Tables 1.2 and 1.3). This paper presented a number of experiments examining the many factors relevant to PER, but does not conclude with a model or complete description. These experiments along with others are summarized in Table 1.4.

Murray and co-workers also studied 'heterophase' ligand exchange reactions.[66] Reactions between organic-soluble C_6S-AuNP and water-soluble triponin protected AgNPs were investigated. Not only ligand transfer but also the transfer of gold

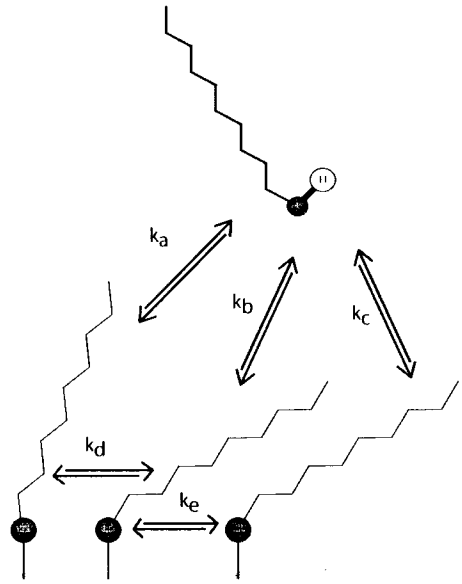

Figure 1.6: 'Edges and Vertices' model of PER, where $k_a >> k_b \geq k_d \geq k_e >> k_c$. Adapted from [61].

from the organic to aqueous phase occurs. This is postulated to be a Au(I) thiolate species. The deliberate addition of Au(I) thiolates to the reaction increases the rate of an exchange reaction between HO-C_6-SH and C_6S-AuNP. Moreover retardation or slowing of the PER in the absence of oxygen is noted. An attempt to unify several sets of results[58, 59, 61, 64] led to the formulation of a reaction model involving a Au(I) thiolate (see Figure 1.7).

Although the quench-based NMR technique is analytically effective it has rather specific requirements. Firstly, one has to be able to separate the solution thiols from AuNP which have bound alkylthiols. Secondly, chain-end chemical distinction is necessary for quantitation.

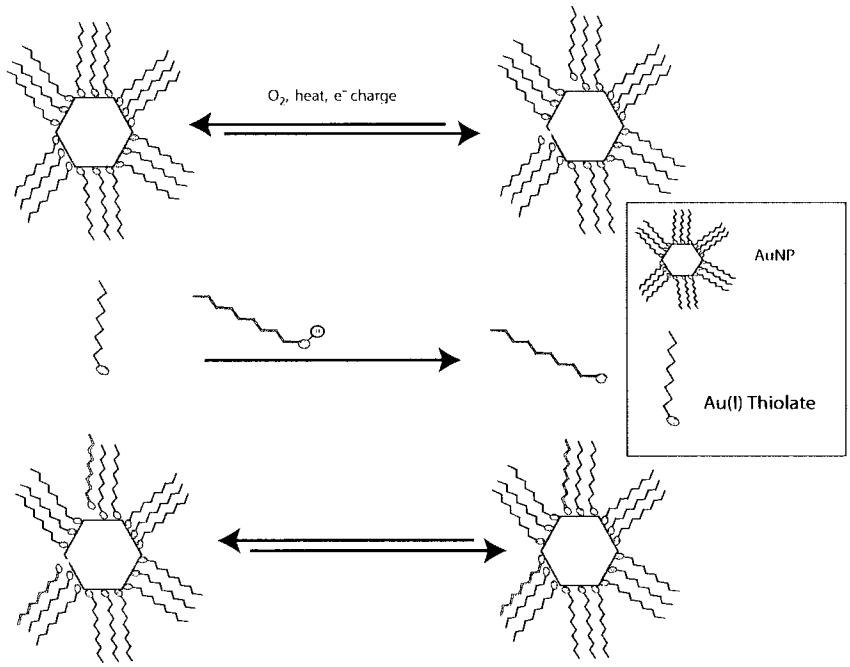

Figure 1.7: Proposed mechanism of Au(I) mediated PER. Adapted from [64].

Table 1.2: Acid/Base effects on extent of PER[a]

Additive	% of ligands exchanged
K^+t-BuO^-	80
Bu_4NClO_4	36
acetic acid	30
none	51

[a] Data taken from [64]. Reactions were performed under nitrogen in THF with C_6S-AuNP(charged to +1 state) with HO-C_6SH and reacted for 1 hour with a 2:3 mole ratio of incoming to bound ligand to bound ligand.

Table 1.3: Solvent effects on PER[a]

	% ligands exchanged	
Solvent	HSC_6OH	$HSC_{12}Br$
toluene	70	60
THF	55	43
methanol	53	0

[a] Data taken from [64], reactions were performed under nitrogen with C_6S-AuNP(charged to +2 state) using HO-C_6SH/$HSC_{12}Br$ ligands and reacted for 1 hour with a 2:3 mole ratio of incoming ligand.

1.8.2 In-Situ Techniques

A number of publications have attempted to circumvent the problem with quench/separation/identification by using direct, *in situ* analytical techniques. These techniques require ligands whose "signal" changes whether they are bound to a AuNP or are free in solution. This is advantageous because it allows for continuous data acquisition. It however invariably requires complex ligands. This complicates the studying of PER because such ligands introduce issues of chemical preference, confounding molecular interactions (attractive and repulsive), and differential solubilities. The following is a case-by-case description and discussion of the *in situ* techniques reported in PER mechanistic studies.

Electron Paramagnetic Resonance Labelling Techniques

The group of Chechik at the University of York (U.K.), have reported a series of experiments to explore PER kinetics using a TEMPO (2,2,6,6-tetramethylpiperidine-1-oxyl) modified disulphide (Figure 1.8).[67–70] This short chain disulphide is able to exchange a maximum of 5% of the ligands on a C_4S- protected nanoparticles, in a 48 hr period.[67] EPR spectroscopy allows for the monitoring of the progress of the ligand exchange since isolated radicals exhibit a triplet signal whereas coupled radicals (like that in the TEMPO disulphide) exhibit a quintet signal.

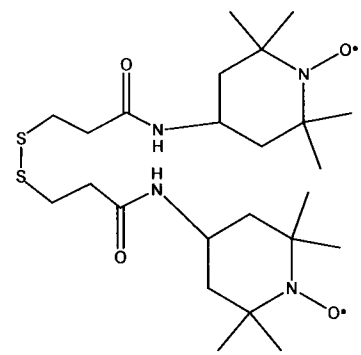

Figure 1.8: TEMPO-based disulphide used by the group of Chechik et. al. to monitor PER.[70]

The quantity of isolated probe increases as the PER proceeds. Deconvolution and integration of the peak allows one to monitor the reaction progress. These researchers worked only in pseudo first-order conditions (large excess of surface bound ligand with respect to the incoming ligand). The reaction was zeroth order with respect to the

incoming ligand (see also Section 1.10.) Because the EPR splitting of the TEMPO decreases during the reaction course it was postulated that the reaction proceeds through a mixed disulphide. This product was not isolatable in sufficient quantities for characterization.[67] In contrast to Murray et al.,[64] the Chechik group found that O_2 has no influence on the reaction rate, but that ageing (the amount of time the NP sample spends in solution after/during synthesis) reduces the rate greatly.[68] A mechanism was proposed whereby the rate limiting step is desorption of an activated alkyl sulphur species from the AuNP surface (Figure 1.9).

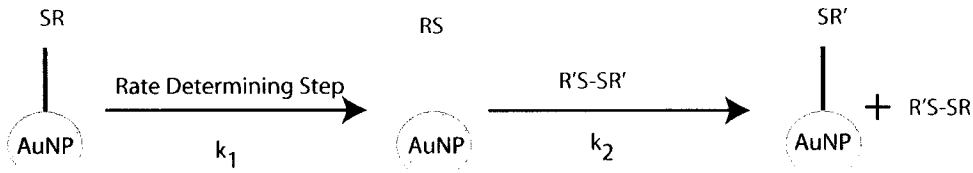

Figure 1.9: Disulphide model of the PER. Adapted from [70].

Fluorescence Labelled Alkylthiol Techniques

Two research groups have used fluorescently-labelled alkylthiol ligands to monitor PER.[71, 72] The fluorescence of a bound fluorophore is quenched due to its proximity to the gold core. Fluorescence signal recovery can be tracked as the PER proceeds if the flourophore is liberated into solution.

Zerbetto et al. used a pyrene-modified alkylthiol to create AuNP.[71] Monitoring of the recovery of the fluorescence signal in the presence of $C_{10}SH$ involved excess incoming ligand conditions(between 1:10 and 1:100 capping:incoming thiol ratio). This results in the reactions reaching the same final fluorescence intensity in the concentration range of incoming alkylthiol used and suggests that complete ligand displacement has occurred. The reaction progress curves were fitted to two consecutive pseudo first-order processes as proposed by Murray (since they are in excess incoming ligand conditions). The reaction has a non-unity (0.33) dependence on incoming thiol concentration. This is attributed to the size difference between the pyrene moiety and the methyl group of the alkylthiol, where several C_{10}alkylthiols molecules adsorb onto the particle for each pyrene-thiol liberated.

Rotello et al. studied the fluorescent signal recovery technique using a Bodipy-thiol ligand.[72] C_5S-AuNP were reacted with the Bodipy-thiol ligand to produce

particles with a 1:1 ratio of Bodipy-thiol to C_5thiol. These particles were then used as a starting material for PER with a series of different branched and unbranched C_4 and C_5alkyl thiol ligands. Although only the first ~60-120 minutes of the reaction were monitored, the reactions were observed to be sensitive to both chain packing and size of the incoming ligands. Chain packing on the surface was shown to reduce the rate of the reaction, but whether this was due to more thiols being displaced by a branched thiol or by its faster exchange rate was not evaluated.

NMR labelled alkylthiols

Two studies have used *in situ* NMR methods to track PER.[73, 74] PER on 1.6nm and 1.1nm AuNP were performed by using phenylethanethiol with different ρ-substituted functional groups. A pulse sequence was used to suppress the signal of the arylthiols bound to the AuNP. This allows one to monitor the PER in real time. The reaction rates and final number of exchanged arylthiols vary depending on the different substitutes. Electron-withdrawing substitutes increase the rate of reaction yielding a positive ρ value in a Hammet plot.[74] The main difference between the large(1.6nm) and small(1.1nm) NP is that the total number of ligand exchanges and the faster rate occurs with the smaller NP. The small NP in fact undergo almost complete exchange. This enables the 'reverse' exchange, where the ρ-substituted phenylethanethiol is initially bound to the AuNP and is exchanged for a phenylethanethiol and yields the same substituent effect (i.e. AuNP with increasing electron withdrawing ligands react faster) in both senses. This implies that the rate determining step in PER involves changes in the bonding of both the incoming *and* outgoing ligands. Thus it appears that both incoming and outgoing ligands play a role in the reaction kinetics and thermodynamic endpoint.[73] This is contrary to previous models where only at long times do capping ligands affect the rate. In this case smaller NP[74] also appear to have a faster reaction rate, although it is difficult to be definitive because only two data points (nanoparticle sizes) were reported.

1.9 AuNP with Mixed Composition Capping Ligands

Although the problem of forming mixed composition AuNP is still a relatively new field, several high profile publications have appeared, emphasizing structural details. The first set of papers by Stellacci and co-workers (MIT)[75, 76] contend that

the capping layer on AuNP formed from 2 or more alkylthiols spontaneously arrange themselves into ordered structures of 'stripes and/or ribbons.' In creating the particles using the Brust-Schiffrin synthesis the authors assume (without performing the requisite analysis) that the mixed RS-AuNP composition is the same as the stoichiometry used in the synthesis, even though previous reports suggest that this will not be the case.[54] Drawing heavily upon geometrical arguments Stellacci et al., contend that the minimum energy of NP ligand arrangement involves these stripe or ribbon configurations. The evidence for these capping layer structures comes from STM images and the apparent solubility of the resulting NP. The STM data are difficult to interpret since imaging 'floppy' organic molecules is complex. Compounding the difficulties in image interpretation is the highly curved surface of the AuNP surface. Stellacci et al. use an empirical solubility scale[75] to correlate qualitative solubility observations to proposed capping layer geometries. The details and underlying assumptions of this correlation are not evident in the publication.

Workentin and Donkers studied the rate of some organic photo reactions on ω-functionalized thiols tethered to AuNP.[77] They draw on the "edge and vertex" model of the PER(Figure 1.6) although Murray himself has never shown any proof of this mechanism (in fact his own test of this model have failed).[61] These researchers use it to create NP whose alkylthiol ligands are believed to reside at highly specific positions such as edges, vertices, and facets. The RS-AuNP were subsequently taken through Norrish type II reactions and the yields/rates were interpreted in the context of reagents being preferentially localized at edge vs. vertex vs. facet positions. It was reported that facet(terrace) ligands react more slowly then those on edges/vertices. A greater reactivity of small(1.8nm) AuNP versus larger(4.5nm) AuNP was observed. This is presumably because of the greater number of facet-bound alkylthiols expected on larger NP.

1.10 Kinetics of Place Exchange Reactions on AuNP

Key elements in elucidating a reaction mechanism are the trapping or direct observation of a reactive intermediate and/or determining the relationship of reaction progress to a kinetic model. Attempts to isolate or detect a reactive intermediate on the reaction pathway in there PER have not been successful. Many studies of PER have therefore related progress curves to mechanistic schemes. These are outlined and evaluated in the following.

1.10.1 "Edge and Vertex" Model

The first paper to study the kinetics and mechanism of the PER was the detailed study of Murray et al. in 1999.[61] This study provides the basis for many subsequent reports[64, 71, 73, 74]. The PER showed an initial fast rate of ligand replacement followed by an approach to an apparent plateau. However, a complete levelling off does not occur in the timeframe of the experiment. The initial rate was observed to vary with the amount of incoming thiol and was fitted to a first order rate law (ν=k[alkylthiol]). However a plot of the initial rate vs. concentration exhibits a non-zero intercept(contrary to the expectation of a first order process). The slow 'second phase' of the reaction combined with the fast 'first' phase suggested an overall reaction involving two processes with two rate constants.

$$\nu_1 = k_1 \, [incoming\ thiol] \qquad (at\ short\ times) \tag{1.5}$$

$$\nu_2 = k_2 \, [incoming\ thiol] \, [capping\ thiol] \quad (at\ long\ times) \tag{1.6}$$

In this model (Figure 1.6) the initial alkylthiol absorption occurs at defect sites on the AuNP surface (i.e. vertices, edges.) The alkylthiols subsequently move from the less reactive terrace sites to the reactive edge and vertex sites in the surface in the slower, 'second phase' of the overall reaction. Subsequent publications from the Murray group applied this reaction scheme to interpret additional kinetic results. The 2002 study,[64] which presented the evidence for the involvement of a soluble Au(I) thiolate in the reaction, suggested that this species is responsible for the non-zero intercept in the rate vs. [ligand] plot.

In situ NMR-derived data were also fitted to this model.[73, 74] The first such study (concentrating on 1.6nm p-arylthiol AuNP) correlates the fitted second-order rate constants and the Hammett substituent parameter, σ, leading to a linear relationship. At shorter reaction times however, the sense of the LFER relationship is reversed. This apparent contradiction (between reaction rates at short and long times and the electron donating/withdrawing nature of the ligands) is explained by elaborating on their previous model, citing proposed differences in the nature of the Au-S bond at different sites (edges vs. terraces). In the follow-up study[74] (concerning 1.1nm p-arylthiol AuNP) the authors seek whether there is a LFER. In this case there is however no distinct LFER.

Zerbetto's group fitted *in situ* fluorescence data at 4 different incoming thiol

concentrations using the Murray "edge and vertex" model (see Section 1.8.2). Since these data involve high ratios of incoming to capping ligand, the kinetics are fitted to two consecutive first-order processes. The dependence of the rate on concentration is not linear(i.e. $k_1 \alpha [incoming\ thiol]^n$ where n$\neq$ 1). This non-integral dependence is attributed to a cooperative dissociation whereby several incoming ligands absorb for each capping ligand desorbed (see Section 1.8.2). The authors do not however examine whether the coverage has changed during the PER.

While certainly the most used and cited model of PER, the Murray "edge and vertex" model has not been well supported by literature data. Many tests of its validity have failed and indeed at times the authors themselves have attempted to propose other models to explain their results.

1.10.2 Chechik Model

The results derived from the in-situ EPR probe work of Chechik et al. are contrary to those of the edge/vertex model. A zeroth order dependence in initial rate on the incoming ligand is observed (although the reaction conditions always involve small numbers of incoming ligand.) By working in pseudo-first order conditions, a simple model based on near-surface disulphide exchange can be derived.

$$\nu = -k_1 \times [capping\ thiol] \times \frac{[incoming\ disulphide]}{[incoming\ disulphide]_o} \tag{1.7}$$

This model was (qualitatively) tested in several experiments. The reaction profiles provide a reasonable fit to the model, but the authors do not perform experiments to see if the rate constant is constant. It appears by their own account that this model is lacking given the statement: "Our simple kinetic was not intended to adequately describe this complexity. Instead, we attempted to unravel some basic details of the main reactions taking place in this system. "[67] The basic difficulty in using those relatively nonreactive disulphides, and always working in pseudo first-order conditions means that this model is difficult to assess.

There have been numerous studies involving PER which show effects by various factors on the rate, these are summarized in table 1.4 below:

Table 1.4: Factors affecting the kinetics and thermodynamics of PER

Factor	Particle	Incoming Ligand	Effect
N_2 vs. air	C_6S-	C_6OH	Lower conversion after 1 hr[64]
Air vs. argon	C_4S-	Tempo Disulphide	No effect [68]
Au(I)salt	C_6S-	C_6OH	Higher conversion after 1 hr[66]
Oxidative charge	C_6S-	C_6OH	As AuNP formal charge ↑, exchange is faster/more complete [64]
Acid/Base effects	C_6S-	C_6OH	More exchange after 1 hour in basic conditions[64]
Solvent polarity	C_6S-	C_6OH	Lower conversion after 1 hr as polarity increased[64]
		$C_{12}Br$	Lower conversion after 1 hr as polarity increased (no reaction in methanol)[64]
Thiol capping ligand length	C_4S-,C_8S-,$C_{12}S$-$C_{16}S$-	$MeO_2CC_{11}SH$	Fewer ligands exchanged with ↑ increasing capping ligand length after 96h[61]
Electron withdrawing groups	Phenylethanethiol	ρ-X-Aryl-SH	More E.W.G. Accelerates (-OCH3 $\geq$ CH3 $\geq$ NO_2) [73]

1.11 Concluding Remarks and Outline of Thesis

Several mechanistic descriptions have been presented for PER. A consensus mechanism has not emerged. A viable kinetic model for the PER must explain both the kinetics of the reaction and the reaction endpoint. Surprisingly few published data sets actually correspond to the kinetic models discussed. The goal of the research summarized in this Thesis is to thus accurately measure the kinetics of the PER and propose a mechanism consistent with both the rate and product composition data.

Understanding the kinetics of the PER will enable scientists to create reproducible NP for the next generation of applications. Until this reaction is fully understood empirical techniques of particle derivatization must be used. Batch-to-batch variability is a serious issue, and only when all the variables that affect the reaction are known and controlled will the PER enjoy widespread use.

Understanding of PER on AuNP will enable creation of AuNP with prescribed ligand composition. It also provides insight into the stability of AuNP. In order for these systems to be used in the variety of chemical environments proposed in the literature, a key question is whether these particles will remain stable (aggregation, decomposition.) By understanding how and under what conditions thiols exchange on and off AuNP, the research should provide methods to create more stable particles.

This Introduction has presented the state-of-the-art of creating AuNP with mixed ligand composition. Research in the field is ongoing and many of the issues presented are under scrutiny. Despite the overall confusion in the literature regarding the kinetics and mechanism of this reaction, there are several agreed-upon facts:

- longer alkylthiol ligand capping layers are thermodynamically more stable than are shorter ones(see Figure 1.5)[61]
- when simultaneously absorbing more than one alkylthiol, the ratio of incoming thiols to one another over time is constant, indicating a thermodynamic equilibrium control of the reaction[59]
- a 1:1 replacement stoichiometry is operative, where for each thiol adsorbed, one thiol is desorbed.[61]
- there is no production of other species (oxidized(sulphites) or reduced(disulphides))[61]
- the reaction is very slow at room temperature where, for example with C6 AuNP it takes over 48 hours to achieve a steady state[61]

References

[1] Schmid, G., Ed.; *Nanoparticles: From Theory to Application;* Wiley-VCH: 2004.

[2] Park, J.; Joo, J.; Kwon, S. G.; Jang, Y.; Hyeon, T. *Ang.Chem. Int. Ed.* **2007,** *46(25),* 2453-2457.

[3] Daniel, M.-C.; Astruc, D. *Chem. Rev.* **2004,** *104,* 293-346.

[4] Yi, J. B.; Ding, J.; Feng, Y. P.; Peng, G. W.; Chow, G. M.; Kawazoe, Y.; Liu, B. H.; Yin, J. H.; Thongmee, S. *Physical Review B (Condensed Matter and Materials Physics)* **2007,** *76,* 224402.

[5] Brust, M.; Walker, M.; Bethell, D.; Schiffrin, D. J.; Whyman, R. *Chem.Commun* **1994,** 801-2.

[6] Nuzzo, R. G.; Allara, D. L. *J. Am. Chem. Soc.* **1983,** *105,* 4481-4483.

[7] Taton, T. A.; Mirkin, C. A.; Letsinger, R. L. *Science* **2000,** *289,* 1757-1760.

[8] Lu, Y.; Liu, J. *Acc. Chem. Res.* **2007,** *40,* 315-323.

[9] Bain, C. D.; Troughton, E. B.; Tao, Y. T.; Evall, J.; Whitesides, G. M.; Nuzzo, R. G. *J. Am. Chem. Soc.* **1989,** *111,* 321-335.

[10] Love, J.; Estroff, L.; Kriebel, J.; Nuzzo, R.; Whitesides, G. *Chem. Rev.* **2005,** *105,* 1103-1170.

[11] Schwartz, D. K. *Ann. Rev. Phys.Chem.* **2001,** *52,* 107-37.

[12] Biebuyck, H. A.; Bain, C. D.; Whitesides, G. M. *Langmuir* **1994,** *10,* 1825-1831.

[13] Nuzzo, R. G.; Zegarski, B. R.; Dubois, L. H. *J. Am. Chem. Soc.* **1987,** *109,* 733-740.

[14] Nuzzo, R. G.; Dubois, L. H.; Allara, D. L. *J. Am. Chem. Soc.* **1990,** *112,* 558-569.

[15] Ulman, A. *An Introduction to Ultrathin Organic Films: From Langmuir-Blodgett to Self-Assembly;* Academic Press:New York: 1991.

[16] Schlenoff, J. B.; Li, M.; Ly, H. *J. Am. Chem. Soc.* **1995,** *117,* 12528-12536.

[17] Widrig, C. A.; Alves, C. A.; Porter, M. D. *J. Am. Chem. Soc.* **1991,** *113,* 2805-2810.

[18] Dubois, L. H.; Nuzzo, R. G. *Annu. Rev. Phys. Chem.* **1992,** *43,* 437-463.

[19] Bourg, M.-C.; Badia, A.; Lennox, R. *J. Phys. Chem. B* **2000,** *104,* 6562-6567.

[20] Zhong, C.-J.; Brush, R.; Anderegg, J.; Porter, M. D. *Langmuir* **1999,** *15,* 518-525.

[21] Dannenberger, O.; Buck, M.; Grunze, M. J. *J.Phys.Chem.B.* **1999,** *103,* 2202-2213.

[22] Karpovich, D. S.; Blanchard, G. J. *Langmuir* **1994,** *10,* 3315-3322.

[23] Peterlinz, K. A.; Georgiadis, R. *Langmuir* **1996,** *12,* 4731-4740.

[24] Georgiadis, R.; Peterlinz, K. A.; Peterson, A. *J. Am. Chem. Soc.* **2000,** *122,* 3166-3173.

[25] Xu, S.; Cruchon-Dupeyrat, S.; Garno, J. C.and Liu, G.-Y.; Jennings, G. K.; Yong, T.-H.; Laibinis, P. E. *J. Chem. Phys.* **1998,** *108,* 5002-5012.

[26] Yan, D.; Saunders, J. A.; Jennings, G. K. *Langmuir* **2002,** *18,* 10202-10212.

[27] Folkers, J. P.; Laibinis, P. E.; Whitesides, G. M. *Langmuir* **1992,** *8,* 1330-1341.

[28] Folkers, J. P.; Laibinis, P. E.; Whitesides, G. M.; Deutch, J. *J.Phys.Chem.* **1994,** *98,* 563-571.

[29] Biebuyck, H. A.; Whitesides, G. M. *Langmuir* **1993,** *9,* 1766-1770.

[30] Bumm, L.; Arnold, J.; M.T., C.; Dunbar, T.; Burgin, T.; Jones, L.; Allara, D.; Tour, J.; Weiss, P. *Science* **1996,** *271,* 1705-1707.

[31] Chidsey, C. E. D.; Bertozzi, C. R.; Putvinski, T. M.; Mujsce, A. M. *J. Am. Chem. Soc.* **1990,** *112,* 4301-4306.

[32] Bain, C. D.; Whitesides, G. M. *J. Am. Chem. Soc.* **1989,** *111,* 7164-7175.

[33] Badia, A.; Lennox, R. B.; Reven, L. *Acc. Chem. Res.* **2000,** *33,* 475-481.

[34] Faraday, M. *Phil. Trans. R. Soc.* **1857,** .

[35] Turkevich, J.; Stevenson, P. C.; Hillier, J. *Faraday Discuss.* **1951,** *11,* 55-75.

[36] Frens, G. *Nautre* **1973,** *241,* 20-22.

[37] Schmid, G.; Pfeil, R.; Boese, R.; Brandermann, F.; Meyer, S.; Calis, G. H. M.; Van der Velden, J. W. A. *Chemische Berichte* **1981,** *114,* 3634-3642.

[38] Corbierre, M.; Lennox, R. *Chem. Mater.* **2005,** *17,* 5691-5696.

[39] Hostetler, M. J.and Wingate, J. E.; Zhong, C.-J.; Harris, J. E.and Vachet, R. W.; Clark, M. R.; Londono, J. D.; Green, S. J.; Stokes, J. J.; Wignall, G. D.; Glish, G. L.; Porter, M. D.; Evans, N. D.; Murray, R. W. *Langmuir* **1998,** *14(1),* 17-30.

[40] Leff, D. V.; Ohara, P. C.; Heath, J. R.; Gelbart, W. M. *J.Phys.Chem.* **1995,** *99,* 7036-7041.

[41] Araki, K.; Mizuguchi, E.; Tanaka, H.; Ogawa, T. *J.Nanosci.Nanotech.* **2006,** *6(3),* 708-712.

[42] Brust, M.; J.Fink,; D.Bethell,; Schiffrin, D. J.; Kiely, C. *J.Chem.Soc.,Chem.Commun* **1995,** 1655-1656.

[43] Yee, C. K.; Jordan, R.; Ulman, A.; White, H.; King, A.; Rafailovich, M.; Sokolov, J. *Langmuir* **1999,** *15(10),* 3486 - 3491.

[44] Chen, S.; Ingram, R. S.; Hostetler, M. J.; Pietron, J. J.; Murray, R. W.; Schaaff, T. G.; Khoury, J. T.; Alvarez, M. M.; Whetten, R. L. *Science* **1998,** *280,* 2098-2101.

[45] Wuelfing, W. P.; Templeton, A. C.; Hicks, J. F.; Murray, R. W. *Anal. Chem.* **1999,** *71,* 4069-4074.

[46] Jung, L.; Campbell, C. *Journal of Physical Chemistry B* **2000,** *104,* 11168-11178.

[47] Whetten, R. L.; Khoury, J. T.; Alvarez, M. M.; Murthy, S.; Vezmar, I.; Wang, Z. L.; Stephens, P. W.; Cleveland, C. L.; Luedtke, W. D.; Landman, U. *Advanced Materials* **1996,** *8,* 428-433.

[48] Whetten, R.; Shafigullin, M.; Khoury, J.; Schaaff, T.; Vezmar, I.; Alvarez, M.; Wilkinson, A. *Acc. Chem. Res.* **1999,** *32,* 397-406.

[49] Luedtke, W. D.; Landman, U. *J.Phys.Chem.* **1996,** *100,* 13323-13329.

[50] Luedtke, W.; Landman, U. *J. Phys. Chem. B* **1998,** *102,* 6566-6572.

[51] Badia, A.; Cuccia, L.; Demers, L.; Morin, F.; Lennox, R. *J. Am. Chem. Soc.* **1997,** *119,* 2682-2692.

[52] Corbierre, M.; Cameron, N.; Lennox, R. *Langmuir* **2004,** *20,* 2867-2873.

[53] Templeton, A. C.; Wuelfing, W. P.; Murray, R. W. *Acc. Chem. Res.* **2000,** *33,* 27-36.

[54] Shon, Y.-S.; Mazzitelli, C.; Murray, R. *Langmuir* **2001,** *17,* 7735-7741.

[55] Rucareanu, S.; Gandubert, V.; Lennox, R. *Chem. Mater.* **2006,** *18,* 4674-4680.

[56] Woehrle, G.; Brown, L.; Hutchison, J. *J. Am. Chem. Soc.* **2005,** *127,* 2172-2183.

[57] Woehrle, G.; Hutchison, J. *Inorg. Chem.* **2005,** *44,* 6149-6158.

[58] Hostetler, M.; Green, S.; Stokes, J.; Murray, R. *J. Am. Chem. Soc.* **1996,** *118,* 4212-4213.

[59] Ingram, R.; Hostetler, M.; Murray, R. *J. Am. Chem. Soc.* **1997,** *119,* 9175-9178.

[60] Weisbecker, C.; Merritt, M.; Whitesides, G. *Langmuir* **1996,** *12,* 3763-3772.

[61] Hostetler, M. J.; Templeton, A. C.; Murray, R. W. *Langmuir* **1999,** *15,* 3782-3789.

[62] Chen, S.; Murray, R.; Feldberg, S. *J. Phys. Chem. B* **1998,** *102,* 9898-9907.

[63] Hicks, J.; Miles, D.; Murray, R. *J. Am. Chem. Soc.* **2002,** *124,* 13322-13328.

[64] Song, Y.; Murray, R. *J. Am. Chem. Soc.* **2002,** *124,* 7096-7102.

[65] Templeton, A.; Hostetler, M.; Kraft, C.; Murray, R. *J. Am. Chem. Soc.* **1998,** *120,* 1906-1911.

[66] Song, Y.; Huang, T.; Murray, R. *J. Am. Chem. Soc.* **2003,** *125,* 11694-11701.

[67] Ionita, P.; Caragheorgheopol, A.; Gilbert, B. C.; Chechik, V. *Langmuir* **2004,** *20,* 11536-11544.

[68] Chechik, V. *J. Am. Chem. Soc.* **2004,** *126,* 7780-7781.

[69] Chechik, V.; Helen, J. W.; Korte, A.; Bruce, C. G.; Caldararu, H.; Ionita, P.; Caragheorgheopol, A. *Faraday Discuss.* **2005,** *125,* 279-91; discussion 293-309.

[70] Ionita, P.; Caragheorgheopol, A.; Gilbert, B. C.; Chechik, V. *J. Am. Chem. Soc.* **2002,** *124,* 9048-9049.

[71] Montalti, M.; Prodi, L.; Zaccheroni, N.; Baxter, R.; Teobaldi, G.; Zerbetto, F. *Langmuir* **2003,** *19,* 5172-5174.

[72] Hong, R.; Fernandez, J. M.; Nakade, H.; Arvizo, R.; Emrick, T.; Rotello, V. M. *Chem. Comm.* **2006,** 2347 - 2349.

[73] Donkers, R.; Song, Y.; Murray, R. *Langmuir* **2004,** *20,* 4703-4707.

[74] Guo, R.; Song, Y.; Wang, G.; Murray, R. *J. Am. Chem. Soc.* **2005,** *127,* 2752-2757.

[75] Jackson, A. M.; Myerson, J. W.; Stellacci, F. *Nat. Mater.* **2004,** *3,* 330-336.

[76] Jackson, A.; Hu, Y.; Silva, P.; Stellacci, F. *J. Am. Chem. Soc.* **2006,** *128,* 11135-11149.

[77] Kell, A.; Donkers, R.; Workentin, M. *Langmuir* **2005,** *21,* 735-742.

CHAPTER 2

Methods

2.1 Synthesis of Gold Nanoparticles

The one-pot facile synthesis of gold nanoparticles was first described in 1994 by Brust and Schiffrin.[1] This synthesis methodology was thoroughly characterized by Murray et al. in 1998.[2] The methodology is able to make 1.1 - 5.2nm AuNPs protected by ω-functionalized alkylthiols. Drawing on these two publications we have modified the procedure slightly to run the reaction faster. The following is a detailed methodology for a typical synthesis.

2.1.1 Synthesis 2nm $C_{10}SH$ stabilized gold nanoparticles

1g of $HAuCl_4$ hydrate salt (49.9 % gold) was dissolved in 50ml Millipore water in a 500ml round bottom flask. To this 4.23g (2.5eq) of tetraoctylammonium bromide (TOAB) dissolved in 200ml of toluene was added. The two-phase mixture was stirred for 20 minutes until the aqueous phase is clear (complete phase transfer of the gold salt.) 610 μl of $C_{10}SH$ (1eq) was added and the reaction was additionally stirred for 5 minutes. Drop-wise addition of 1.11g $NaBH_4$ (10 eq) in 50 ml Millipore water caused an immediate reaction causing the orange coloured organic phase to turn black indicating nanoparticle formation. The reaction was allowed to continue for another 3 hours. The organic phase was separated in a 500 ml seperatory funnel and washed 3 times with Millipore water, to remove all ions from it. The organic phase was then placed back into the 500 ml round bottom flask and rotovaced to near dryness. To the resulting thick black slurry(if rotovaced to dryness 20ml toluene was added) 300ml of anhydrous ethanol was added to precipitate the AuNPs while leaving any unreacted thiols in solution. AuNP were collected by vacuum filtration on a 60ml fine glass frit

Table 2.1: Parameters used for TGA analysis of RS-AuNP

Time	Temperature	Ramp °C/min	Notes
0	RT	40	
1.5	110	Hold	Ensure that all solvents used are evaporated
6.5	700	120	Removal of ligands
11.5	700	N/A	Ensure all ligands are removed

and also washed with 2x 50ml ethanol and 2x 50ml acetone(care must be taken to not allow the particles to dry on the frit). The waxy NP mass was then collected into a sample vial and left overnight in a dessicator to remove residual solvent.

2.1.2 Variation on Synthesis

Alkylthiol length

Alkylthiols from C_6 to C_{14} were used for particle synthesis. These were used with the above method, using the same molar ratio(Au:thiol.) Shorter chain alkylthiols yielded more powdery AuNP samples, while longer chains created more waxy-like samples.

AuNP core size

Smaller AuNP core sizes were synthesized by decreasing the Au:thiol ratio during synthesis(to 1:4) and completing the synthesis at 0 °C resulting in 1.7nm core NP. Larger particles were made at room temperature by increasing the Au:thiol ratio to 1:0.13, resulting in 3.5nm NP.

2.2 Particle Characterization

To ensure particles were free of residual thiols, a sample was subjected to ^{1}H NMR analysis (in d_6-benzene.) An absence of sharp peaks indicates removal of residual thiols, since thiols bound to the gold nanoparticle have their peaks broadened due to their slow rotation in solution.[2] This step is critical in the kinetics experiments as the rest of our procedure assumes that there are no free capping thiols in solution at t=0. An example of a NMR spectrum of clean C_{10}AuNPs is shown in Figure 2.1

The product's Au:thiol ratio was evaluated using thermogravametric analysis (TGA). 5mg of purified AuNPs were placed on an annealed platinum pan, and in a N_2 atmosphere heated to 700 °C using the procedure in Table 2.1. The final product after heating appeared to be pure gold (metallic and yellow.)

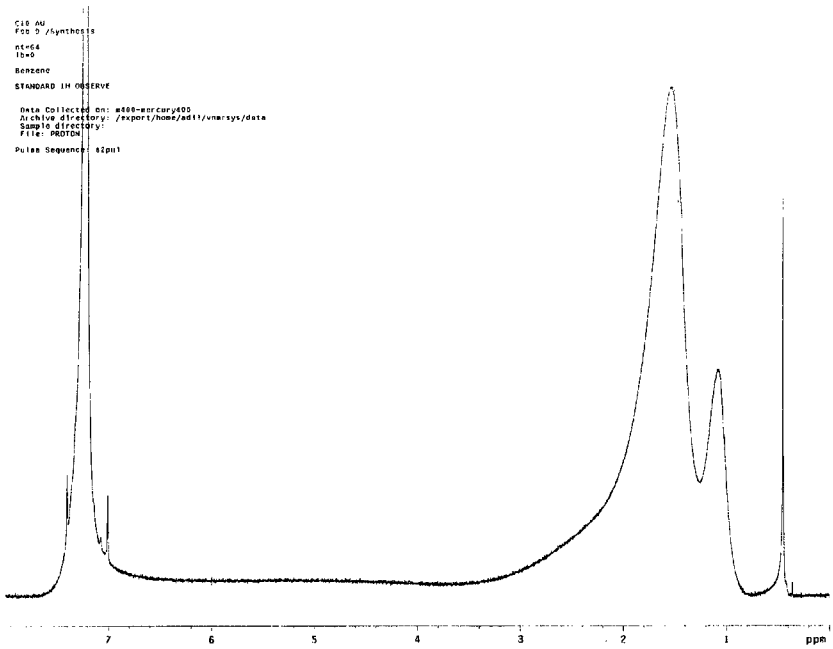

Figure 2.1: NMR spectra of C_{10}AuNP in d_6-benzene. Note that the peak at 0.4ppm is due to residual water.

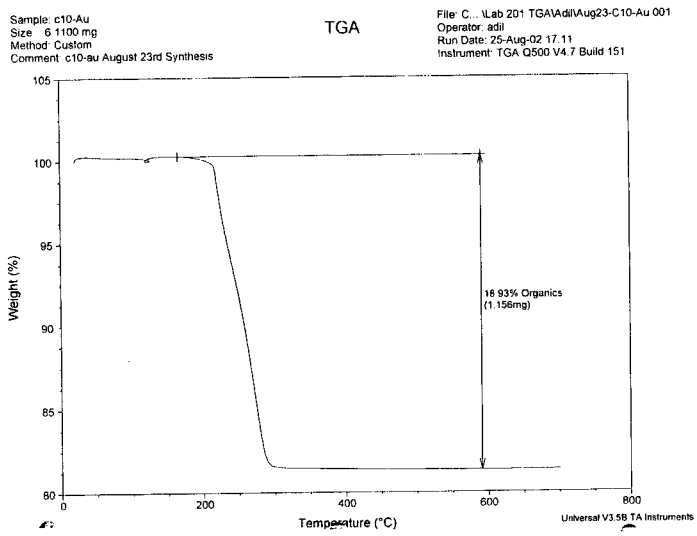

Figure 2.2: TGA of C_{10}AuNPs, the loss of mass is attributed to the burning of the organic ligands attached to the gold nanoparticle core.

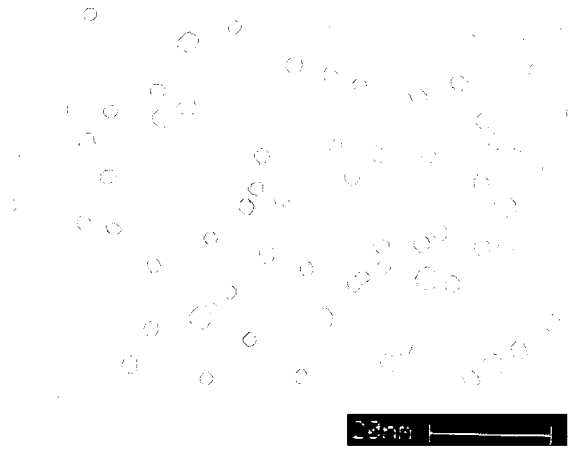

Figure 2.3: Left:TEM image of a sample of of C_{10}AuNPs. Right:Image analysis by Matlab, the red circles are the particle outlines found by the program.

Particle size was determined using TEM. A sample of particles is dispersed in toluene, a drop placed onto a Si/SiO grid, and then allowed to dry (by wicking) on filter paper. Images were obtained on a Philips CM200 transmission electron microscope using an acceleration voltage of 200 kV. The 3 in. $\times$ 4 in. negatives were scanned at a resolution of 300 dpi using an Epson 1200 photo scanner and its negative adaptor. The resulting images were evaluated using a custom written Matlab program utilizing DIPimage libraries.[1] The program utilizes a set of image filters(median, Laplace) before thresholding the image to obtain the particle area by pixels, which is converted to a diameter using the spherical approximation. Appendix A reports the program code. A minimum of 200 particles were counted to obtain the size and dispersion of nanoparticle samples. An example of the behaviour of the program for a particular sample is shown in Figure 2.3.

2.3 Evaluation of Place Exchange Reactions

All previous reports of PER kinetics relied on methods where the ligands were chemically different (e.g. by NMR, EPR or fluorescence.) These reporter groups change the chemical behaviour of the two thiols because of solution solubility and/or monolayer packing properties. Literature in the field of 2D SAMs has shown that these chemical properties (solubility, packing) can greatly influence the resultant composition of the monolayer (see Section 1.3.2). In order to simplify the study of PER we

[1] See http://www.diplib.org/

developed a methodology to simplify the exchange reaction by using ligands that are chemically similar.

The main experiment used by the Murray group involves a lengthy workup. Moreover the technique employed for analysis (^{1}H NMR) is not particularly sensitive nor accurate ($\pm$ 5 %) in terms of quantity. Indeed each datapoint requires user input to correct for the different vials used in analysis. Using error-prone data makes it difficult to evaluate rate laws; where the evalutaion procedure invariably involves fit-testing of data to a series of experiments.

Both GC and HPLC are able to differentiate alkylthiols with as little as one carbon change in chain length with high accuracy (baseline separation in both) and reproducibility ($\pm$ 1.5 %). Early reports indicated that the exchange of thiols had a 1:1 stoichiometry (later confirmed by our own experiments), which made it facile to use the solution concentrations as an indicator of particle composition.[4] The difficulty then is to be able to detect the alkylthiols at the concentrations typically employed in PERs (10mg/ml of AuNPs).

Our first attempts utilized C_{10}AuNPs with C_{14}SH using the quench technique of Murray[4]. After quenching 10ml aliquot of the reaction in 150 ml ethanol, the solution was filtered on a 60 ml glass frit and washed additionally with ethanol and acetone. The resultant clear solution was rotovaped to remove the excess solvent. The flask was then washed with 5ml of ethanol to dissolve the thiols remaining. This solution was then subjected to analysis by GC to yield the solution concentration of thiols. Due to the many steps in the workup, the error on the resulting solutions was large and difficult if not impossible to interpret.

Eventually we developed a method that yielded a high accuracy and was highly reproducible. The method is as follows. Solutions of 10 mg/ml C_{10}AuNPs were made up (in toluene for GC or hexane for HPLC analysis) at 25°C under argon. The reactions were initiated by syringe injections of the requisite amount of incoming ligand (thiol or disulphide) into the reaction vial. Data points are collected at regular intervals by precipitating 1ml aliquots of the reaction mixtures in 10 ml ethanol and separating the supernatant by filtration using a glass frit. The solution was transferred to a sample vial, suitable for analysis by GC or HPLC.

2.3.1 GC analysis of PER products

An Agilent 6890 GC fitted with a 5 % phenyl dimethylsiloxane column and a FID detector was used for analysis. Early experiments relied on manual injection of

Table 2.2: Parameters used for GC analysis of alkylthiol solutions

Thiol Pair	Initial Temperature(°C)	Initial Hold Time(min)	Final Temperature(°C)	Final Hold Time(min)
C_6, C_{10}	110	1.5	180	0
C_{10}, C_{12}	160	1	200	0.5
C_{10}, C_{14}	160	1	250	1
C_6, C_{14}	110	1.5	250	1
Common Parameters				
Parameter	Value			
Injection Volume(μl)	5			
Ramp (°C/min)	20			
Pressure (psi)	14.8			
Split Ratio	20:1			
Inlet Temperature (°C)	325			

samples, while later ones utilized an autosampler to provide greater throughput and greater injection volume accuracy. Table 2.2 lists the parameters used for the analysis of alkylthiol chains in solution.

For each pair of thiols used a calibration plot with at least 4 data points was prepared using the same thiol combination. A plot of solution ratio vs. peak area ratio was prepared and the resulting linear relationship was used for subsequent analysis. The GC had to be recalibrated after any work to the inlet linear, column, run parameters and/or prolonged periods of inactivity. An example calibration plot is shown in Figure 2.4 for C_{10} and C_{12} thiols.

GC applied to this problem has a large dynamic range, excellent accuracy ($\pm$ 1.5 %), and excellent reproducibility ($\pm$ 5 %). A demonstration of this can be seen in Figure 2.5 which shows the kinetics of exchange of two different place exchange reactions, performed with the same thiol pairs, but the particles were synthesized for different times. This enables one to differentiate between different rate laws such as Langmuir 1^{st} and Langmuir 2^{nd} order. Without this level of accuracy and reproducibility, such distinctions cannot be supported. However despite numerous attempts, the GC instrument used is unable to detect the dialkyldisulphides ($> (C_{10}S)_2$) used in this study.

2.3.2 HPLC analysis of PER products

In order to expand our methodology to detect disulphides as well as thiols a procedure employing HPLC was developed. The filtrate composition was analyzed

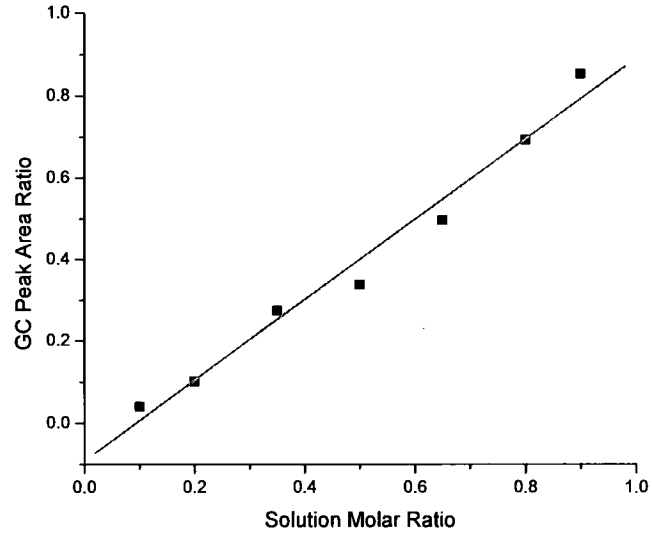

Figure 2.4: Calibration plot of $C_{10}SH$ and $C_{14}SH$ using the GC with an FID detector. Solid line is fit to linear regression of form y=mx+b, m=0.98, b=-0.09, R^2=0.98.

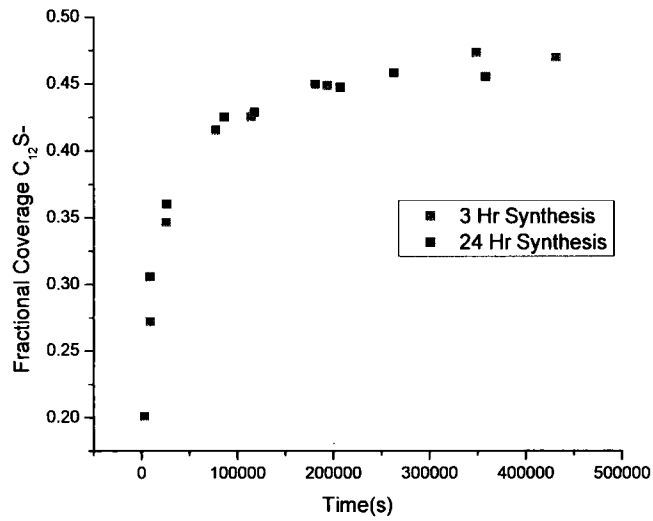

Figure 2.5: Reaction of $C_{12}SH$ with $C_{10}S$-AuNP using the GC. The AuNP samples were separately synthesized, but otherwise the reaction conditions are identical.

using an Agilent 1100 HPLC, with a Zorbax SB-C18 column and UV detector at 206nm. For each analysis 10 μl of analyte solution was injected and eluted with a 55 % isopropanol/acetonitrile solution. By tracking the reaction three main peaks corresponding to the three different disulphides (C_{10} disulphide, C_{1012} asymmetric disulphide, and the C_{12} disulphide) are observed. Alkylthiols could also be detected using this method but GC was faster and more accurate for this analysis. HPLC alkylthiol detection did however provide a useful test to ensure that no disulphide-thiol interconversion was occurring. Using a varible wavelength detector(VWD) we were able to lower our detection limits by choosing an appropiate wavelength(206nm) for the -S-S- bond in dialkyldisulphides. Utilizing this wavelength had the added benefit that both C_{10} and C_{12} dialkyldisulphides had the same intensity of detector response, so that peak areas were indicative of solution concentrations, negating the need for repeated calibrations. By using isocratic elution conditions , the time between runs was reduced enabling higher throughput and simpler cleaning of the column between runs. Table 2.3 lists the other parameters used for the HPLC method.

Table 2.3: HPLC parameters for the analysis of alkylthiol and dialkyldisulphide solutions

Parameter	Value
Injection loop volume (μl)	10
Flow rate (ml/min)	0.50
UV detector wavelength (nm)	206

The HPLC has the ability to seperate and detect dialkyldisulphides. This enables the development of experiments not possible with the GC method. HPLC's lesser sensitivity and longer analysis time precluded its greater use however.

These two separations provided for the development of facile and powerful techniques for the analysis of AuNP and their reaction with alkylthiols/dialkyldisulphides. This enabled the critical evaluation of both the kinetics and thermodynamics of PER with the accuracy and reproducibility necessary to differentiate kinetic laws and mechanistic details.

2.3.3 Fitting to Kinetic Models

Data were fit using OriginPro^{TM} version 7.5. The nonlinear least squares fitting (NLSF) was comupted using the Levenberg-Marquardt method that minimizes the chi^2 parameter . This method utilizes partial derivatives of the function with respect to the fit parameters to find the optimum parameter values.

References

[1] Brust, M.; Walker, M.; Bethell, D.; Schiffrin, D. J.; Whyman, R. *Chem. Commun.* **1994**, 801-802.

[2] Hostetler, M. J. W.; Wingate, J. E.; Zhong, C.-J.; Harris, J. E.; Vachet, R. W.; Clark, M. R.; Londono, J. D.; Green, S. J.; Stokes, J. J.; Wignall,G. D.; Glish, G. L.; Porter, M.D.; Evans, N. D.; Murray, R. W. *Langmuir* **1998**, 14, 17-30.

[3] Badia, A.; Lennox, R. B.; Reven, L. *Acc. Chem. Res.* **2000**, 33, 475-481.

[4] Hostetler, M. J.; Templeton, A. C.; Murray, R. W. *Langmuir* **1999**, 15,3782-3789.

APPENDIX A

NP Size Function

The following function calculates the sizes of NPs in a TEM image. It uses user input to adjust threshold parameters which vary image by image.

A.1 Program Code

```
 function [ np_area ] = np_size_function( ImFilePath,SavePath,length_of_scale_bar_nm )
%%%%%%%%%%%%%%%%%%%%%%%%%%%%%%%%%%%%%%%%%%%%%%%%%%%%%%%%%%%%%%%%%%%%%%%%%%%%%%%
%%%%%%%%%%%%%%%%%%%%%%%%%%%%%%%%%%%%%%%%%%%%%%%%%%%%%%%%%%%%%%%%%%%%%%%%%%%%%%%
%% Estimation of nanoparticle size determined from image%%
%% Jeff Shepherd, Sept. - 2005
%% Edited by Adil for batch processing
%%%%%%%%%%%%%%%%%%%%%%%%%%%%%%%%%%%%%%%%%%%%%%%%%%%%%%%%%%%%%%%%%%%%%%%%%%%%%%%
%%%%%%%%%%%%%%%%%%%%%%%%%%%%%%%%%%%%%%%%%%%%%%%%%%%%%%%%%%%%%%%%%%%%%%%%%%%%%%%
%%%%%%%%%%%%%%%%%%%%%%%%%%
% Image File Parameters %
%%%%%%%%%%%%%%%%%%%%%%%%%%
complete = 'Repeat';
while strcmp(complete,'Repeat')
Image_extension = 'TIFF';            % raw image prefix

median_iterations = 2;
min_np_size = 0;     % area nm
max_np_size = 20;    % area nm
bloomitfactor = 1;
laplaces=4; %# of laplace transformations
dilas=2; %#of dilations/ersoion
inpthresh='240';
thresh=240;
image_resolution_calculated =1;
thresh_feedback='No';
dipinit_ws = [800,800];
```

```
dipfig -unlink
%%%%%%%%%%%%%%%%%%%%%%%%%%%%%%%%%%%%
% calculate resolution in nm/pixel %
%%%%%%%%%%%%%%%%%%%%%%%%%%%%%%%%%%%%

% read in the image
dipfig(10,'image',[200,800,dipinit_ws]);
image = readim(ImFilePath,Image_extension)
% crop out the scale bar
scale_bar = dipcrop(10);
% segment the scale bar to binary value
scale_bar_binary = threshold(scale_bar,'isodata',Inf);
%Make sure we have a valid length of scale bar
while  image_resolution_calculated < 10 | image_resolution_calculated > 200
% dilate the thin scale bar
scale_bar_binary_dila = bdilation(scale_bar_binary,bloomitfactor,-1,0);
% find length of scale bar in number of pixels
length_of_scale_bar_pixels = measure(scale_bar_binary_dila,[],
{'Dimensions'},[],1,0,0);
% extract data from measure function
image_resolution_calculated = length_of_scale_bar_pixels(1:1).Dimensions(1);

    if bloomitfactor > 5
        disp('unable to acquire length bar skipping file')
        np_area=0;
        return;
    end
    bloomitfactor = bloomitfactor+1;
end
%display bloomit factor
variables=strcat('Bloom It Factor:',num2str((bloomitfactor-1)),
'Image Resolution Calculated:',num2str(image_resolution_calculated));
disp(variables)
% compute resolution
resolution_of_image = length_of_scale_bar_nm/image_resolution_calculated;

dipfig(11,'c',[200,350,dipinit_ws])
% apply a median filter to smooth image if necessary
if median_iterations > 0
    image_med_filt = medif(image,median_iterations,'rectangular');
    % read in original median filtered image
    c=image_med_filt
else
    c=image
end
```

```
%%%%%%%%%%%%%%%%%%%%%%%%%%%%%%%%%%%%%%%%%%%%%%%%%%%%%%%%%%%%%%%%%%%%%%%%
% find nanoparticles and calculate their area in nm^2 %
%%%%%%%%%%%%%%%%%%%%%%%%%%%%%%%%%%%%%%%%%%%%%%%%%%%%%%%%%%%%%%%%%%%%%%%%

% crop a region of interest
croped_image = dipcrop(11);
dipfig(11,'c',[1,50,dipinit_ws]);
c=croped_image
% enhance features with a laplace operator
enhanced_features = laplace(croped_image,laplaces);
% histogram equalization of enhanced features
features_hist_equal = hist_equalize(enhanced_features);
% numerically threshold image
dipfig(12,'d',[1000,50,dipinit_ws])
while strcmp(thresh_feedback,'No')
    prompt = strcat('Enter Threshold[', inpthresh, ']:');
    features_thresh = features_hist_equal>thresh;
    d=features_thresh
    dlg_title = 'Input for Threshold';
    thresh_feedback = questdlg('Is the Threshold OK','Threshold Feeback',
'Yes','No','Yes');
    if strcmp(thresh_feedback,'No')
        inpthresh = inputdlg(prompt,dlg_title)

    m = cell2mat(inpthresh)
    str = mat2str(m)
    thresh=str2num(str);
    end
end
features_thresh_dila = berosion(features_thresh,dilas,-2,1);
% remove features touching the edge of image
features_thresh_eros = bdilation(features_thresh_dila,dilas,-2,0);
d=features_thresh_eros
features_no_edge = brmedgeobjs(features_thresh_eros,1);
% analysis of features excluding np's that are too big or too small
if min_np_size > 0
    min_np_size = min_np_size/(resolution_of_image*resolution_of_image);
    min_np_size = ceil(min_np_size);
else
end

if max_np_size > 0
    max_np_size = max_np_size/(resolution_of_image*resolution_of_image);
    max_np_size = ceil(max_np_size);
else
```

```
end

features_analysis = measure(features_no_edge,croped_image,'size',[],1,
min_np_size,max_np_size);
% convert measured data into an array
analysis_array = features_analysis(1:end).size;
% calculate feature size based on resolutiona
np_area = resolution_of_image*resolution_of_image*analysis_array;
% plot data
figure(1);
plot(np_area);


%%%%%%%%%%%%%%%%%%%%%%%%%%%%%%%%%%%%%%%%%%%%%%%%
% make an image for all the features found %
%%%%%%%%%%%%%%%%%%%%%%%%%%%%%%%%%%%%%%%%%%%%%%%%

% convert 1's in image to 255
mask_image_a = features_thresh*255;
% define edges
feature_outlines_a= varif(mask_image_a,2,'elliptic');
% threshold outlines
outline_mask_a = threshold(feature_outlines_a,'isodata',Inf);
% overlay image with outlines
all_features_found = overlay(croped_image,outline_mask_a,[255 0 0]);


%%%%%%%%%%%%%%%%%%%%%%%%%%%%%%%%%%%%%%%%%%%%%%%%
% make an image for all the features analysed %
%%%%%%%%%%%%%%%%%%%%%%%%%%%%%%%%%%%%%%%%%%%%%%%%

%make an image for all features analysed
mask_image_b = features_no_edge;
% label objects within bc's
labeled_image_b = label(mask_image_b,2,min_np_size,max_np_size);
% threshold to binary values
labeled_image_thresh_b = labeled_image_b>2;
% convert to 1's and 255's
labeled_image_thresh_b_255s = labeled_image_thresh_b*255;
% define edges
feature_outlines_b = varif(labeled_image_thresh_b_255s,2,'elliptic');
% threshold outlines
outline_mask_b = threshold(feature_outlines_b,'isodata',Inf);
% overlay image with outlines
features_analsed = overlay(croped_image,outline_mask_b,[255 0 0]);
```

```
dipfig(14,'f',[600,50,dipinit_ws])
f = features_analsed
%%%%%%%%%%%%%%%%%%%%%%%%%%%%%%%%
% write area data out to a file %
%%%%%%%%%%%%%%%%%%%%%%%%%%%%%%%%


complete=questdlg('Is the Fitting OK?','Finding Feeback','Yes','Repeat',
'Skip Image','Yes');
if strcmp(complete,'Skip Image')
    np_area=0;
    return;
end
end

fid = fopen(strcat(SavePath), 'wt+');
fprintf(fid,'%15s\t%15s\t%15s\t%15s\t%15s\t%15s\n','Median Iterations','Min NP Area',
'Max NP Area','Laplaces','Medians','Threshold');
fprintf(fid,'%f\t%f\t%f\t%f\t%f\t%f\n',median_iterations,min_np_size,max_np_size,
laplaces,dilas,thresh);
fprintf(fid,'%s\n','Calculated np area');
fprintf(fid,'%15s\t%15s\n','NP Number','Np Area (nm^2)');
for i=1:length(np_area)
fprintf(fid,'%f\t%f\n',(i), np_area(i));
end
fclose(fid);
```

CHAPTER 3

Place Exchange Reactions of Alkyl Thiols on Gold Nanoparticles

Several models of the exchange reaction have been presented in the literature (see Section 1.10). To date each experiment has used labelled alkylthiols with different solubilities and chain packing. This complicates the interpretation of the results. Using the techniques developed in Chapter 2, alkylthiols with little chemical distinction are utilized to examine PER of RS-AuNP.

3.1 Abstract

The kinetics and equilibrium position of place exchange (alkylthiol-for-alkylthiol) reactions of gold nanoparticles are reported. These reactions were monitored via a gas chromatography analysis of structurally similar incoming and outgoing alkylthiols, as a function of time. The place exchange reactions described here proceed to an equilibrium position, where $K_{eq} \approx 1$. The product-time data follow Langmuir diffusion kinetics.

3.2 Introduction

Place or ligand exchange reactions on gold nanoparticles (AuNPs) have been extensively used to create new functionalized NPs.[1] This reaction allows one to use a well characterized AuNP sample (e.g., C_6S-AuNP) as an entry point to a host of other AuNPs, with a range of functionalities. AuNPs with electrochemical,[2] fluorescent,[3] and bio-active[4] ligands have thus been prepared using n-alkylthiol-AuNPs as the starting materials. Not only is the introduction of new functionality to the NP important, but so is control of how many new ligands are on the Au core. In many situations, controlling the number of exchanged ligands is an important determinant of eventual properties. This control inevitably stems from an understanding of the kinetics and mechanism of the ligand exchange process. To date, kinetics studies have concluded that the ligand exchange process is associative (S_N2-like)[5, 6], dissociative (S_N1-like),[7–9] or combinations thereof.[10] Each study has had to employ pairs of ligands, where one or both have a label appropriate to the analytical methodology used. Ligand pairs with quite different terminal groups have therefore been used (e.g., methyl/ferrocene,[6] methyl/methyl ester,[6] methyl/alcohol,[7] methyl/ pyrene,[8] and methyl/TEMPO[8, 9, 11]).

In the related binary 2D SAM system, the terminal group is known to be an important determinant of the final SAM composition. If the terminal groups are quite different, the preparation solution often requires a large excess of one of the alkylthiols to produce, for instance, a 1:1 binary SAM.[12, 13] Such a terminal group dependence is likely transferable to the nanoparticle system given the similarities between the 2D and 3D (i.e., NP or monolayer-protected cluster) SAMs.[14]

3.3 Experimental Methods

Recognizing the problem introduced by labelled alkylthiols, we have developed a GC product analysis method which allows one to study the alkylthiol-for-alkylthiol exchange reaction where the chains only differ in length. Briefly, the reactions were followed using a modified version of the published reaction-quench process.[6] However, to obtain accurate and reproducible results, the purification procedure was simplified. AuNPs were dissolved in toluene to yield 10 mg/ml solutions. These solutions were kept under an Ar atmosphere at 25 °C. Reactions were initiated by adding an appropriate quantity of alkylthiol via syringe injection. The reaction progress was tracked by removing 1 ml aliquots of solution and precipitating the NPs via introduction of 10 ml of ethanol. The AuNPs were separated from the supernatant containing free thiols via filtration with a fine glass frit. The quantity of unbound alkylthiols was determined by GC using a 5 % phenyl dimethylsiloxane column and a FID detector. GC applied to this problem has a large dynamic range, excellent accuracy ((1.5 %), and excellent reproducibility (5 %).) Excellent run-to-run reproducibility of kinetic traces is observed when working with the same batch of AuNPs. However, some inter-batch variability is observed. This inter-batch variability does not alter the form of the kinetics fit (see below) but affects the value of the fitted parameter (the rate constant). To minimize this batch-to-batch variability, kinetics experiments were performed from samples of large (ca. 1 g in $HAuCl_4$) AuNP preparations. Particles were synthesized using the standard two-phase Brust-Schiffrin[15, 16] synthesis using Au:C_{10}SH:TOAB:$NaBH_4$ in a 1:1:2.5:10 molar ratio. Nanoparticles were characterized by ^{1}H NMR (for free ligand), TEM (2.2 $\pm$0.2 nm), and TGA (18-21 % organic content) analyses.

3.4 Results

Figure 3.1 presents the time progress of reactions of C_{12}SH with C_{10}Au-NP, where the (incoming ligand):(outgoing ligand) ratio ranges from 9:1 to 1:4. The reaction proceeds in a progressive, rather than discontinuous (e.g., bi- or multiphasic) manner over 100 h, and reaches a limiting value corresponding to the ligand ratio of the experiment. An excellent fit is obtained when the entire time course data are applied

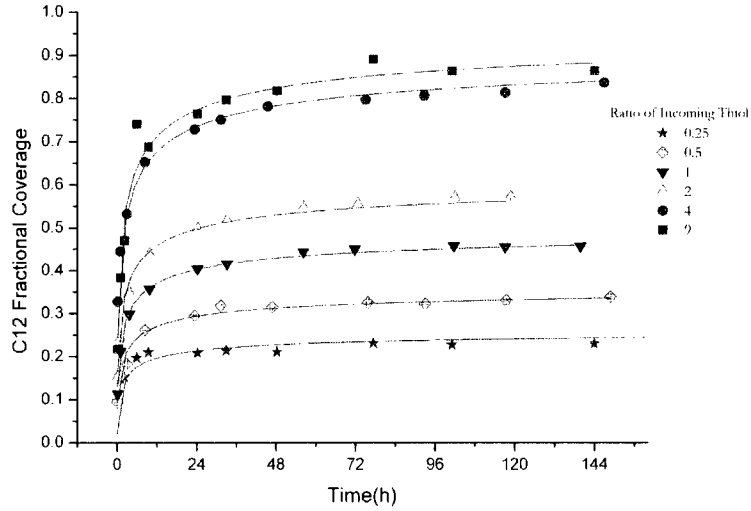

Figure 3.1: Time progress of reactions of C12SH with C10-AuNPs at different incoming to outgoing ligand ratios. Solid lines are fits to second-order diffusion-limited Langmuir model (eq 3.1).

to a second order Langmuir diffusion-limited rate equation:[17, 18]

$$\Theta(t) = \frac{Ak\sqrt{t}}{1 + k\sqrt{t}} \tag{3.1}$$

A number of alternative kinetics models, including other Langmuir, first-order, and second-order models, yield either inappropriate or lesser quality fits than those to eq 3.1 (see Supporting Information). It is significant that the exchange/adsorption kinetics of thiols to 2D gold surfaces also adhere to simple[19, 20] or diffusion-limited[21–23] Langmuir kinetics. The implications of a $K_{eq} \approx 1$ are clear. Under the reaction conditions used ($C_{12}SH$ with $C_{10}Au$-NP, 25 °C, toluene as a solvent), there is no discernible discrimination between an outgoing ligand rebinding to the NP surface and an incoming ligand binding to the NP surface. The chemical nature of the outgoing and incoming species has been postulated as being a thiyl radical,[24] thiolate,[10] or disulphide.[9] The kinetics as presented here do not, however, provide insight into these mechanistic details.

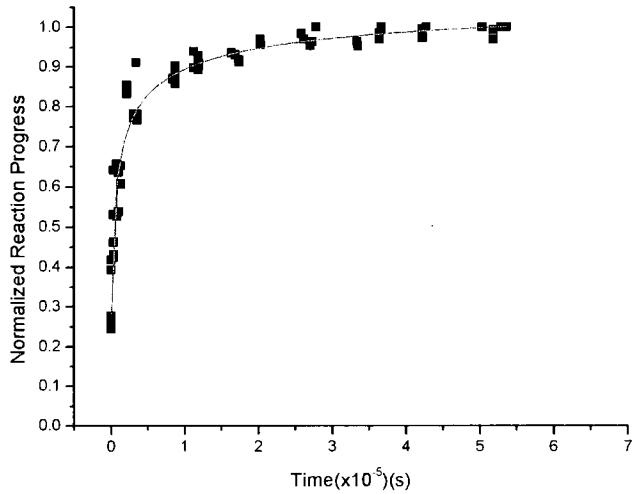

Figure 3.2: Normalized reaction progress for data in Figure 3.1. Solid line is fitted to a second-order diffusion-limited Langmuir model (eq 3.1). Fitting values: A = 1.10 (±0.01), k = 0.0137 (±0.008), r^2=0.96.

Table 3.1: Summary of Alkylthiol Place Exchange Reactions:$C_{12}SH$ with $C_{10}Au$-NP

Incoming $C_{12}SH$: outgoing $C_{10}Au$-NP thiol ratio	final coverage of incoming thiol ($C_{12}SH$) [a]	predicted final coverage [b]	yield
0.27	0.23	0.21	1.08
0.49	0.34	0.33	1.00
1.06	0.46	0.52	0.88
2.12	0.57	0.68	0.84
3.95	0.84	0.80	1.05
9.56	0.86	0.91	0.95
		mean	0.97 ±0.09

[a] Calculated from the last experiment point obtained in each reaction

[b] Final predicted coverage of the incoming $C_{12}SH$ if the replacement occurs with a 1:1 stoichiometry.

Figure 3.3 provides additional evidence that the extent of reaction is determined by the molar ratio of incoming to outgoing ligand. When studying the C_{10}AuNP reaction with $C_{14}SH$, we observe that addition of a second equivalent of $C_{14}SH$ to a reaction whose conversion has already reached a limiting value results in additional conversion and a new limiting value consistent with $K_{eq} \approx 1$. This is relevant to previous work, which concluded that a complete exchange of alkylthiols is not possible

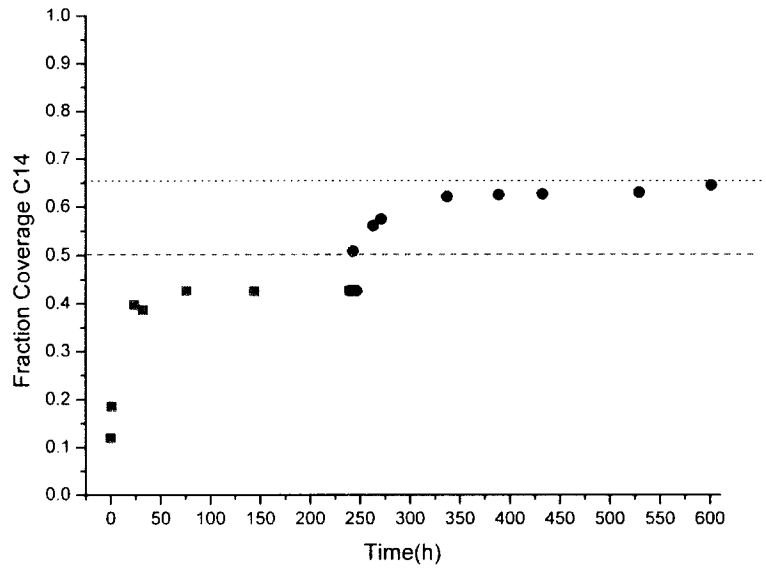

Figure 3.3: Place exchange reaction of C_{10}AuNP with C_{14}SH. After 250 h, a second equivalent of C_{14}SH was added.

for particles with greater C_4 chains.[6] This conclusion leads to a complex mechanism involving multiple types of binding sites on the NP, some of which are nonexchangeable. Although the data presented here do not preclude there being an interchange of ligands on the NP surface, they also do not require that there be a population of nonexchangeable ligands. The observed $K_{eq} \approx 1$ requires a large incoming:outgoing ligand ratio (≥ 100) to establish whether complete exchange has occurred. However, the limitations of the GC method used here preclude monitoring the kinetics for an incoming:outgoing ligand ratio ≥ 10.

3.5 Conclusion

In summary, we have demonstrated that the place exchange reaction between C_{10}S-Au NP and C_{12}SH follows Langmuir diffusion kinetics. The reaction rate notably has a zero-order dependence in the incoming ligand concentration. A $K_{eq} \approx 1$ in the C_{10}/C_{12} case is observed for the reaction performed in toluene at 25 °C With this information in hand, the opportunities and restrictions of the place exchange reaction as a preparative reaction are now clarified.

3.6 Acknowledgements

We thank NSERC (Canada), FQRNT (Quebec), and Genome Quebec for support of this research.

References and Notes

[1] Brust, M.; Kiely, C. J. *Colloids Surf. A*,**2002**, 202, 175-186.

[2] Hostetler, M. J.; Green, S. J.; Stokes, J. J.; Murray, R. W. *J. Am. Chem.Soc.* **1996**, 118, 4212-4213.

[3] Demers, L. M.; Mirkin, C. A.; Mucic, R. C.; Reynolds, R. A., III; Letsinger, R. L.; Elghanian, R.; Viswanadham, G. *Anal. Chem.* **2000**, 72,35-41.

[4] McIntosh, C. M.; Esposito, E. A., III; Boal, A. K.; Simard, J. M.; Martin, C. T.; Rotello, V. M. *J. Am. Chem. Soc.* **2001**, 123, 7626-7629.

[5] Montalti, M.; Prodi, L.; Zaccheroni, N.; Baxter, R.; Teobaldi, G.; Zerbetto, F. *Langmuir* **2003**, 19, 5172-5174.

[6] Hostetler, M. J.; Templeton, A. C.; Murray, R. W. *Langmuir* **1999**, 15, 3782-3789.

[7] Song, Y.; Murray, R. W. *J. Am. Chem. Soc.* **2002**, 124, 7096-7102.

[8] Ionita, P.; Caragheorgheopol, A.; Gilbert, B. C.; Chechik, V. *J. Am. Chem.Soc.* **2002**, 124, 9048-9049.

[9] Ionita, P.; Caragheorgheopol, A.; Gilbert, B. C.; Chechik, V. *Langmuir* **2004**, 20, 11536-11544.

[10] Song, Y.; Huang, T.; Murray, R. W.*J. Am. Chem. Soc.* **2003**, 125, 11694-11701.

[11] Chechik, V. *J. Am. Chem. Soc.* **2004**, 126, 7780-7781.

[12] Folkers, J. P.; Laibinis, P. E.; Whitesides, G. M. *Langmuir* **1992**, 8, 13340-13346.

[13] Folkers, J. P.; Laibinis, P. E.; Whitesides, G. M.; Deutch, J. *J. Phys. Chem.* **1994**, 98, 563-571.

[14] Badia, A.; Lennox, R. B.; Reven, L. *Acc. Chem. Res.* **2000**, 33, 475-481.

[15] Brust, M.; Walker, M.; Bethell, D.; Schiffrin, D. J.; Whyman, R. *Chem.Commun.* **1994**, 801-802.

[16] Hostetler, M. J. W.; Wingate, J. E.; Zhong, C.-J.; Harris, J. E.; Vachet, R. W.; Clark, M. R.; Londono, J. D.; Green, S. J.; Stokes, J. J.; Wignall, G. D.; Glish, G. L.; Porter, M. D.; Evans, N. D.; Murray, R. W. *Langmuir* **1998**, 14, 17-30.

[17] Where A is the final fractional coverage, is the fractional surface coverage of the incoming thiol, and k is the rate constant.

[18] In these experiments, we note that the rate of reaction is proportional to the surface coverage of incoming ligand and to the solution fraction of incoming ligand, both of which scale with (1 - θ(t)). This leads to the observed second-order Langmuir kinetics. Diffusion of the active species to the surface has previously been reported to be the limiting factor in 2D exchange reactions; see ref [21]

[19] Biebuyck, H. A.; Bain, C. D.; Whitesides, G. M. *Langmuir* **1994**, 10, 1825-1831.

[20] Schessler, H. M.; Karpovich, D. S.; Blanchard, G. J. *J. Am. Chem. Soc.* **1996**, 118, 9645-9651.

[21] Georgiadis, R.; Peterlinz, K. P.; Peterson, A. W. *J. Am. Chem. Soc.* **2000**, **122**, 3166-3173.

[22] Yan, D.; Saunders, J. A.; Jennings, G. K. *Langmuir* **2002**, 18, 10202-10212.

[23] Peterlinz, K. A.; Georgiadis, R. *Langmuir* **1996**, 12, 4731-4740.

[24] Ionita, P.; Gilbert, B. C.; Chechik, V. *Angew. Chem., Int. Ed.* **2005**, 44,3720-3722.

APPENDIX B

Derivation of Diffusion-Limited Second Order Langmuir Kinetics

Langmuir first presented a description of the adsorption of gases onto crystal surfaces in 1918.[1] This thermodynamic relationship, became known as the 'Langmuir isotherm'. It describes gas-adsorption to a surface as an irreversible statistical process where:

$$\frac{d\Theta}{dt} \propto 1 - \Theta \tag{B.1}$$

integrating yields the time-dependent coverage[2]:

$$\Theta(t) = 1 - e^{-kt} \tag{B.2}$$

Formation kinetics of 2-D SAMs are limited by the rate at which thiols can be delivered to surface leading to a diffusive term in addition to the constraints of an empty surface-site imposed by Langmuir kinetics. The flux to the surface, J, can be given by:[3]

$$J = c\left(\frac{D}{\pi}\right)^{0.5} t^{-0.5} \tag{B.3}$$

where c is the bulk concentration and D is the diffusion coefficient

Combining the Langmuir and diffusion models leads to a diffusion-controlled Langmuir model where:

$$\frac{d\Theta}{dt} = J(1 - \Theta) \tag{B.4}$$

However, in our case we have the solution concentration changing with time (most models assume this to be constant as the surface area is small cf. the solution concentration). This can be incorporated into the final equation by changing the concentration term c:

$$c = c_o(1 - \Theta) \tag{B.5}$$

where c_o is the initial bulk concentration

Setting k as:

$$k = \left(\frac{D}{\pi}\right)^{0.5} \tag{B.6}$$

we can express the coverage as:

$$\frac{d\Theta}{dt} = kc_o(1 - \Theta)^2 t^{-0.5} \tag{B.7}$$

Integrating Equation B.7 gives[3]:

$$\Theta(t) = \frac{2kc\sqrt{t}}{1 + 2kc\sqrt{t}} \tag{B.8}$$

This is the form of the Langmuir equation used in the fittings in the equations here, however some arguments made were out of context for the AuNP case. Diffusion to the surface in our case is not bulk diffusion through a surface layer, but rather diffusion through the pre-existing SAM layer on the gold. This explains the extremely slow kinetics observed in PERs cf. the formation kinetics cited in the above derivation. In addition, although the form of the equations are correct, the scaling of the equations with concentration cannot be solved and we have been unable to fully derive the second order diffusion-limited Langmuir kinetics from first principles. This precludes us from using the fitted values of k to obtain the diffusion values of the process.

References

[1] Langmuir, I. *J. Am. Chem. Soc.* **1918,** *40,* 1361-1403.

[2] Dannenberger, O.; Buck, M.; Grunze, M. J. *J.Phys.Chem.B.* **1999,** *103,* 2202-2213.

[3] Yan, D.; Saunders, J. A.; Jennings, G. K. *Langmuir* **2002,** *18,* 10202-10212.

APPENDIX C

Fitting of PER Kinetics Data to Models

There are several approaches one can take when faced with reaction progress data such as shown in Figure C.1. One commonly used method, used extensively by Murray[1–4], is to impose a multi-exponential fit to the data. This *de facto* imposes a reaction scheme on the system which can be very difficult to test with standard chemical or mechanistic (kinetics) tools because of the arbitrariness of transitions in the fits.

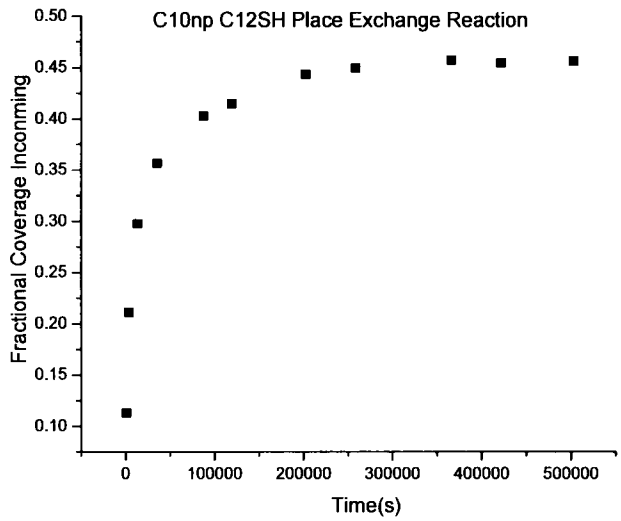

Figure C.1: Reaction of $C_{12}SH$ with $C_{10}AuNP$.

C.0.1 Traditional Kinetic Models

Fitting of the experimental data to traditional first and second order reactions yields unsatisfactory results. First order only is effective for the first 3 data points, and second order can be 'forced' to fit the last few points, but neither can account for the entire time course. While Murray has argued that this is the sequence of rate laws governing the PER reaction on RS-AuNPs, fitting to Langmuir type kinetics yields excellent fits to the entire set of data. Moreover, the rate constants and scaling with concentration make sense without the use of convoluted arguments (See Section 1.10).

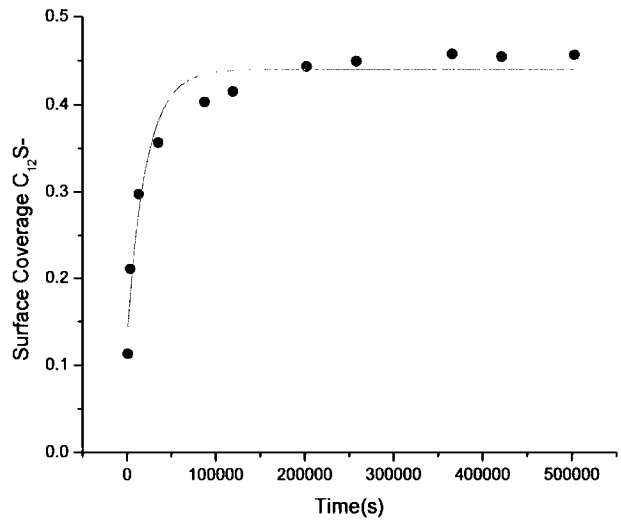

Figure C.2: Reaction of $C_{12}SH$ with $C_{10}AuNP$. Fit is to first-order kinetics rate law.

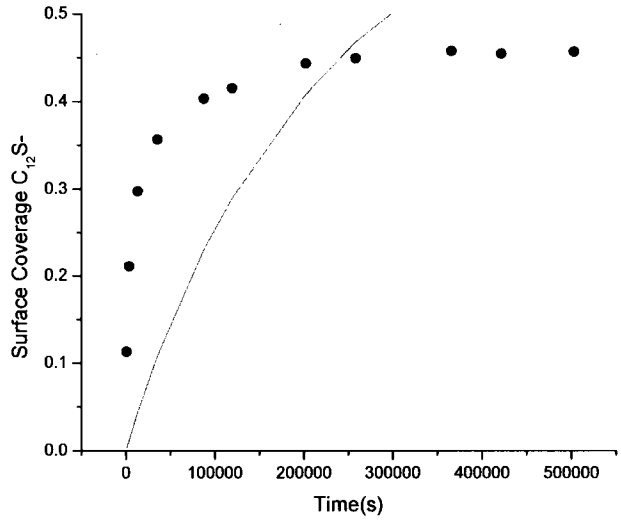

Figure C.3: Reaction of $C_{12}SH$ with $C_{10}AuNP$. Fit is to a second-order rate law.

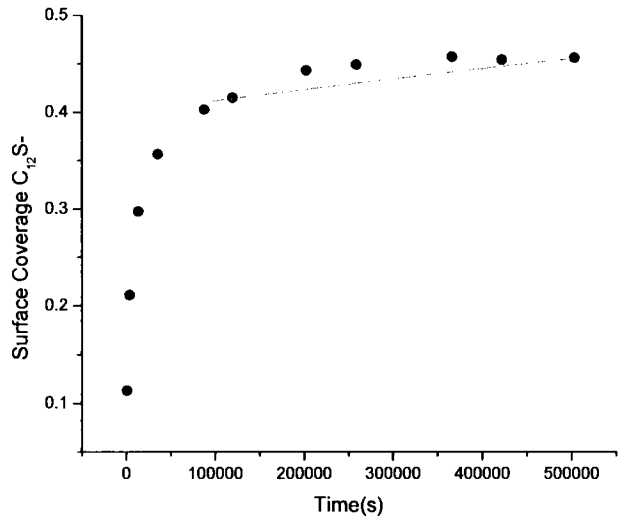

Figure C.4: Reaction of $C_{12}SH$ with $C_{10}AuNP$. Fit is to second-order rate law, selected to fit the last data points.

C.0.2 Langmuir Kinetic Models

The reaction (1:1 reaction of C_{10}AuNP with C_{12}SH) was fitted to Langmuir kinetics. While the fitting distinction between, first- and second-order Langmuir diffusion models may appear small, when fitting multiple data sets simultaneously the second-order Langmuir diffusion fit is clearly the best (Figure C.9).

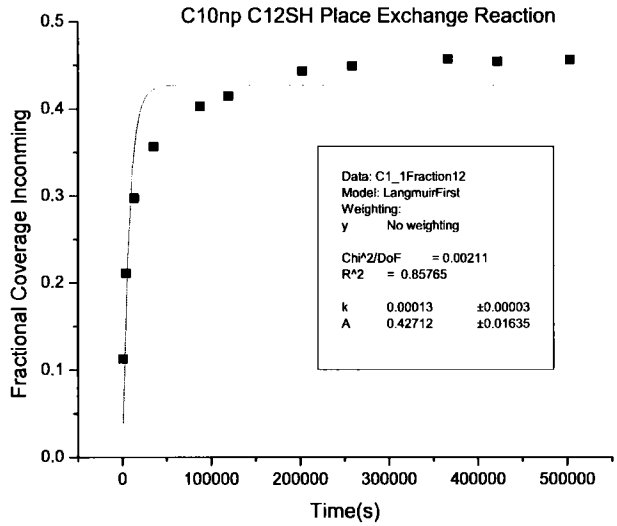

Figure C.5: Reaction of C_{12}SH with C_{10}AuNP. Fit is to first-order Langmuir kinetics.

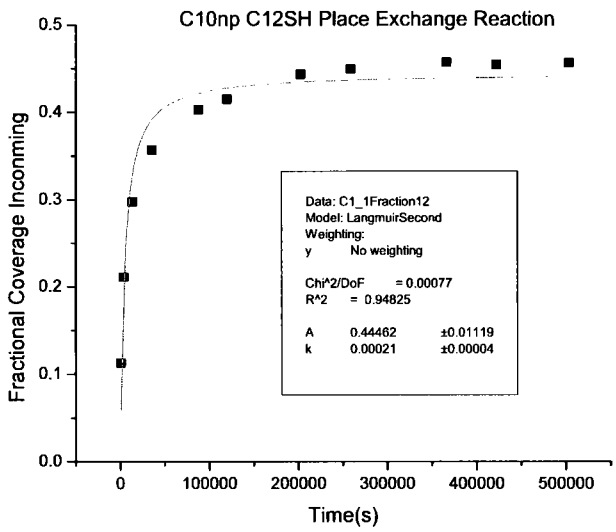

Figure C.6: Reaction of $C_{12}SH$ with $C_{10}AuNP$. Fit is to second-order Langmuir kinetics.

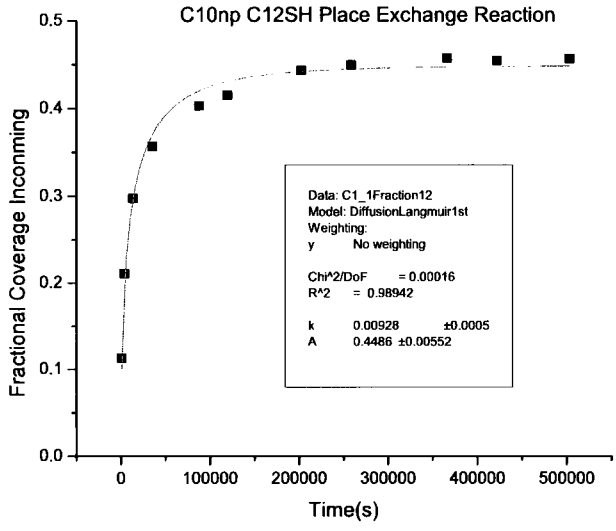

Figure C.7: Reaction of $C_{12}SH$ with $C_{10}AuNP$. Fit is to first-order diffusion limited Langmuir kinetics.

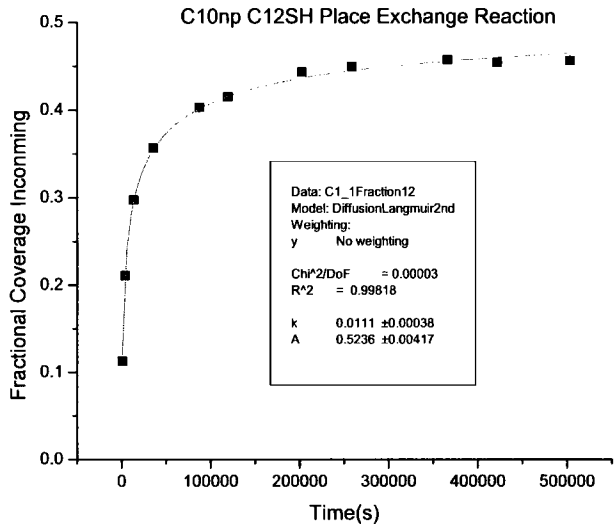

Figure C.8: Reaction of $C_{12}SH$ with $C_{10}AuNP$. Fit is to second-order diffusion limited Langmuir kinetics.

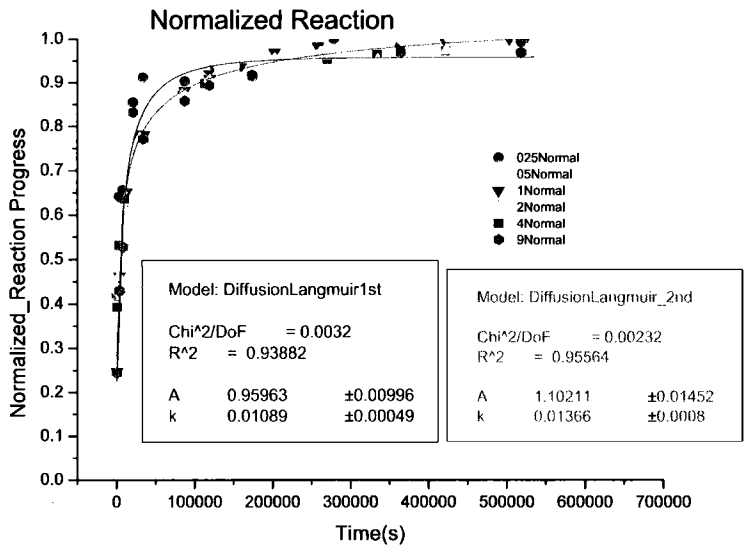

Figure C.9: Reaction of $C_{12}SH$ with $C_{10}AuNP$ at 6 different concentrations, with all plots normalized by their final value. Fits are to first-order diffusion limited Langmuir kinetics(blue) or second-order diffusion limited Langmuir kinetics(red) respectively.

References

[1] Song, Y. and Murray, R. *J. Am. Chem. Soc.* 2002, 124, 7096-7102

[2] Donkers, R.L., Song, Y., and Murray, R.W.*Langmuir*, 2004, 20(11):4703–4707.

[3] Guo, R.,Song, Y., Wang, G. and Murray, R.W.*J. Am. Chem. Soc.*, 2005, 127(8):2752–2757.

[4] Hostetler, M. J.; Templeton, A. C.; Murray, R. W. *Langmuir* 1999, 15,3782-3789.

APPENDIX D

Fitting to Existing Literature Data

There have been several attempts to model the kinetics of PER (see Section 1.10). One of the chief problems with proposed schemes to date is that they are only able to work under specific conditions (excess incoming or capping ligand) or they are not applicable to other experiments. To show the applicability of second order diffusion limited Langmuir kinetics to experiments, beyond those of the alkylthiol-for-alkylthiol case, fittings are provided to literature published experiments by Murray[1] and Zerbetto[2].

As seen in Figures D.1 and D.2, the fits of these data to Equation 3.1 are excellent. Of note is the fact that these fits are excellent over the full range of experimental data. This is especially noteworthy given that the data in Figure D.1, for example, had previously been only fitted to two sequential exponentials.[1]

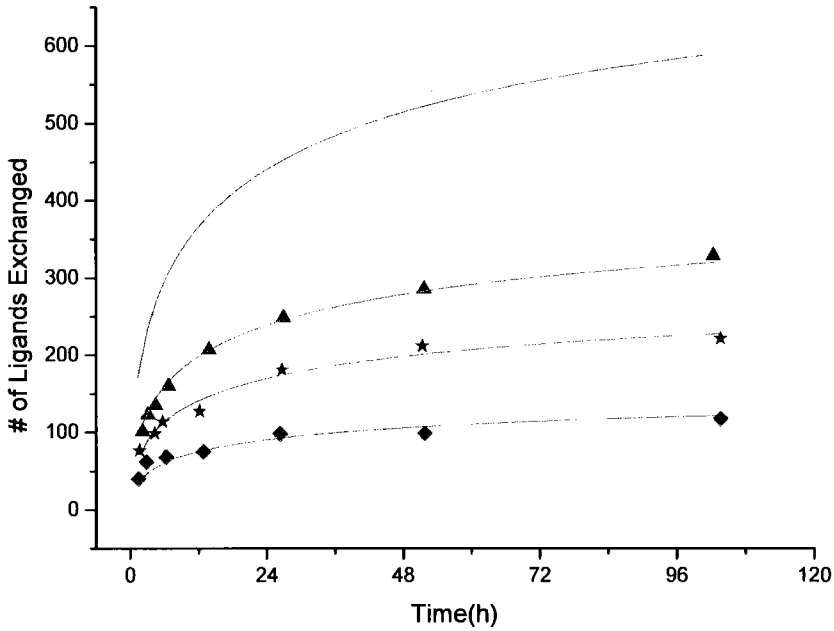

Figure D.1: Second order diffusion limited Langmuir kinetics fitted to data from [1]. Reaction is ω-ferrocenyloctanethiol with C_8AuNPs for various concentrations of FcC_8SH: 1.7×10^{-3} M (black squares); 1.2×10^{-3} M (red circle); 4.1×10^{-4} M (blue triangle); 1.6×10^{-4} (green inverted triangle). Solid curves are fittings to second order diffusion limited Langmuir kinetics (eq. 3.1) and were simultaneously fitted using only one rate constant, k (0.2122 $h^{-\frac{1}{2}}$), r^2=0.98.

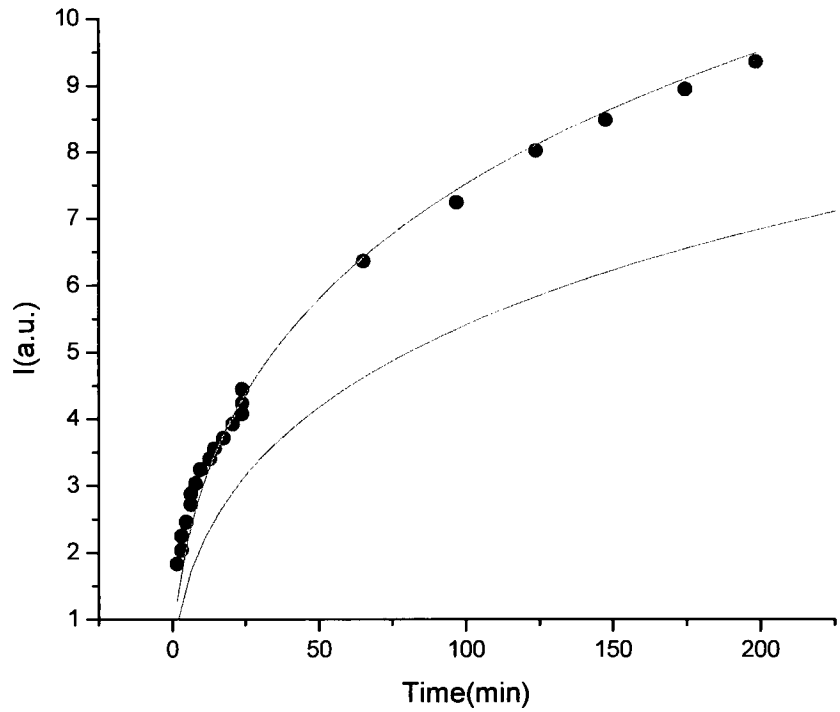

Figure D.2: Second order diffusion limited Langmuir kinetics fitted to data from [2]. Reaction is of C_{10} with pyrene-modified C_{10}AuNPs for various concentrations of C_{10}SH: 1.7×10^{-4} M (green triangle); 1.3×10^{-3} (blue circles). Solid curves are fittings to second order diffusion limited Langmuir kinetics (eq. 3.1) and were simultaneously fitted using only one rate constant, k (0.03996 $\text{min}^{-\frac{1}{2}}$), r^2=0.98.

References

[1] Hostetler, M. J.; Templeton, A. C.; Murray, R. W. *Langmuir* **1999**, 15, 3782-3789.

[2] Montalti, M.; Prodi, L.; Zaccheroni, N.; Baxter, R.; Teobaldi, G.; Zerbetto, F. *Langmuir* **2003**, 19, 5172-5174.

CHAPTER 4

The Kinetics and Mechanism of the Place Exchange Reaction on Gold Nanoparticles:Dialkyldisulphide for Alkylthiol

This paper was submitted to J. Am. Chem. Soc. It is co-authored by Elisa Fuller, and R. Bruce Lennox. The text below is a verbatim copy of the submitted paper.

In Chapter 3 the reaction kinetics of PER of alkylthiols on RS-AuNPs were determined. However this previous study did not address molecular details of the mechanism. Attempts to find a suitable trap to identify a reactive intermediate proved unsuccessful. Dialkyldisulphides however do react with RS-AuNPs, giving insight into the mechanism of the PER.

4.1 Abstract

Thiol protected gold nanoparticles were reacted with dialkyldisulphides. The major product of the reaction was a mixed disulphide, with one half from the surface bound thiol, and the other half from the dialkyldisulphide. The reaction proceeds in an almost linear fashion over a period of 16 days monitored. Kinetics can be fit to a 2^{nd} order Langmuir diffusion rate law similar to the alkylthiol case. These observations lead us to postulate a similar mechanism between alkylthiol and dialkyldisulphide exchange reactions with alkylthiol gold nanoparticles.

4.2 Introduction

Place exchange reactions(PER) are increasingly used to derivatize pre-synthesized gold nanoparticles (AuNP) for optoelectronics and biological applications. Owing to its mild conditions and facile workup, this reaction has become the method of choice for the creation of multifunctional AuNP.[1] Nonetheless, the understanding of its kinetics and mechanism is incomplete. Similarly, in the parallel and more mature field of alkylthiol(RSH) self assembled monolayers on gold surfaces (2D SAMs), no consensus description of the exchange reaction mechanism is available. In both cases there clearly is a need for further understanding of this important and much-used reaction.

In our previous report on exchange kinetics of alkylthiols concerned with alkylthiol-protected gold nanoparticles(AuNP),[2] we found that the kinetics of the reaction followed a 2nd order diffusion limited Langmuir rate law. The reaction proceeds to a stoichiometric endpoint and the rate is independent of incoming thiol concentration. Although this work addressed the reaction kinetics, questions about the molecular details of the mechanism remain. Given that valuable mechanistic information can be derived from identifying reactive intermediates (or lack thereof), we have examined a number of radical traps[3] over a range of conditions. No evidence was found for an alkylthiol radical being involved in the reaction. However, the well documented alkylthiol-dialkyldisulphide reaction does proceed and the kinetics of this reaction at AuNPs provides valuable mechanistic insight.

Dialkyldisulphides have previously been reported to react with alkylthiol AuNPs[4] although only 3-5% of the alkylthiol ligands react with C_4S-AuNPs. Reaction of napthyl-based disulphides with alkylthiol 2D-SAMs leads to a mixed disulphide detected in solution, suggesting that a similar mechanism governs the alkylthiol and

disulphide exchange reactions.[5] The disulphide reaction is very slow and only 20% of the alkylthiol monolayer reacts in 115 h, whereas 100% reacts in 20 h in the alkylthiol-napthylthiol monolayer reaction. This prior work suggests that detailed kinetics and product identification of the dialkyldisulphide/RS-AuNP reaction might provide new insight.

4.3 Results and Discussion

To this end, C_{12} disulphide was reacted with C_{10}S-AuNP. The asymmetric C_{1012} disulphide appears at early times and increases in quantity in a monotonic fashion over the 16 day observation window. Only at long times ($\geq$4d) does the C_{10} disulphide appear. These observations indicate that the intact C_{12} disulphide reacts with the surface-bound C_{10} thiolate and that there no significant quantity of C_{10} (as thiol, thiolate or thiyl radical) nor C_{10} disulphide have spontaneously left the gold surface via dissociative processes. The observed C_{10} disulphide thus arises from a surface-based reaction between outgoing C_{1012} asymmetric disulphide molecules. This also means that the reaction is limited by very slow kinetics rather than there being a very small number of reaction sites.

To ensure that the incoming disulphides in solution were reacting with the AuNPs, a sample of AuNPs that had been washed with ethanol was subjected to iodine decomposition.[8] Subsequent HPLC analysis provides the C_{10}:C_{12} ratio on the nanoparticle. The relative solution composition was 14% C_{10}(86%C_{12}) while that on the AuNP was 9%C_{12}(91%C_{10}). Control reactions in the absence of added thiol or disulphide produce no evidence of either thiol or disulphide in solution after several days under the same reaction conditions. In sum there is no evidence that either thiol or disulphide spontaneously desorb from the AuNP surface in any measurable asymmetric quanitity.

$$\begin{aligned} Au\left(SC_{10}\right)_n + C_{12}SSC_{12} &\leftrightarrows Au\left(SC_{10}\right)_{n-1}\left(SC_{12}\right)_1 + \\ & \quad C_{10}SSC_{12} \qquad (4.1) \\ Au\left(SC_{10}\right)_n\left(SC_{12}\right)_m + C_{10}SSC_{10} &\leftrightarrows Au\left(SC_{10}\right)_{n-1}\left(SC_{12}\right)_{m+1} + \\ & \quad C_{10}SSC_{10} \qquad (4.2) \end{aligned}$$

The observed kinetics were fit to various rate laws. Calculating the extent of

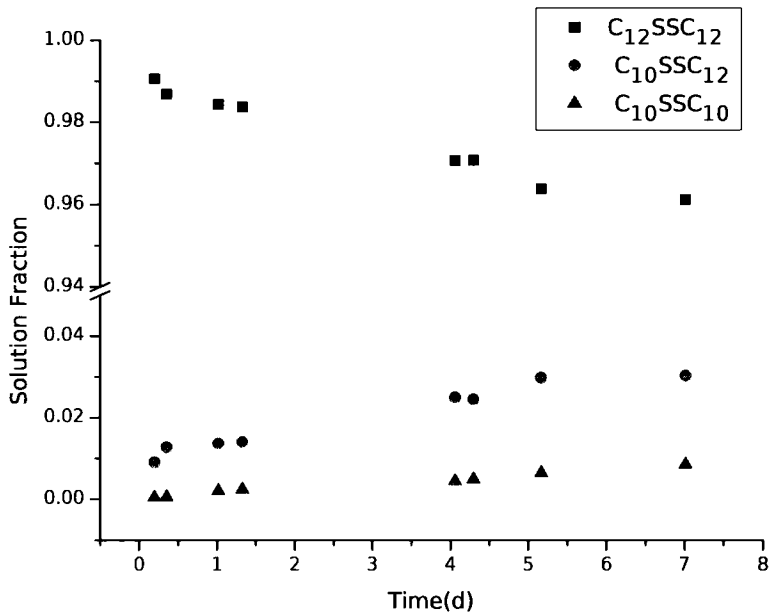

Figure 4.1: Reaction of C_{12} disulphide with C_{10}S-AuNP. [7] Note the discontinuity on the y-axis.

exchange as:

$$\%exchange = \frac{2 * [C_{12}disulphide]_o}{[thiol]_o} \times \left([C_{10}disulphide] + \frac{[C_{1012}disulphide]}{2}\right) \tag{4.3}$$

we can test kinetic models. The kinetic data was applied to several rate laws.[6] The concentrations are derived from the HPLC analysis.[7]These reactions were found to best fit second-order Langmuir diffusion kinetics, as per the alkylthiol-alkylthiol:[2]

$$\Theta(t) = \frac{A * k\sqrt{t}}{1 + k\sqrt{t}} \tag{4.4}$$

The analysis is limited to the fact that only the first 5-10 % of the reaction can be monitored.[9] The rates are independent of the disulphide concentration, where the rates for exchange of these three concentration ratios of disulphide:total to thiol (0.26, 0.50, 0.74) were 5, 2.5, 2.9 ($\times 10^{-4}$) respectively. The observed rate constant is 20-fold less than in the alkylthiol case.[2]

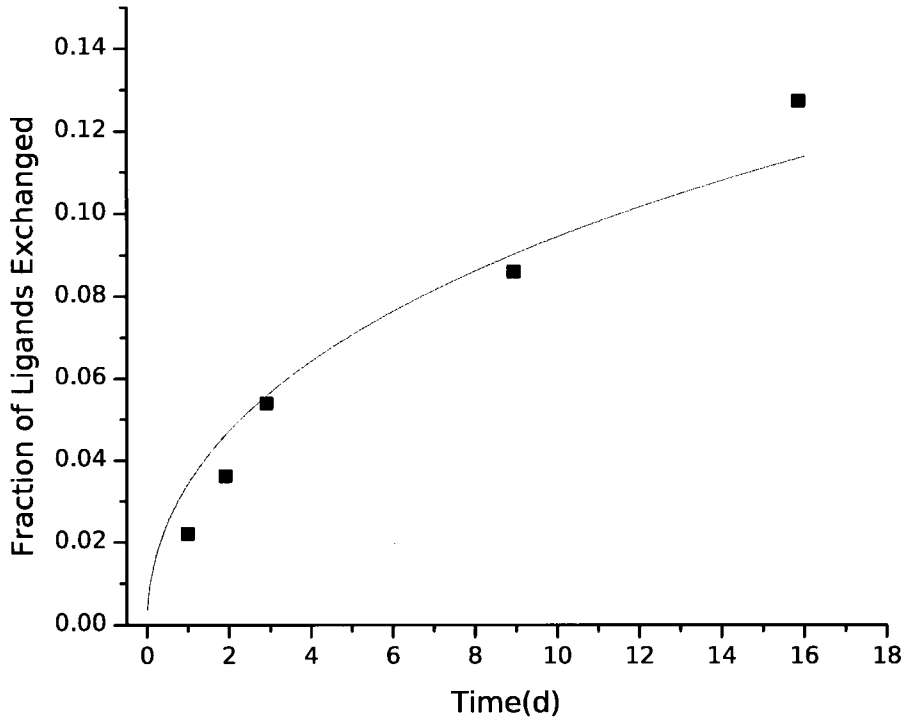

Figure 4.2: Reaction of one equivalent C_{12} disulphide onto C_{10}S-AuNP.[9]

All the reactions studied exhibit similar reactions rates, within the limitations of the data. The adherence to second order diffusion Langmuir kinetics and a zeroth order dependence on incoming thiol concentration points to the exchange reaction mechanism being the same in the C_{12} disulphide-C_{10}AuNP case as for the C_{12}SH-C_{10}AuNP case.

A reaction involving transfer of a hydrogen atom or thiyl radical to the surface-bound ligand, as per the suggestion of Schlenoff for 2D SAM PERs[5] is in accord with our results. Although we observe a zeroth order dependence in incoming ligand like that of Chechik et al.,[4] there is no apparent limit to the quantity of exchange.

The EPR technique however is limited to the quantity of reaction progress that can be monitored. Crucial to the present study is the observation of the mixed disulphide as the predominant product. This is clear evidence that an associative mechanism is in play and that the incoming ligand is actively involved in the reaction. This would otherwise have been uncertain given the zeroth order dependence on the incoming disulphide concentration. The rate-limiting kinetics do not involve these bond making/breaking processes, but instead involve some physical process, possibly penetration of the capping layer by the incoming ligand.

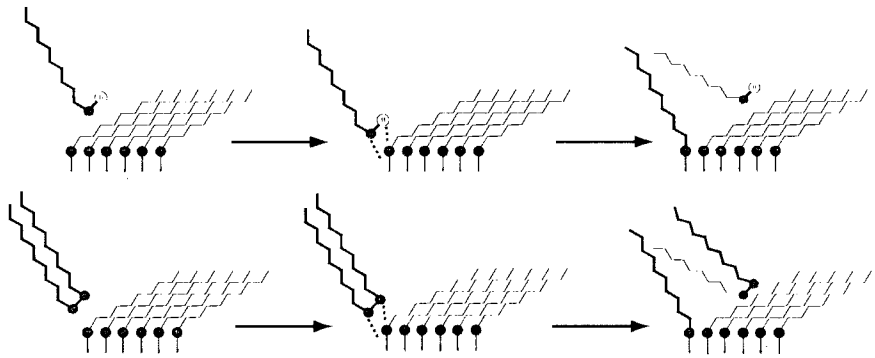

Figure 4.3: Proposed reaction scheme of thiol(A) and disulphide(B) exchange on AuNPs

4.4 Conclusion

The products of the C_{12} disulphide plus C_{10}S-AuNP reaction and adherence to 2nd order Langmuir diffusion kinetics point to a similar, associative process governing the disulphide and thiol exchange reactions. The rate of the disulphide reaction is ca. 20-fold slower however, consistent with steric access in the associative mechanism being important in defining the kinetics.

Acknowledgement. We thank NSERC (Canada), FQRNT (Quebec),and Genome Quebec for support of this research.

Supporting Information Available: Additional figures and table. This material is available free of charge via the Internet at http://pubs.acs.org.

4.5 Methods

Particles were synthesized using the standard two-phase Brust-Schiffrin synthesis[10] with a 1:1:2.5:10 molar ratio of Au:Thiol:TOAB: $NaBH_4$. Particles were characterized

by ^{1}H NMR for free ligand[11], TEM of the gold core(2.2 $\pm$ 0.2nm) and TGA (18-21 % organic content).

Dialkyldisulphides were synthesized by oxidation of the alkylthiols with iodine in ethanol.[12] Reactions were analyzed using an adaptation of a GC-based method recently published.[2] Briefly, solutions of 10 mg/ml C_{10}AuNPs were made up in hexanes at 25°C under argon. The reactions were initiated by syringe injections of the requisite amount of C_{12} disulphide into the reaction vial. Data points were taken at regular intervals by precipitating 1ml aliquots of the reaction mixtures in 10 ml ethanol and separating the supernatant by filtration using a glass frit. The filtrate composition was analyzed using HPLC(Agilent 1100, Zorbax SB-C18 column and UV detector at 206nm); 10 μl of analyte solution was injected and eluted with a 55 % iso-propanol\acetonitrile solution for each sample. By tracking the reaction we see three main peaks corresponding to the three different disulphides (C_{10} disulphide, C_{1012} asymmetric disulphide and the the C_{12} disulphide.)

References and Notes

[1] Templeton, A. C; Wuelfing, W. P.; and Murray, Royce W.*Acc. Chem. Res.*,**2000** ,33,27-36.

[2] Kassam, A.; Bremner; G., Clark, B.; Ulibarri, G.; and Lennox, R.B. *J. Am. Chem. Soc.*, **2006**, 128, 11, 3476 - 3477.

[3] Traps studied include:Butylated hydroxytoluene,α-tocopherol and cis-2-octene.Chechik and colleagues previously reported that alkylthiyl free radicals were not observed in the presence of classic spin traps during the alkylthiol-alkylthiol exchange reaction. Ionita. P; Gilbert,B. ; Chechik, V. *Angew.Chemie(Int. Ed.)*,**2005** , 44, 3720-3722.

[4] Ionita, P.; Caragheorgheopol, A.; Gilbert, B. C.; Chechik, V. *Langmuir* **2004**, 20, 11536-11544.

[5] Kolega, R. R.; Schlenof, J. B. *Langmuir* **1998**, 14, 5469-5478.

[6] Traditional 1^{st},2^{nd} reaction equations were fitted as well as 1^{st},2^{nd} order Langmuir with and without diffusion limitations. See Supplementary material.

[7] Where the [C_{10}disulphide] and [C_{1012}disulphide] refer to the normalized solution concentration, i.e. [C_{10}disulphide] + [C_{1012}disulphide] + [C_{12}disulphide]=1. This comes from equations 1 +2, whereby a mixed disulphide is one PER and a C10 disulphide is two exchange reaction, the first term, gives a ratio of solution bound thiol initially to the number of moles of disulphide available for exchange.

[8] Hostetler, M. J.; Templeton, A. C.; Murray, R. W. *Langmuir* **1999**, 15,3782-3789.

[9] Owing to the difficulty of fitting curves to reaction profiles before they have plateaued we impose final plateau values on the fittings.

[10] Brust, M.; Walker, M.; Bethell, D.; Schiffrin, D. J.; Whyman, R. *Chem. Commun.* **1994**, 801-802.

[11] Badia, A.; Lennox, R. B.; Reven, L. *Acc. Chem. Res.* **2000**, 33, 475-481.

[12] Bain, C. D.; Biebuyck, H. A.; Whitesides, G. M. *Langmuir* **1989**, 5,723-7.

APPENDIX E

Alternative Kinetics Models Applied to the Dialkyldisulphide-for-Alkylthiol Reaction Data

E.0.1 Alternative Fittings

Note that although a first order equation fits the data well. A test of a first order reaction is the linear relation between substrate(incoming disulphide) concentration and observed reaction rate. Shown in Figure S-2, the observed rate constant does not appreciably decrease with incoming disuphide concentration, and certainly does not have an intercept close to 0. This was also the case in the alkylthiol case, where first order kinetics were reported by Murray.[2]

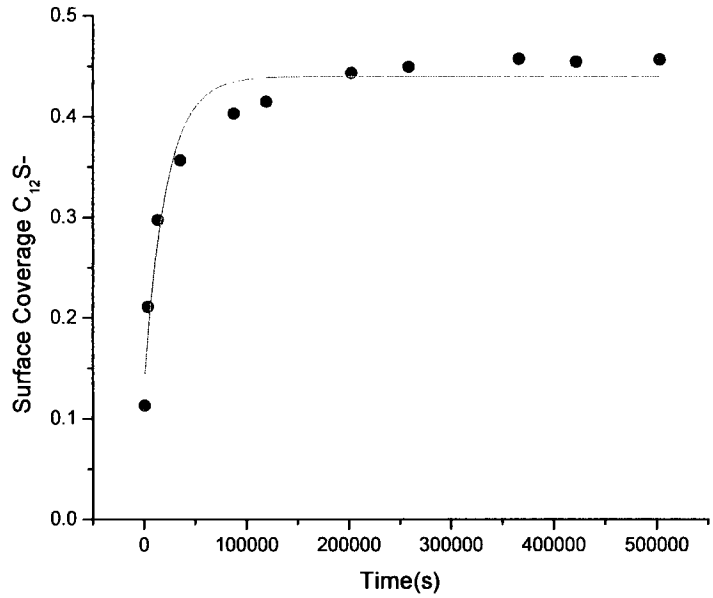

Figure E.1: First Order Fitting of 1 equivalent C_{12} Disulphide onto C_{10}S-AuNP.

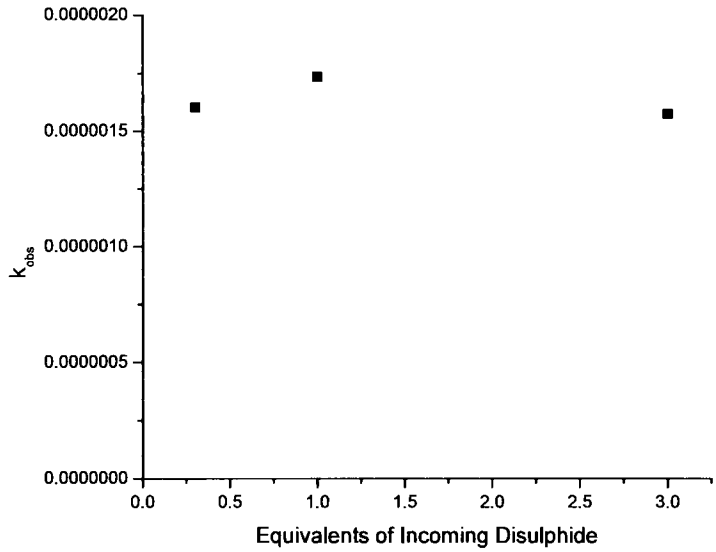

Figure E.2: Observed first order rate constant (k_{obs}) for concentrations observed. The non-zero intercept is not conducive to a first order mechanism.

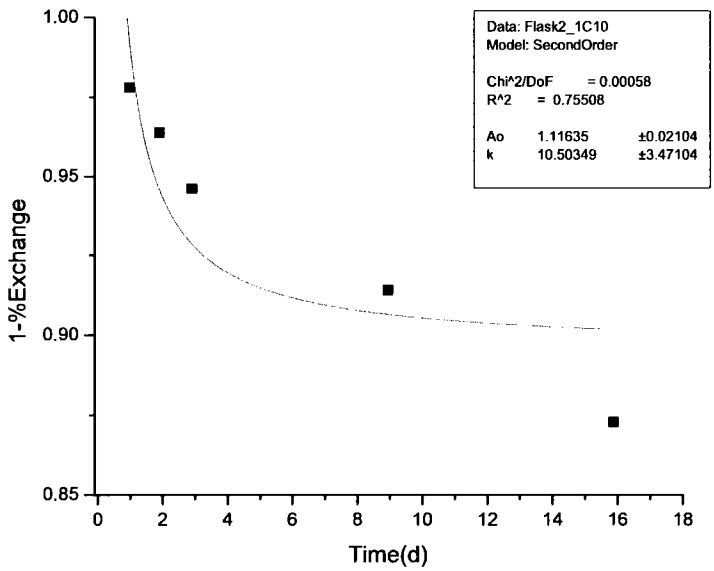

Figure E.3: Second Order Fitting of 1 equivalent C_{12} Disulphide onto C_{10}S-AuNP.

Various different Langmuir type kinetics were fit to the reaction profiles. It is difficult to unequivically differentiate between models, due to the extremely slow kinetics, however the data presented are not inconsistent with the diffusion Langmuir kinetics.

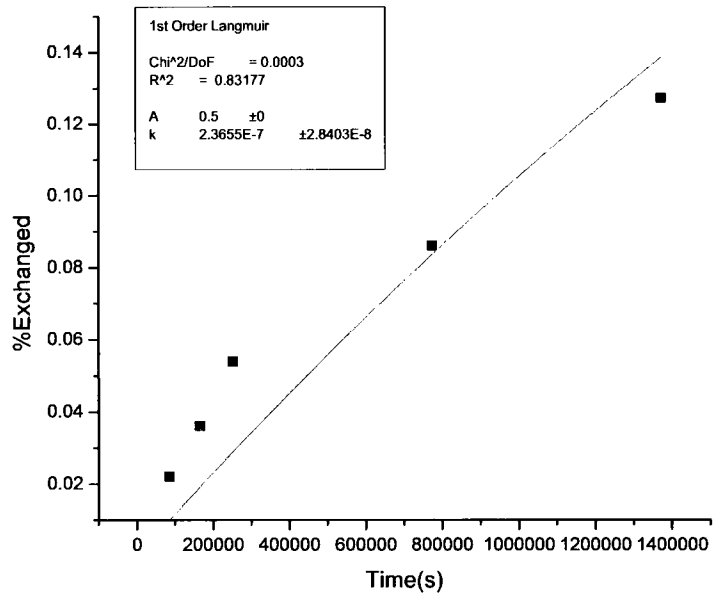

Figure E.4: Langmuir Fittings of 1 equivalent C_{12} Disulphide onto C_{10}S-AuNP fitted line is to Langmuir 1st order kinetics

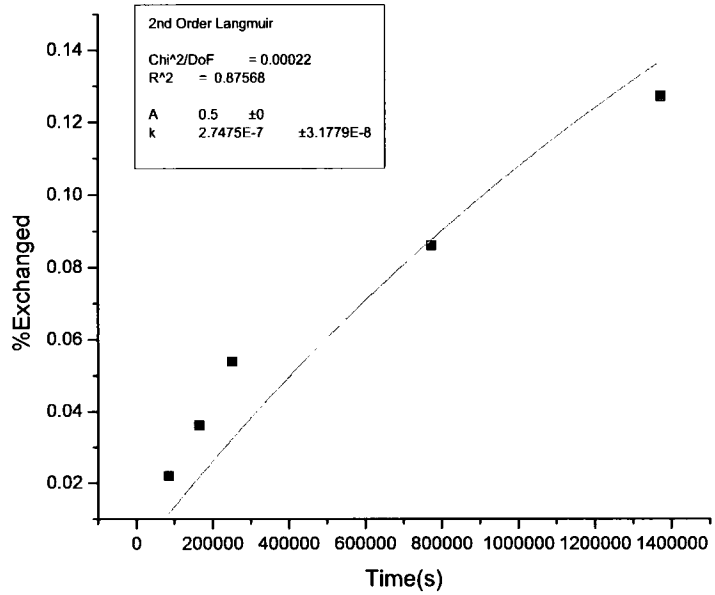

Figure E.5: Fitting of 1 equivalent C_{12} Disulphide onto C_{10}S-AuNP fitted line is to Langmuir 2nd order kinetics

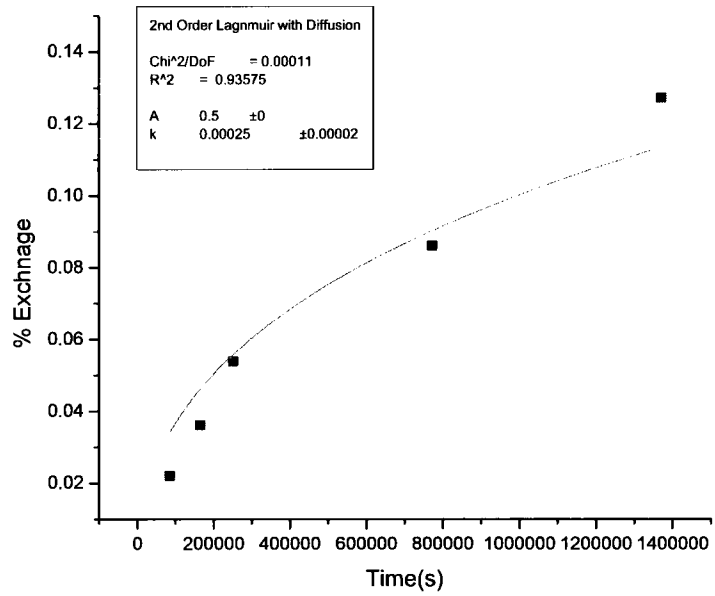

Figure E.6: Fitting of 1 equivalent C_{12} Disulphide onto C_{10}S-AuNP fitted line is to diffusion limited 1st order Langmuir kinetics

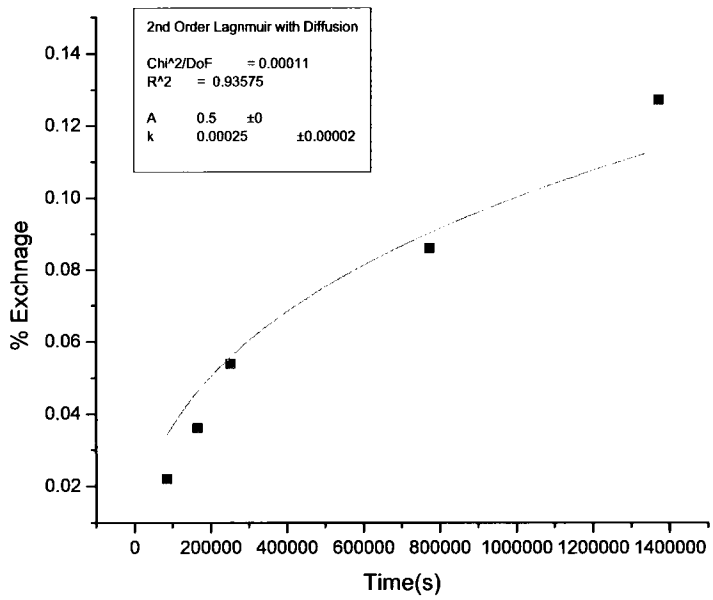

Figure E.7: Fitting of 1 equivalent C_{12} Disulphide onto C_{10}S-AuNP fitted line is to diffusion limited 2nd order Langmuir kinetics

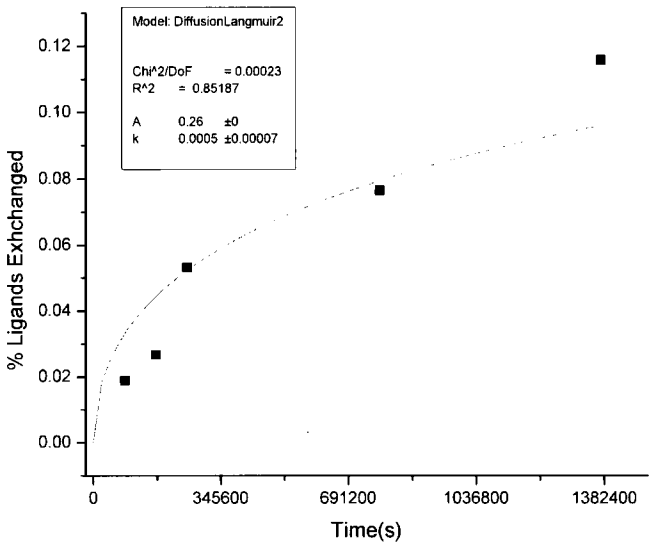

Figure E.8: Reaction of C_{12} disulphide onto C_{10}S-AuNP (0.33 equivalents). Fit is to second-order diffusion limited Langmuir model.

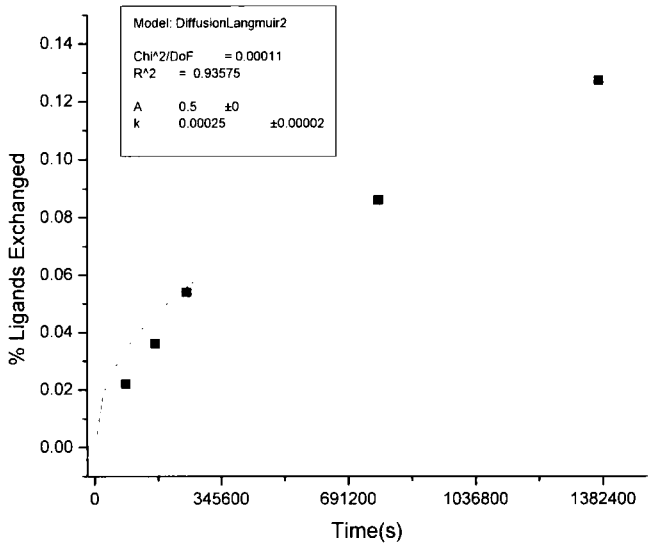

Figure E.9: Reaction of C_{12} disulphide onto C_{10}S-AuNP (1 equivalent). Fit is to second-order diffusion limited Langmuir model

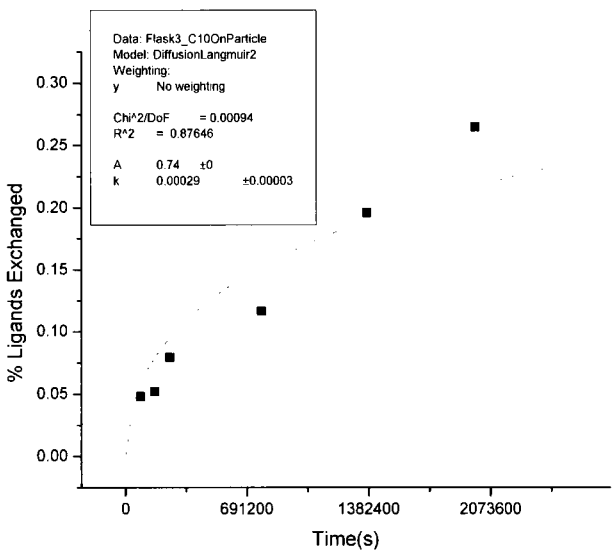

Figure E.10: Reaction of C_{12} disulphide with C_{10}S-AuNP (3 equivalents). Fit is to second-order diffusion limited Langmuir model

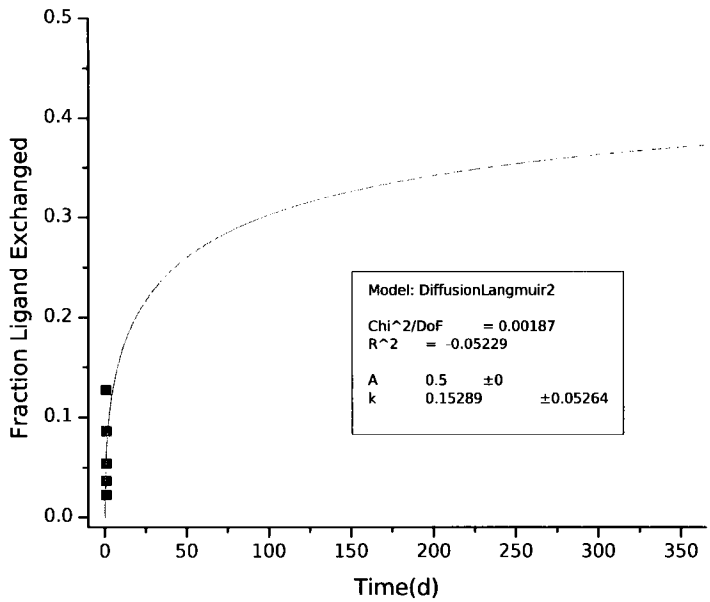

Figure E.11: Reaction of C_{12} disulphide onto C_{10}S-AuNP (1 equivalent). Fitting is to a 2nd Order Langmuir diffusion model, with the fit line extended to show up to 90 % completion.

Table E.1: Rate constants of disulphide exchange from second order Langmuir fittings

A	k$*10^{-4}(\sqrt{s})$
0.26	5
0.50	2.5
0.74	2.9

References

[1] Kassam, A.; Bremner; G., Clark, B.; Ulibarri, G.; and Lennox, R.B. *J. Am. Chem. Soc.* **2006** 128, 11, 3476 - 3477.

[2] Hostetler, M. J.; Templeton, A. C.; Murray, R. W. *Langmuir* **1999**, 15,3782-3789.

CHAPTER 5

Characteristics of the Alkylthiol-for-Alkylthiol Exchange Reaction Kinetics of Gold Nanoparticles

This paper is to be submitted to Langmuir. It is co-authored by Glen Bremner, Jeff L. Shepherd and R.Bruce Lennox.

Chapters 3 and 4 described the reaction kinetics and gave insights into the mechanism of PER of RS-AuNP. However the scope of factors which affect the rate of the PER remain unaddressed. Examination of the physical parameters affecting the rate including incoming- and capping- ligand alkylthiol chain size, AuNP core size, and solvent effects leads to a convergent mechanism of PER of alkylthiols on RS-AuNP.

5.1 Abstract

Place exchange reactions are used to create thiol-protected gold nanoparticles with a range of ligand compositions. The factors that determine the kinetics of this reaction are explored by systematically changing the chain length of both the incoming and initial alkylthiol ligand as well as gold core size. A convergent picture of the exchange reaction emerges where is it best described as a surface-localized reaction, with diffusion of the incoming alkylthiols to the surface as the principle limiting factor in the kinetics of the reaction.

5.2 Introduction

Gold nanoparticles(AuNP) with more than one type of ligand are finding application in drug delivery, biosensors, medical imaging, etc.[1] The main method of preparing nanoparticles with multiple ligand types is the place exchange reaction(PER) between solution-based alkylthiols and alkylthiol-capped AuNP. In order to rationally prepare NP with a defined ligand composition both, the mechanism and controlling factors of the PER must be understood.

To this end our recent studies[2] of PERs of alkylthiol-for-alkylthiol and dialkyldisulphide-for-alkylthiol provide a new framework to understand the factors affecting these reactions. When the incoming and outgoing chains are chemically similar the reactions proceed to a well-defined endpoint, at a rate that is independent of the concentration of the incoming alkylthiol. The kinetics of the reaction adhere to a 2nd order diffusion limited Langmuir rate law, where the coverage Θ is given by[2]:

$$\Theta(t) = \frac{Ak\sqrt{t}}{1 + k\sqrt{t}} \tag{5.1}$$

where A=ratio of incoming alkylthiol/total alkylthiol, k=rate constant($s^{-1/2}$).

This report explores the dependence of the rate and final composition in the chainlengths of the incoming and outgoing ligands. These results provide further differentiation between the diffusion-restricted surface reaction mechanism[2] and the "edge and vertex" mechanism described by Murray and co-workers.[6]

5.2.1 Previous Work

The existence of a thermodynamic endpoint of the alkylthiol-for-alkylthiol reaction was first demonstrated by Murray and coworkers.[6] AuNP capped with different alkylthiols (C_4-C_{16}) were reacted with a C_{11}-methyl ester thiol as the incoming ligand. The final particle composition (after 96h) of reaction was determined by NMR. An increased chain length of the alkylthiol-AuNP results in lesser conversion. This effect is more pronounced at higher incoming:outgoing ligand ratios. These results led to the development of the "edge and vertex" model of PER, where RS chains are activated towards reactivity by being localized at low coordinate sites (edges, vertices) as opposed to the higher coordinate terrace sites. Multiexponential fits to the data assigned a fast reaction to the edge/vertex sites and a slower reaction at the terraces or migration from the terraces to edges/vertices. Large changes in the NP/capping layer composition are precluded, since the ligands on the NP must migrate to the edge/vertices to react.

Murray et al.[13, 14] have also described the PER of arylthiols on small Au_{38} and Au_{140} NP. The smaller NP(Au_{38}) are able to completely exchange all their original capping ligands in $\sim$ 2 h[14] whereas the Au_{140} NP exchange only 40-50 %,[13] presumably because of the lesser mobility of their terrace-localized ligands. In addition, para-substituted electron withdrawing groups(EWG) (to the linking thiol) lead to faster reactions in both senses (EWG-SH with phenyl-C_2-S-AuNP and the reverse, where phenyl-C_2-SH react with EWG-S-AuNP.) These results are consistent with the rate limiting step of the PER involving both an incoming and outgoing ligand.[14]

In our work the second-order diffusion limited Langmuir rate law is shown to fit all PER performed at different incoming:capping alkylthiol ratios with a single rate constant.[2] Which factors affect this rate constant is crucial to the rational design of mixed composition AuNPs. This report is thus an exploration of the physical parameters that affect the rate of PER. An understanding of the mechanism of the PER will lead to a model that can be used to interpret and rationally use the PER.

5.3 Methods

Reactions were followed using the previously described procedure,[2] with modifications made to the GC method to accommodate the different alkylthiols used. Briefly, AuNP were dissolved in toluene to yield 10 mg/ml solutions. These solutions were maintained under an Ar atmosphere at 25 °C. Reactions were initiated by adding

an appropriate quantity of alkylthiol via syringe injection. The reaction progress was tracked by removing 1 ml aliquots of solution and precipitating the NPs via introduction of 10 ml of ethanol. The AuNP were separated from the supernatant (containing free thiol) via filtration with a fine glass frit. The quantity of unbound (free) alkylthiols was determined by GC using a 5 % phenyl dimethyl-siloxane column and a FID detector. For each thiol pair(incoming, outgoing) a calibration of the different thiol ratios expected was performed and used to convert the peak areas to solution mole ratios. Particles were synthesized using the two-phase Brust-Schiffrin[4, 5] synthesis using Au:C_{10}SH:TOAB:$NaBH_4$ in a 1:1:2.5:10 molar ratio for C_6, C_{10} and C_{14} AuNP. Two additional C_{10}AuNP samples were synthesized so that a range of NP sizes: large(3.5 nm), medium (2.0 nm) and small (1.7 nm) were available. Au:thiol ratios of 1:4 and 8:1 (at 0 °C) respectively provided large and small samples. All NP were characterized by ^{1}H NMR (for free ligand), TEM, and TGA. Resulting analyses are shown in Table 5.1.

Table 5.1: Characterization of AuNP samples used in this study

Particle	% organic[a]	Diameter[b]	Std. Dev.	n[c]	Au atoms[d]	Au:thiol[e]
C_{10}AuNP	21.63					
C_6AuNP	14.57	2.2	0.6	760	329	3.5
C_{14}AuNP	27.14	2.5	0.7	261	483	3.2
C_{10}AuNP 'small'	23.15	1.7	0.5	4751	152	2.9
C_{10}AuNP 'large'	14.31	3.5	0.7	272	1325	5.3
C_{10}AuNP 'standard'	20.17	2.0	0.4	4181	247	3.5

[a] determined by TGA under O_2 conditions
[b] determined by assessment of TEM images
[c] number of NP counted in size TEM determination
[d] estimated with TEM data assuming sperical NP
[e] evaluated from TEM and TGA data

5.4 Results

The reaction between incoming alkylthiols (C_6 to C_{14}) and C_{10}-S-AuNP in toluene are shown in Figure 5.1. Each reaction reaches a similar plateau value in terms of fraction of ligands exchanged, demonstrating that the reaction endpoint is not dependent on the incoming alkylthiol composition. Within experimental scatter,

each reaction proceeds with the same rate constant. Incoming ligands as chemically different as C_6SH and $C_{14}SH$ (notably) show the same kinetics form and a similar endpoint.

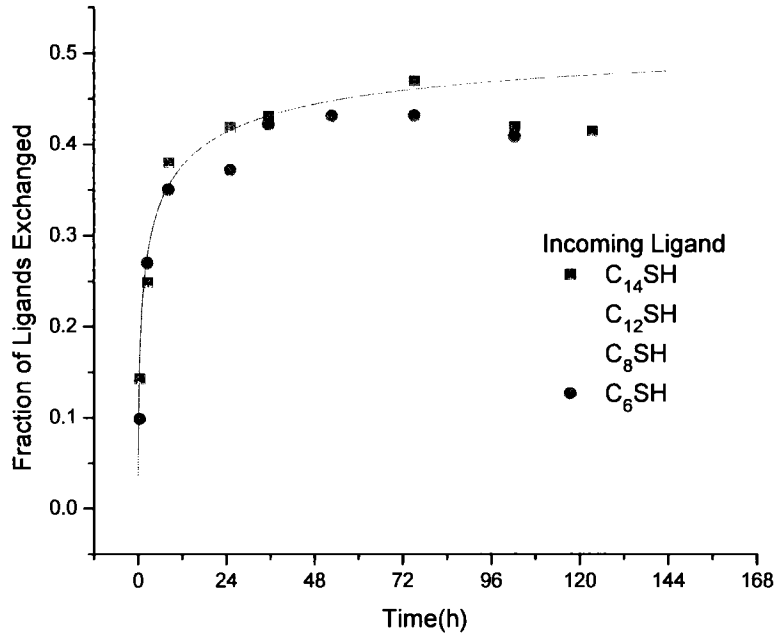

Figure 5.1: Reaction of C_6, C_8, C_{12} and C_{14} alkylthiols with C_{10}-AuNPs. The solid curve is the fit to equation 5.1

To further test the dependence of the reaction on chainlength, C_6S- and $C_{14}S$-protected AuNPs were reacted with two different alkylthiols. $C_{10}SH$ and $C_{14}SH$ were used as the incoming ligand in reactions with C_6-S-AuNPs. The observed reaction rates do not depend on the incoming chain length (Figure 5.2). Similarly, when C_{14}-S-AuNPs react with $C_{10}SH$ and C_6SH, the resulting rates are similar (Figure 5.3). We thus conclude that the chainlength of the incoming ligand does not affect the reaction rate if the incoming ligands are otherwise chemically similar (i.e. n-alkylthiols in this case).

While the incoming ligand chainlength does not affect the reaction rate for a given AuNP, the rate does depend on the outgoing ligand chainlength (Table 5.2). The rate constant, k, increases 4-fold in the reaction with $C_{10}SH$, going from C_6S- to $C_{14}S$-AuNPs.

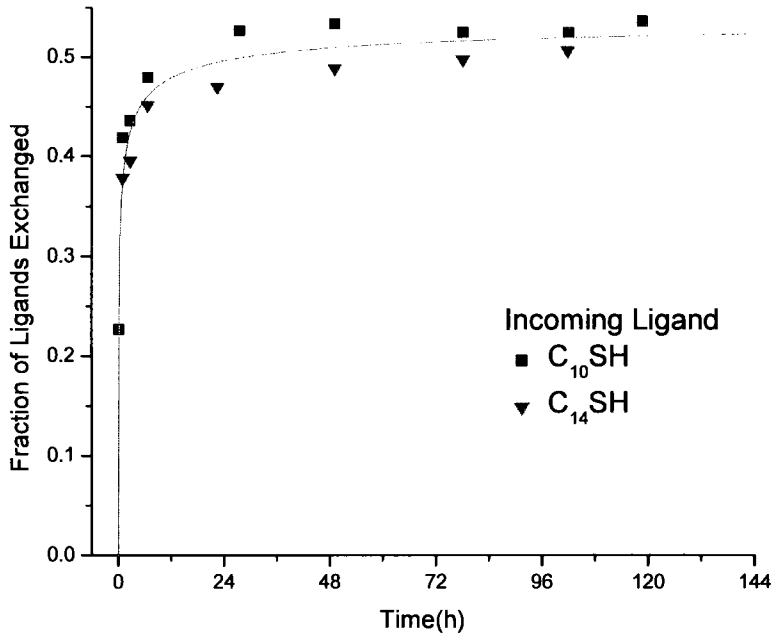

Figure 5.2: Reaction of C_{10} and C_{14} alkylthiols with C_6-AuNPs.

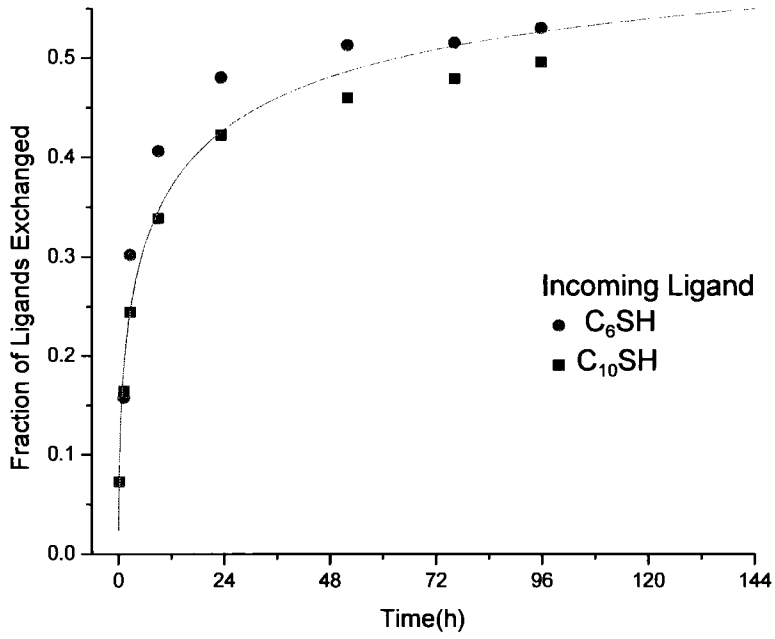

Figure 5.3: Reaction of C_6 and C_{10} alkylthiols with C_{14}-AuNPs.

Table 5.2: Kinetic data derived from application of Equation 5.1

Initial Ligand	Incoming Ligand	$k*10^{-2}s^{-\frac{1}{2}}$ [a]
C_6NP	$C_{10}SH$	3.3
$C_{10}NP$	$C_{12}SH$	1.2
$C_{14}NP$	$C_{10}SH$	0.8

[a] All three kinetic curves were simultaneously fitted using only one final 'A' value.

A mechanism which is dependent on the nature of the capping ligand is thus indicated. In the alkylthiol-for-alkylthiol PER the rate is dependent on the penetration of the incoming ligand into the existing alkylthiol capping layer.

5.4.1 Effect of NP core size on PER rate

Both the rate and extent of the reaction changes significantly with increasing size (Figure 5.4 and Table 5.3). The rate constant derived from fitting increases over 4-fold going from 1.7nm to 3.5nm cores. This trend is contrary to the expectations of the "edge and vertex" model.[6] The extent of reaction also increases with NP size. Although the gold atom-to-alkylthiol ligand ratio is potentially an important variable in any mechanistic study where electronic effects are being modulated, it has only been followed in one study.[14] It is not straightforward to prepare AuNP with different core sizes with the same ligand. Moreover, size effects are difficult to discern given the polydispersity of the core when the Brust-Schiffrin synthesis is used. Nonetheless, by varying the Au:RSH ration as per [5], we have prepared both a sample which is larger (3.5nm) than that used in the studies described above, and one that is smaller (1.7 nm).

Table 5.3: Rate constants of different sized AuNPs samples.

Size(nm)	A	$k*10^{-2}s^{\frac{-1}{2}}$
1.8	0.50	0.6
2.2	0.55	1.1
3.5	0.61	2.6

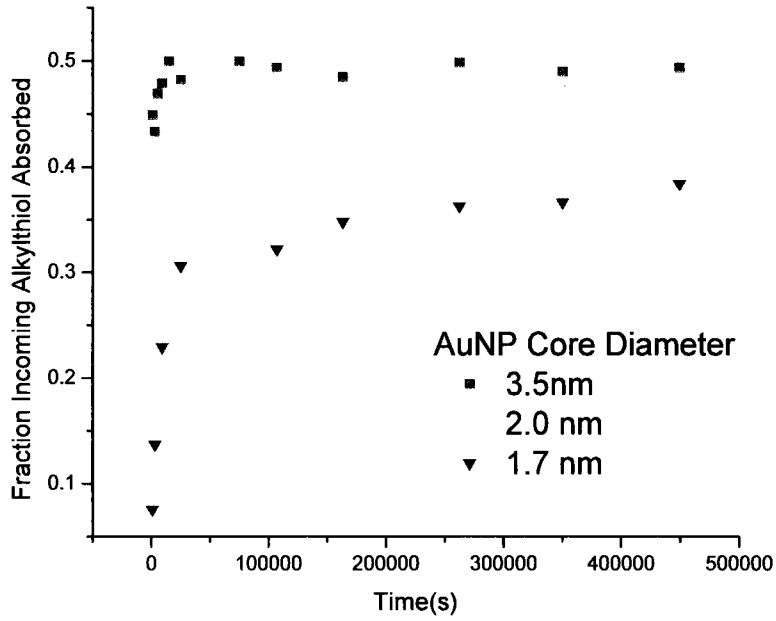

Figure 5.4: Reaction of C_{12} alkylthiol with three different core sizes of C_{10}-AuNPs.

This rate dependence on core size might originate from physical or structural differences in the different samples tested. It is first important to establish that the size of the gold core does not change during the reaction, given that it is known that alkylthiols can 'etch' AuNPs at high concentrations and/or temperatures.[9, 10] Neither TEM - derived sizes nor UV-Vis spectra before and after the reaction indicate that the NP size changes during the reactions.

Two ^{1}H NMR experiments were performed to assess whether the quantity of free alkylthiol changes during the reaction. ^{1}H NMR experiments allow for the *in situ* monitoring of the quantity of released alkylthiol. By using an internal standard (TMS), the change in the quantity of the β-methylene (delta=2.1ppm) of the free alkylthiol is measured. If there is a net thiol flux on (or off) the AuNP the NMR signal from thiols bound to the AuNP core are greatly broadened[13]. Any changes in the sharp resonance reports (assesed by integration of the peak) free alkylthiol in solution. No change in the quantity of the β-methylene relative to the TMS (tetramethylsilane) standard is in fact observed. An alkylthiol titration was then performed to determine whether these NP have a latent capacity to absorb free alkylthiols. In other words, do these as-prepared NP have uncoordinated gold sites? To do so would suggest that

at some early stage an adsorption, rather than an exchange, reaction has occurred. Standard solutions of $C_{10}SH$ in d_6-benzene with a dioxane internal standard(3.3ppm) were thus prepared to address this question. Experiments were carried out on both the 2.0nm and 3.5nm nanoparticles. A linear relationship between the quantity of added alkylthiol and the NMR signal area(R^2=0.99,0.97) results, with a near zero intercept. These data indicate that these AuNP release an equal number of alkylthiols as newly absorbed alkylthiols. These AuNP remain the same size (in terms of the core) during a PER and each releases a ligand in response to an incoming ligand.

There is currently only one model described in the literature that rationalizes the dependence of core size on the kinetics. Murray's 1999[6], "edge and vertex" model proposes that exchange reactions on AuNP (similar to those for 2D SAMs) are localized at edge and vertex sites on the gold nanoparticle's truncated octahedon core. The model arises from several details observed by Murray (but notably, not by us.) The most notable of these is the difficulty in completely exchanging all ligands from a AuNP. Two papers using ρ-arylthiols[13, 14] report reaction on two different sized particles(1.1nm and 1.6nm respectively) with the same incoming ligands. More complete and faster exchange occurs for smaller particles.[14]

The size dependent results presented here are not consistent with the "edge and vertex" model because smaller NP (cf. large NP) have a greater porportion of their ligand contents at edge and vertex sites than at terrace sites. A larger rate constant is thus expected, and not a lesser one, if the "edge and vertex" model is operative.

There are at least two possible origins of the core size effect. The first derives from the Heath and Gelbart[12] analysis of NP stability. The size of AuNPs in the Brust-Schiffrin synthesis was proposed to be controlled by two competing factors: the system's(thiol and gold) effort to reduce the gold-thiol surface energy balanced by the lower free energy of thiol monomers in solution. According to this model NP below 1.6nm will have a large driving force to form larger particles to reduce the gold-thiol surface energy. NP larger than ~5nm show a small difference in energy for each thiol in solution as a function of the reduction of their surface area. This leads to a regime where growth of the NP leads to little or no reduction in the total energy of the system. The NP thus have little (free energy) incentive to grow, even in diminishing thiol concentrations. Even though this publication [12] examines only the conditions of AuNP synthesis, these results can be translated to PER if one presumes that the equilibrium between thiols in solution and those on the NP determine the

exchange kinetics. The free energy change(large for small NPs) is then a controlling determinant in the rate constant. This proposition is intriguing and would account for the observed rate changes observed both here and in much of the work of reported from the Murray laboratory.[13, 14]

The second explanation derives from the AuNP electrochemistry work of Murray and others[11, 15] where the AuNP can be oxidized or reduced (producing $\pm 1, \pm 2, \pm 3$, etc. states). When their oxidized (+1) NP are introduced in the PER, the reaction rate is slightly faster (1.3 times) cf. the neutral NP.[7] It is not known however what the electrochemical potential of the reaction solution is during the synthetic process i.e. at open circuit (OCP). Moreover it is likely that different sized NP have different E° values and thus even at ambient OCP conditions, NP might exist in a different net charge state. It is significant that the E° values are quite accessible at ambient and Murray et al. have noted that as-synthesized samples exist as a 0/+1 mixture.

A method to test the importance of the redox state of the NP involves fixing the solution potential using redox "buffers". To determine if the solution potential affects the rate, three solutions pinned at different potentials using the ferrocene/ferrocinium couple were investigated. The solution potentials(vs. Ag/AgCl), fixed by the Nernst potential, were 800 mV(20mM Fe^+), 515 mV (10mM Fe^0/10mM Fe^+), and 305 mV (20 mM Fe^0.) Based on previous work[7, 11, 16] the difference between the 800 mV solution and the 305 mV solution should correspond to a difference of two oxidation states of the NP. However, no rate difference is observed when NP fixed at these three potentials are subjected to PER conditions described here. If a size-E° relationship indeed exists, it is not consistent with the observed reaction rates.

5.4.2 Other methods of PER rate control.

To determine if there is a change in rate with solvent polarity, three solvents of different dielectric constants were used in a model (C_{12} alkylthiol with C_{10}-AuNPs in toluene) PER: hexanes(ϵ =2.0), dichloromethane(ϵ =9.1), and the extensively used toluene(ϵ =2.4). The observed rate is found to be invariant over this range of solvent polarities.

To test if a radical species is an intermediate along the reaction pathway, two common trapping agents for radicals (BHT and α-tocopherol) were added to the reaction. These reagents however produced no effect in either the form or rate of the reaction.

5.4.3 Mechanism

To date, two mechanisms of AuNP PER have been presented. Murray and coworkers have produced a large body of results which converge to a model where the reaction involves displacement of soluble Au(I)-thiolate species, which then is involved in mediating the reaction.[7] Chechik et al.[8] on the other hand, suggest that the reaction is surface limited by the creation of a surface or near surface activated alkylsulphur species.

In the field of 2D Au-RS SAMs, Schlenoff and co-workers also proposed that the reaction is surface bound[3](as does [8]) with both incoming alkylthiols and disulphides reacting with a similar mechanism of surface bound ligand exchange as Figure 5.5. In the case of alkylthiols the product is a new alkylthiol, and in the case of disulphides the product is a mixed disulphide. This description parallels our recent findings that disulphides react with alkylthiol-protected AuNP to yield a mixed disulphide (See Chapter 4).

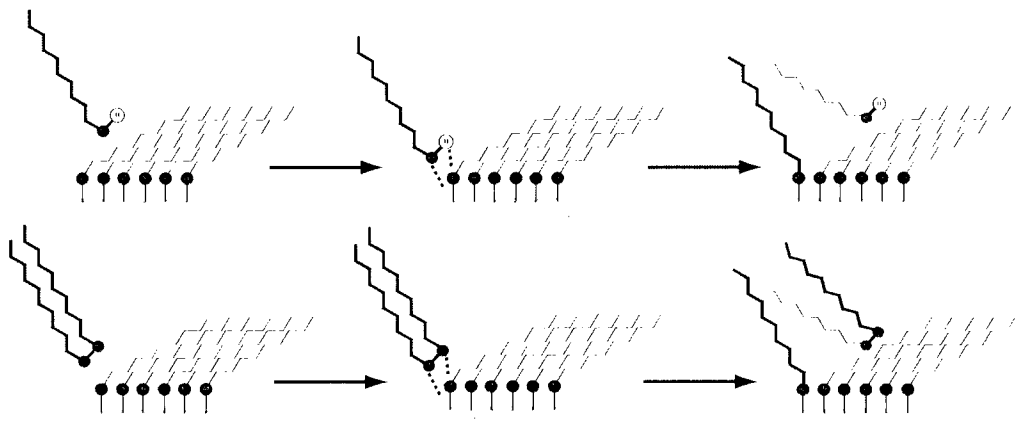

Figure 5.5: Proposed scheme of alkylthiol and dialkyldisulphide reaction with alkylthiol-capped AuNPs

The results presented here and in our prior work[2] converge to yield five principle conclusions:

i) that the exchange reaction is an equilibrium reaction, and proceeds to a stoichiometric endpoint.[2]

ii) the main determinant of reaction rate is the capping ligand binding to the AuNP

iii) reactive radical intermediates are not on the reaction pathway

Table 5.4: Kinetic models applied to alkylthiol-for-alkylthiol and dialkyldisulphide-for-alkylthiol PER. indicates that observed phenomena and model are inaccord, × indicates conflicting observations and model, ? unknown relationship.

	Model			
	Edge and Vertex	Surface Reactive Intermediate	Au(I) Thiolate	2nd Order Langmuir Diffusion
Zeroth order in [Incoming ligand]	×			
Kinetic fits to entire reaction profile	×		?	
End point ($K_{eq} \approx 1$)	×	×		
Capping alkylthiol length	×	?		
Reaction with dialkyldisulphides	?		×	
Rate invariance with E°	×	?	×	
Rate invariance with solvent	?		×	
Reaction in inert atmosphere	×		×	
Size dependence	×	?	?	?

iv) the rate is not significantly modulated by changes in the solution potentials

v) the PER of disulphides with AuNPs follows similar kinetics as alkylthiols with AuNP, but is 20-fold slower.

The question as to what is the composition of the rate limiting step in the reaction is a complex one. Adherence to diffusion-limited kinetics, (Equation 5.1) prevents there being a direct rate law attribution of the chemical components of the rate limiting step. Previous hypotheses[2, 7, 8, 14] suggested that the rate limiting step involves either:

i) the incoming and outgoing ligands in some unspecified coupling[2, 14], or

ii) dissociation of a Au(I) thiolate species into solution[7], or

iii) dissociation of an unspecified alkylsulphur species from the surface [8]

The observations reported here are only reconcilable if the limiting step in the PER is the diffusion of an incoming ligand through the NP ligand layer. The slower rate of disulphide reaction is attributable to its greater bulk, and hence lesser ability to reach to the AuNP surface. If the rate was indeed controlled by the dissociation of a reactive species into solution, one would expect that the rates of alkylthiol and disulphide exchange would be similar. Instead the model summarized in Figure 5.5 is consistent with all the data reported here and in related studies.

5.5 Conclusion

The rate of the PER of alkylthiols with RS-AuNPs is determined largely by the nature of capping ligand on the AuNP surface. The emerging picture of these PERs is one where a surface or near-surface reaction involves both incoming and outgoing ligands as a factor in determining the rate.

5.6 Acknowledgements

TEM imaging was performed by Dr. David Liu(Dept. of Physics, McGill.) Dr. Ian Burgess conducted the solution potential measurements of the ferrocene/ferrocinium solutions. Dr. Paul Xia ran the NMR and helped in the design of the NMR experiments.

References

[1] Schmid,G.*Ed.* Nanoparticles: From Theory to Application,Wiley-VCH;2004.

[2] Kassam, A.; Bremner; G., Clark, B.; Ulibarri, G.; and Lennox, R.B. *J. Am. Chem. Soc.* **2006**, 128, 11, 3476 - 3477.

[3] Kolega, R. R.; Schlenof, J. B. *Langmuir* **1998**, 14, 5469-5478.

[4] Brust, M.; Walker, M.; Bethell, D.; Schiffrin, D. J.; Whyman, R. *Chem. Commun.* **1994**, 801-802.

[5] Hostetler, M. J. W.; Wingate, J. E.; Zhong, C.-J.; Harris, J. E.; Vachet, R. W.; Clark, M. R.; Londono, J. D.; Green, S. J.; Stokes, J. J.; Wignall,G. D.; Glish, G. L.; Porter, M.D.; Evans, N. D.; Murray, R. W. *Langmuir* **1998**, 14, 17-30.

[6] Hostetler, M. J.; Templeton, A. C.; Murray, R. W. *Langmuir* **1999**, 15, 3782-3789.

[7] Song, Y. and Murray, R. *J. Am. Chem. Soc.* **2002**, 124, 7096-7102

[8] Ionita, P.; Caragheorgheopol, A.; Gilbert, B. C.; Chechik, V. *Langmuir* **2004**, 20, 11536-11544.

[9] Wilcoxon, J. P. and Provencio, P. *J.Phys.Chem.B.* **2003**, 107, 12949-12957.

[10] Maye, M. M., Zheng, W., Leibowitz, F.L., Ly, N.K., and Zhong, C. *Langmuir* **2000**, 16, 490-497.

[11] Quinn, B. M., Liljeroth, P., Ruiz, V., Laaksonen, T., and Kontturi, K. *J. Am. Chem. Soc.*, **2003**, 125(22), 6644-6645.

[12] Leff, D.V., Ohara, P.C., Heath, J.R. and Gelbart, W.M. *J. Phys. Chem.*,**1995**, 99(18), 7036-7041.

[13] Donkers, R.L., Song, Y., and Murray, R.W.*Langmuir* **2004**, 20(11), 4703-4707.

[14] Guo, R.,Song, Y., Wang, G. and Murray, R.W.*J. Am. Chem. Soc* **2005**, 127(8), 2752-2757.

[15] Chen, S., Murray, R.W., and Feldberg, S.W.*Journal of Physical Chemistry B*, **1998**, 102(49), 9898-9907.

[16] Lice, G.C., Zelakiewicz, B.S., Constantinescu, M. and Tong, Y.*J.Phys.Chem.B.* **2004**, 108, 19896-19900.

APPENDIX F

Additional Data Reported in Chapter 5

Table F.1: Rate constants of reaction of different incoming ligands with C_{10}-AuNP.

Incoming Ligand	A [a]	$k*10^{-2}h^{-\frac{1}{2}}$ [a]
C_6	0.51 (0.03)	0.57 (0.11)
C_8	0.56 (0.02)	0.69 (0.11)
C_{12}	0.55 (0.02)	0.82 (0.12)
C_{14}	0.51 (0.02)	0.67 (0.12)

[a] Fitting errors are shown in parentheses.

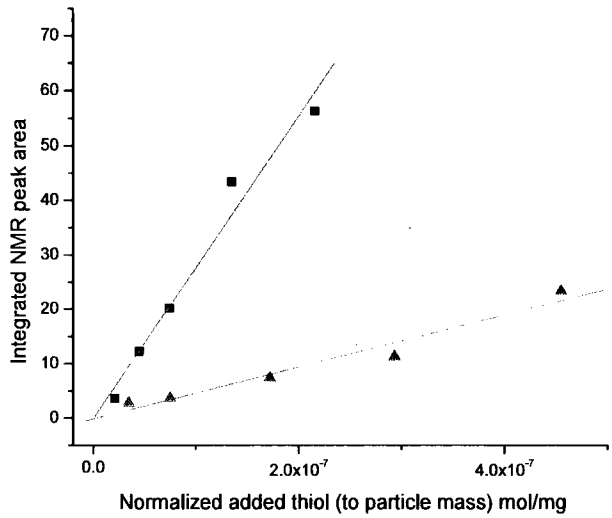

Figure F.1: Addition of thiols to 3.5nm(blue) and 2.0nm(red) AuNP samples. Fitting is to a linear regression for both 3.5nm($m=2.8\times10^{8}$,$b=-0.09$,$r^2=0.97$) and 1.7nm($m=4.8\times10^{7}$,$b=-0.16$,$r^2=0.96$) NP respectively.

CHAPTER 6

Conclusions, Contributions to Original Knowledge, Future Work and Outlook

6.1 Conclusions

The research reported in this Thesis has developed a methodology that greatly simplifies the analysis of the place exchange reaction of alkylthiols with alkylthiol-protected gold nanoparticles. This methodology allows for the study of this reaction in the absence of strong thermodynamic differences between the incoming and capping ligands. This provides for a detailed study into the kinetics and mechanism of this reaction. By combining the results presented in this Thesis a convergent description of PERs on RS-AuNPs emerges. The principle results are:

1. The place exchange reaction between RS-Au NP and alkylthiols and dialkyldisulphides follows second order Langmuir diffusion kinetics; the former is 20-fold faster than the latter.

2. The reaction rate is zero-order in the incoming ligand concentration for both alkylthiols and dialkyldisulphides.

3. A value consistent with $K_{eq} = 1$ is observed when there is little chemical distinction between thiols used, as is the case for alkylthiols from C_6 to C_{14} and in the case of reaction of C_{12} dialkyldisulphides with C_{10}AuNPs.

4. The reaction of C_{12} dialkyldisulphides with C_{10}AuNPs produces the C_{1012} mixed dialkyldisulphide as the major product.

5. The rate of exchange of alkylthiols onto AuNPs is determined largely by the nature(chain length) of the capping ligand on the AuNP surface.

The emerging picture of exchange reactions of alkylthiol-capped AuNPs is that of a surface, or near-surface, reaction that involves both incoming and outgoing ligands as factors in determining the rate. Based on all of the observations presented here a model of the exchange reaction has been developed (Figure 6.1.)

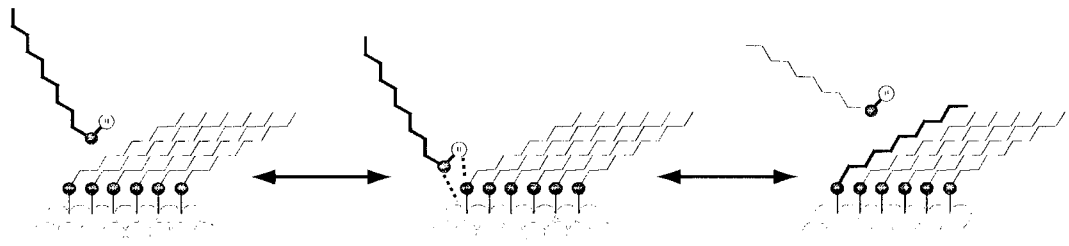

Figure 6.1: Proposed reaction scheme of thiol exchange on AuNPs

6.2 Contributions to Original Knowledge

The development of a methodolgy to study PER of alkylthiols and dialkyldisulphides for alkythiol-protected AuNPs with little chemical distinction enabled study of PER. Carrying out the reaction in the absence of overbearing forcing factors enabled detailed study of the kinetics and parameters influencing the reaction. The chief results are thus:

i) Kinetics of alkylthiol and dialkyldisuphides exchange reaction on RS-AuNP were determined to follow a second order Langmuir diffusion model.

ii) Reaction endpoints of PER were found to be in accord with $K_{eq} = 1$.

iii) Factors effecting the rate of reaction (solvent, chainlength, core size) in alkylthiol-for-alkylthiol exchange reactions were clearly identified, and the magnitudes of their affect on both the extent (A) and reaction rate constant (k) were identified.

iv) Study of the use of perturbing agents (electrochemical buffers, spin traps, solvent) on PER kinetics were explored.

6.3 Future Work

1. The conclusions to this research highlight both the limitations as well as the opportunities of the PER. Equilibrium reactions are awkward to use synthetically and small changes in the equilibrium constant (K_{eq}) can cause significant changes in the particle composition. Creating new nanoparticles within this framework will be both challenging and rewarding. One possible method to create new particles is to use temperature jumps to turn exchange reactions 'on' and 'off' over a sub-second to second timeframe. This may enable the reproducible creation of NP with a known composition, or at the least, NP with a small and well defined number of new ligands.

2. Our work and that of others[1] have suggested that dithiols should react much slower or not at all in PER. These NP would have improved stability cf. alkylthiols and could be used in environments where exchange is undesrible. These reactions have not yet been described in the literature.

3. RS-AuNP are being applied to many biological (cellular applications); the extent to which the PER is a problem or opportunity has to be explored with model incoming ligands such as (glutathione, cysteine, polypeptides and thiosugars).

6.4 Outlook

Since publishing our first paper on the subject 1 year ago,[2] other research groups have begun to use its framework to understand the reaction kinetics of PERs. Two papers have been published that evaluate the K_{eq} value for the alkylthiols[3, 4] used, which is one of the chief findings of this first paper. The prior models (presented in the Introduction) will have less impact on the field, as we believe that their extension can lead to erroneous results and conclusions. This new framework will allow researchers to develop and create multifunctional AuNPs with controled composition.

References

[1] Kolega, R. R.; Schlenoff, J. B. *Langmuir* **1998,** *14,* 5469-5478.

[2] Kassam, A.; Bremner, G.; Clark, B.; Ulibarri, G.; Lennox, R. *J. Am. Chem. Soc.* **2006,** *128,* 3476–3477.

[3] Kalsin, A. M.; Kowalczyk, B.; Wesson, P.; Paszewski, M.; Grzybowski, B. A. *J. Am. Chem. Soc.* **2007,** *129,* 6664-6665.

[4] Nerambourg, N.; Werts, M. H. V.; Charlot, M.; Blanchard-Desce, M. *Langmuir* **2007,** *23,* 5563-5570.